



Università
degli Studi
di Pavia

Dipartimento
di Fisica
“A. Volta”



DOTTORATO DI RICERCA IN FISICA – XXI CICLO

NON CLASSICAL STATES IN INTERFEROMETRY

dissertation submitted by

Giovanni De Cillis

to obtain the degree of

DOTTORE DI RICERCA IN FISICA

Supervisor: Prof. Lorenzo Maccone

Referee: Dott.ssa Maria Bondani

Giovanni De Cillis

PhD thesis – University of Pavia

Printed in Pavia, Italy, November 2008

ISBN 978-88-95767-16-1

*a Pina e a Nicola,
al loro cuore,
per sempre giovane.*

Voi non avete patria, perché voi siete inammissibili a questa società!
(Giovanni Paolo II, Roma, Estate 1982)

Acknowledgments

I would like to thank my Supervisor Prof. Lorenzo Maccone for giving me the opportunity to work in a such exciting research field. I am grateful and honored to have worked with so distinguished scientist like him.

My thanks go also to Matteo Paris and Stefano Olivares for their support and for their availability to collaborate with my reserch project.

A particular thank to my thesis official referee, Maria Bondani for reading carefully my work and for her precious suggestions.

I also wish to express my acknowledgement to Paolo Perinotti and Giulio Chiribella, for their promptness to answer to all my questions. Finally I would like to thank Prof. Lucio Claudio Andreani for his very interesting lectures during the second study year.

Voglio ringraziare Ettore Bernardi e Davide Mascoli, colleghi della scuola di Dottorato, per la loro amcizia, seppur non ricca di incontri. Quei pochi momenti condivisi, comunque, per me valgono tanto (Grazie Ettore per essere venuto fino in Brianza quella sera!!!).

Ringrazio Chiara, per il suo sostegno che mi aiuta a capire quanto io valga.

Ringrazio mamma e papà, perché mi sopportano e mi perdonano sempre.

Ringrazio Papa Benedetto XVI e chi con lui, difende l'uomo e la sua ragione e non cede a compromessi nella ricerca della verità.

Infine Ringrazio Dio che mi ha portato fin qua.

Contents

Introduction	1
1 Phase estimation and Interferometry	5
1.1 Statistical aspects of quantum mechanics	6
1.1.1 Description of experimental measurement	6
1.2 Estimation strategies for QET	7
1.3 Phase estimation problem	8
1.3.1 Optimal single mode phase estimation for global QET	10
1.4 Phase estimation in interferometry	12
1.4.1 Fock state interferometry	13
1.5 Comments	17
2 A review on Gaussian states	21
2.1 Some preliminary notions	21
2.2 Gaussian states	23
2.2.1 Purity of Gaussian states	24
2.2.2 Single mode Gaussian state	24
2.2.3 Bipartite Gaussian states	25
2.3 Noisy evolution of gaussian states	26
3 Interferometry with Gaussian states	27
3.1 Set-up dynamics	27
3.2 Hilbert-Schmidt distance	30
3.3 Uhlman's fidelity	34
3.4 Concluding remarks	37
4 Quantum metrology with loss in Bosonic systems	39
4.1 Physical information encoding	40
4.2 Description of lossy map	41
4.3 Quantum estimation with NOON state	42
4.3.1 NOON States and the Heisenberg Limit	42
4.3.2 NOON state Phase Measurement in the Presence of Loss	43

4.4	Partially entangled states	46
4.4.1	Entanglement between groups	47
4.5	m&m states	50
5	Grouping photons	55
5.1	NOON-LIKE State	55
5.1.1	Ideal case	55
5.1.2	Lossy case	57
5.2	Comments	64
6	Robustness in absolute phase estimation	67
6.1	Canonical phase measurement	68
6.2	Robust strategy	68
6.2.1	Ideal measurement	69
6.2.2	Noisy measurement	70
6.3	Towards interferometric framework	72
	Conclusions	75
A	Symplectic transformations	79
B	Characteristic function	81
C	A remark about parameters κ	83
D	Calculation of damped NOON-like	85
E	Calculation of damped MN-loss	87
F	Analitical evaluation of $(\Delta A)^2$ for the m&m state	89
	Bibliography	92

Introduction

New topics in physics are related to the possibility of performing ultraprecise measurements. Among these measurements, interferometry is the technique that has given the most spectacular achievements. Of historical importance are, among others, measurement apparatuses like the Mach-Zehnder or the Michelson interferometers. Today, the use of this technique applied to several research fields, both fundamental and applicative, is still important: some examples are the detection of gravitational waves, quantum lithography, optical gyroscopes, radio telescopes etc.

Essentially, interferometry consists in the measurement of the phase shift between different optical paths in the arms of an interferometer. Such phase shift can be generated, for example, by changing the refractive index of one of the arms; by means of a measurement of a suitable observable, information on the relative phase can be recovered and in turn, information on some characteristics of a media, such as the refractive index, can be obtained with a certain precision. Since the phase is not directly measured, but is inferred from the measurement of an observable, it is said that a phase estimation is performed: this is an application of the estimation theory by means of optical interferometry.

The quantum mechanical noise that is intrinsic in any measurement (and is a consequence of the Heisenberg uncertainty relations) implies that the precision on the parameter that has to be estimated is limited by the so called *Shot Noise* (SN), at least if only classical states are employed. However, if states that exhibit quantum features, such as entanglement or squeezing, are employed then the SN can be beaten. This is the most exciting discovery of the last years concerning this research field and experimental realizations have been given primarily in quantum optics, where quantum mechanics is applied to phenomena involving light.

The SN beating moreover is not the last step. In the last decade a way to ideally reach the ultimate limit in precision phase measurements, the so called *Heisenberg Limit* (HL), has been also proposed: Unfortunately, an experimental proof of this case is very demanding, due to the high sensitivity to noise of the states of light necessary to achieve this limit. We will encounter cases in

optics for which the loss of only one photon prevents from reaching the HL.

A fundamental question naturally arises, namely: "what is the best strategy to extract information on some parameter in precision measurement when noise is introduced?" We have tried to answer to this question in the quantum optics domain.

Most of the previous literature analyzes the best strategy in estimations of phase shifts and absolute phases exploiting the results of the *Quantum Estimation Theory* (QET) initially developed by Holevo [30] but neglecting the problem of the loss of photons. Only very recently [38, 39], an investigation in this direction was performed.

In the present work I will present a simple but robust absolute phase estimation strategy that could be also used in the interferometric domain. This result is very important because it suggests how to perform a robust measurement in a very simple way.

If we move to multimode interferometry, the application of QET in the presence of noise becomes more complex since mixed multipartite states are involved. Nevertheless, the study of these states allows one to introduce a heuristic but efficient criterion to see whether a quantum state can or cannot be robust to the loss of photons, namely if it can still carry information on the phase parameter with an acceptable precision. Such a criterion consists in degrading the entanglement of a multipartite *Maximally Entangled State (MES)* in order to have a multimode *Partially Entangled State (PES)*. The key idea, first proposed in [29], in which the use of partially entangled light was suggested in order to have an enhancement in the estimation of position of some light sources, is that a less entangled state can tolerate the loss of some photons at the cost of a lower precision in the estimation of the phase. In this way we see that a tradeoff between robustness and precision naturally emerges. A contribution to this multimode interferometry has been also given by presenting some theoretical measurement strategies in which a particular PES is used. We will concretely see how this method can give in principle good results in terms of robustness to loss of photons. Moreover, we will clarify that the maximally entangled states are not always so sensitive to noise, at least in quantum optics, and a particular class of MES can also be employed in noisy measurements as demonstrated by Huver et al. in [38].

As already mentioned, interferometry can be exploited for different aims: so in addition to the above research we have also investigated the problem of discriminating between two optical absorbers characterized by different transmissivities. We have analyzed a simple optical scheme based on the entangling property of the beam splitter when squeezed light is employed. The most important result is that such simple optical set-up can give better performance than the one in which the light field is put directly in the medium for some values of the experimental parameters. We have limited our analysis to the so called *Gaussian states*, a particular class of states easily obtainable in the laboratory.

The aim of this thesis has been to suggest several theoretical methods in quantum optics for phase estimation in the presence of noise and to contribute to the understanding of the tradeoff between precision and robustness. There is still very scarce literature on this problem and a more exhaustive analysis is needed in order to give a more realistic description. I have structured the thesis in this way:

In **Chapter I** a brief review on fundamental notions of quantum theory and QET specialized to the phase parameter is given. At the end of the chapter a revisit of a result presented in [42] where the realization of a particular interferometric measurement is given and consequently some problems concerning the realistic limitations that can be encountered by an experimenter are discussed.

Chapter II is devoted to the presentation of the main characteristics of the Gaussian states and their behaviour under noise. We present some well known results from the continuous variable domain. The plan of the chapter has been taken from [63]. In **Chapter III** I present our original method to be used in the discrimination of damping constants. It uses the *Hilbert-Schmidt distance*, a figure of merit that can be easily handled with Gaussian states. The following three chapters deal with the phase estimation problem:

Chapter IV considers the task of phase estimation in bosonic systems. I present how to ideally reach the HL. The NOON state, to which much attention has been devoted, is presented as a special case of a more general class of maximally entangled interferometer input states. The map describing the loss of photons which will be widely used in the rest of the thesis is also given. At this point, when we will see the expression of a MES evolved under the noisy map, we heuristically introduce the idea of grouping photons as a possible way to fight the high sensitivity to loss. In the end I consider the so called *m&m* states and I present their property in a slightly different way than the one used in [38] where these states are studied for the first time. So in **Chapter V** we show qualities and limitations of our strategies that employ PES starting from the idea of grouping photons of MES. So far we have studied the performance of some schemes that involve multimode interferometry. In **Chapter VI** the single phase estimation problem is addressed and the robust strategy previously mentioned is explained. In this case we will consider the canonical phase measurement performed on the optimal phase state evolved under the noisy map. Such method is a candidate as an alternative strategy to those in which one finds the optimal state evolved under noise and searches for a suitable measurement. In the end, a perspective to interferometric set-up is given and a preliminar way to perform measurement in presence of noise is suggested. **Chapter VII** contains conclusion and outlooks.

Chapter 1

Phase estimation and Interferometry

In physics there are several quantities that are not directly accessible, either in principle or due to experimental impediments. The value of the quantity of interest in these cases should be obtained by indirect measurements and inferred by inspecting a set of data coming from the measurement of some observable, or a set of observables.

Quantum estimation theory (QET) [30] is the theory that provides a way to find the optimal measurement that gives the best estimation; it is divided into two branches: *Global* QET, which finds the most suitable cost function averaged over all the possible values of the parameter to be estimated, and *Local* QET, which searches for the optimal measurement that minimizes the variance of a quantity called estimator, at a fixed value of the parameter [1, 2, 3, 4, 5].

Global QET and Local QET have been applied to find optimal measurements and to evaluate lower bounds on precision for the estimation of parameters imposed by unitary transformations such as single-mode phase [7, 9], displacement [10], squeezing [11, 12] for bosonic systems, and to estimation problems with open quantum systems and non unitary processes [15]: to finite dimensional systems [16], to optimally estimate the noise parameter of depolarizing [17] or amplitude-damping [18], and for continuous variable systems to estimate the loss parameter of a quantum channel [20, 21, 22, 19].

In this chapter we will encounter both these paradigms of QET and we will see how estimation can be performed by means of an interferometric set-up with non classical states of light. First of all a brief review will be given on the fundamental notion of quantum theory and QET which will be suddenly specialized for the phase estimation problem. After this introduction, a particular phase measurement by means of a Mach-Zehnder interferometer will be given.

1.1 Statistical aspects of quantum mechanics

Statistical theory of quantum measurement has become one of the most important research fields in quantum physics. It investigates the relation between the physical world and the elements of the operator formalism. In this framework the notion of observable describes the experimental procedure that produces an outcome, namely the result of the observation, according to some probability distribution. For this reason we will see that to some quantities there is no associated a self-adjoint operator observable, but a more suitable mathematical object called POVM, *positive operator valued measure*.

1.1.1 Description of experimental measurement

In the present section some essential notions on the mathematical description of the measurement process will be given.

In quantum mechanics, the measurement operation is given by a set of operators called POVM, namely a *Positive Operators Valued Measure* satisfying the following requirements:

$$P(B) \geq 0 \quad \forall \text{ set of events } B \quad (1.1)$$

$$P(\Omega) = 1 \quad (1.2)$$

$$P(\cup_{n=1}^{\infty} B_n) = \sum_{n=1}^{\infty} P(B_n) \quad (1.3)$$

$$\forall B_m : B_m \cap B_n = \emptyset, m \neq n$$

where Ω is the set of all possible outcomes which can be continuous (consider for example the possible positions of a particle in the space \mathbb{R}^3) or discrete (the only two outcomes in a Stern and Gerlach experiment).

By means of these operators, it is possible to assign a rule that predicts the probability of possible events through the Born's rule

$$p(B|\rho) = \text{Tr}[P(B)\rho], \quad (1.4)$$

once the state ρ of the system is given. Expression (1.4) reads: $p(B|\rho)$ is the probability of obtaining a particular event B provided that the system was prepared in the state ρ . So we see that it is possible to associate a state ρ to a probability distribution $p(B|\rho)$, and this association is made possible thanks to the operator $P(B)$: this is the description of the statistics of an experiment.

Properties (1.1) of the POVM guarantee, for any state ρ , the positivity and the normalization of the probability distribution (1.4) and the additivity of probabilities for disjoint events, respectively.

The canonical description of a quantum measurement by means of *projectors valued measure* (PVM) can be recovered thanks to the following fundamental theorem:

Theorem 1 (Naimark extension) *Any POVM P for the Hilbert space \mathcal{H} can be extended to a PVM E on a larger Hilbert space $H \supseteq \mathcal{H}$, namely*

$$P(B) = P_{\mathcal{H}}E(B)P_{\mathcal{H}} \quad (1.5)$$

where $P_{\mathcal{H}}$ is the projector onto \mathcal{H} .

From now on POVM will be referred as to a quantum observable. Since the term "observable" denotes a self-adjoint operator with its spectral decomposition made of orthogonal projectors, one might prefer to call observable only the PVM¹. But, as we have seen, thanks to Naimark theorem it is always possible to associate a PVM to POVM and so to call "observable" any given POVM.

After this introduction we can now present some notion of global QET.

1.2 Estimation strategies for QET

As previously mentioned, QET principally searches for the best estimation strategy, namely the experimental procedure that optimizes the recovery of the information on the parameter to be estimated, in a more proper language, it can be said: *the procedure that optimizes the decoding of the signal with respect to a given optimality criterion*. It is well known that when classical information is encoded into quantum systems, its read-out suffers the intrinsic quantum limitation of discriminating among nonorthogonal states.

So the problem is to find the optimal POVM. This mathematical object is very important in QET because it both describes the quantum measurement and the classical data processing (recovered from the Born's rule) which are the two stages that constitute a QET strategy.

For completeness we give the formal description of the typical situation in QET as clearly presented in [32]: The classical information is encoded into a parametric family of signal states, denoted by

$$S(\Theta) = \{\rho_{\theta} \in \mathcal{S}(\mathcal{H}) | \theta \in \Theta\}, \quad (1.6)$$

where $\theta \in \Theta$ is a multidimensional parameter and Θ is the space of outcomes. One is interested in extracting, from the unknown signal state ρ_{θ} , the value of some classical parameter $\omega \in \Omega$, which is in general a function of θ . It can happen that $\omega = \theta$ and this is the *state estimation*. In this case one has to produce the best possible guess of the state of the system under the hypothesis that the latter is prepared in a state of the parametric family $S(\Theta)$. Then a measurement is performed, consequently one extracts from the system an array of experimental data and finally a data analysis producing the estimation on ω is done.

Now we analyze the problem of the phase estimation. Initially an overview will be given on the main result concerning QET and an elegant and simple example will be analyzed in order to understand such result.

¹As it will be now clear, actually a PVM is a POVM with the additional property $P(B_1)P(B_2) = P(B_1 \cup B_2)$.

1.3 Phase estimation problem

In this section a series of general results will be given concerning the problem of phase estimation. We analyze a method to beat the shot noise limit expected by QET by means of the strategy described by *Giovannetti et al.* in [27] and one of the most important result obtained by Holevo about single mode phase estimation concerning the optimal measurement strategy will be shown.

As previously mentioned, both global and local QET have been applied to find optimal measurements and to evaluate lower bounds on precision over shot noise for the estimation of phase parameters ϕ . Such overcoming of the shot noise precision can be seen by means of the the following generalized uncertainty relation valid whatever is the measurement scheme employed [4]:

$$\Delta\phi\Delta h \geq \frac{1}{2\sqrt{\nu}}. \quad (1.7)$$

ν is the number of times the estimation is repeated, $\Delta h = \langle h^2 \rangle - \langle h \rangle^2$ is the variance of the generator h of an unitary trasformation \mathcal{U}_ϕ through which the phase is introduced in the system.

The most important and exciting results in this research field is that in the presence of systems characterized by quantum features such as entanglement or squeezing, it is possible to a have precision bound on the phase ϕ beyond the typical shot noise limit and the so called Heisenberg limit can be reached. A simple and elegant way to see this is given in quantum metrology and a similar argument it will be repeated here for the sake of clarity.

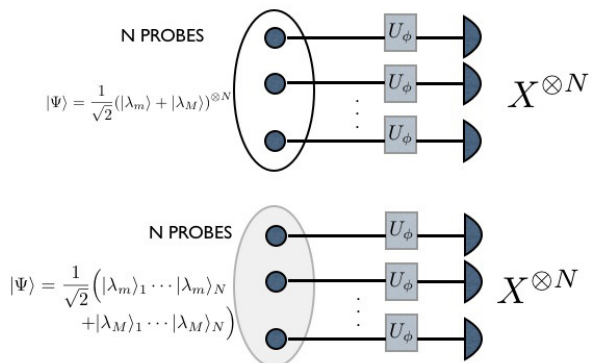


Figure 1.1: Estimation strategies employing a fully separable state (top) and a maximally entangled state (bottom).

Following the general framework of [27], let us take a N probe state (see

1.3. Phase estimation problem

fig. (1.1))

$$|\Psi\rangle = \frac{1}{\sqrt{2}}(|\lambda_m\rangle + |\lambda_M\rangle)^{\otimes N}, \quad (1.8)$$

where $|\lambda_m\rangle$ and $|\lambda_M\rangle$ are the eigenvectors of a known hermitian operator H corresponding respectively to the minimum and maximum eigenvalues λ_m and λ_M . A phase is introduced in the system by means of the operator

$$U_\phi^{\otimes N} \quad (1.9)$$

with $U_\phi = \exp(-i\phi H)$ acting on each probe, and we have the state

$$U_\phi^{\otimes N} |\Psi\rangle. \quad (1.10)$$

If the observable

$$X := |\lambda_m\rangle\langle\lambda_M| + |\lambda_M\rangle\langle\lambda_m| \quad (1.11)$$

is measured separately on each probe, which means a measurement of the observable $X^{\otimes N}$ on the state (1.10), we obtain:

$$\langle X^{\otimes N} \rangle = \langle X \rangle^N = \cos^N[(\lambda_M - \lambda_m)\phi] \quad (1.12)$$

$$\langle (X^{\otimes N})^2 \rangle = 1 \quad (1.13)$$

$$\Delta X^{\otimes N} = \sqrt{1 - \cos^{2N}[(\lambda_M - \lambda_m)\phi]}. \quad (1.14)$$

Through the error propagation formula, for nu repetition of the measurement, it can be seen that

$$\begin{aligned} \Delta\phi &= \frac{1}{\sqrt{\nu}} \Delta X^{\otimes N} / \left| \frac{\partial \langle X^{\otimes N} \rangle}{\partial \phi} \right| = \\ &= \frac{1}{\sqrt{\nu}} \frac{\sqrt{1 - \cos^{2N}[(\lambda_M - \lambda_m)\phi]}}{|-N \cos^{N-1}[(\lambda_M - \lambda_m)\phi] \sin[(\lambda_M - \lambda_m)\phi]|}. \end{aligned} \quad (1.15)$$

which for the values $\phi = k\pi$, $k = 0, 1, 2, \dots$ reaches the minimum (see fig. (1.2)):

$$\Delta\phi_{min} = \frac{1}{\sqrt{\nu} N (\lambda_M - \lambda_m)}. \quad (1.16)$$

This bound is the *shot noise* SN.

If now $|\Psi\rangle$ can be entangled (see fig. 1.1):

$$|\Psi\rangle = \frac{1}{\sqrt{2}} \left(|\lambda_m\rangle_1 \cdots |\lambda_m\rangle_N + |\lambda_M\rangle_1 \cdots |\lambda_M\rangle_N \right), \quad (1.17)$$

by measuring again the observable X of Eq. (1.11) separately on each probe, one has:

$$\langle X^{\otimes N} \rangle = \cos[N\phi(\lambda_M - \lambda_m)]$$

and the standard deviation

$$\Delta X^{\otimes N} = |\sin[N\phi(\lambda_M - \lambda_m)]|.$$

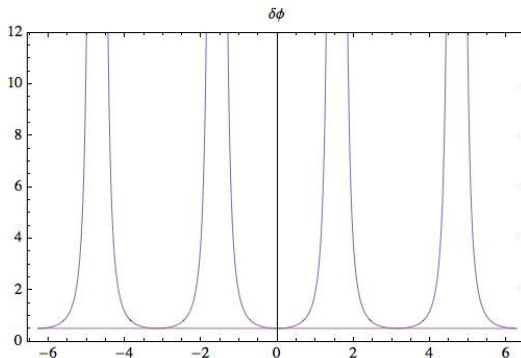


Figure 1.2: Plot of $\delta\phi$ of Eq. (1.15), as a function of ϕ , dotted line is shot noise. $N = 4$

After repeating ν times the experiment, from Eq. (1.15) one obtains:

$$\Delta\phi = \frac{1}{\sqrt{\nu} N(\lambda_M - \lambda_m)} \quad (1.18)$$

So it is possible to ideally reach the so-called *Heisenberg limit* consisting in a scaling law of

$$1/N \quad (1.19)$$

and to cross the shot noise limit for which the scaling law is

$$1/\sqrt{N}. \quad (1.20)$$

It is worth to stress that such an argument, that is much closer to the spirit of local QET for the bound (1.7), derives from the Cramer-Rao inequality; moreover in [27] the theoretical framework refers to the use of a general (biased or unbiased) estimator.

We conclude reminding that these results of quantum metrology are still valid if a sequential configuration, in which a single probe is utilized N times, is employed; an experimental realization has been recently given in [26].

1.3.1 Optimal single mode phase estimation for global QET

Turning to global QET, as explained in section 1.2, the main problem is to find the best estimation strategy. In this subsection we will present the result of Holevo who obtained the optimal strategy for phase estimation.

The family of states (1.6) is

$$\rho_\phi = U_\phi \rho_0 U_\phi^\dagger \quad \text{with} \quad \phi \in [0, 2\pi], \quad (1.21)$$

1.3. Phase estimation problem

$\rho_0 = |\psi_0\rangle\langle\psi_0|$ being a generic initial state that will be assumed to be pure.

Such a family of states is called *covariant* and the unitary operators U_ϕ represent an unitary group which in this case is the abelian group $U(1)$ of the rotations along one axis. So the problem is a covariant estimation problem which in turn requires an optimal *covariant* POVM which will be denoted as $d\mu(\phi_*)^2$.

In global QET we introduce a *cost function* $C(\phi_*, \phi)$ which quantifies the cost of estimating ϕ_* if the true value of the parameter is ϕ : the cost will be minimum when $\phi_* = \phi$ and will increase as the estimate ϕ_* goes away from ϕ .

The optimal estimation strategy consists in minimizing the average cost defined as:

$$\bar{C} = \int_0^{2\pi} d\phi p_0(\phi) \int_0^{2\pi} d\phi_* C(\phi_*, \phi) p(\phi_*|\phi), \quad (1.22)$$

where $p_0(\phi)$ is the a priori probability density for the true value ϕ , $p(\phi_*|\phi)$ is the conditional probability of estimating ϕ_* given the true value ϕ , namely:

$$p(\phi_*|\phi) = \text{Tr}[d\mu(\phi_*)\rho_\phi], \quad (1.23)$$

This is called the Bayesian criterion: in the typical situation ϕ is *a priori* uniformly distributed, i.e. $p_0(\phi) = 1/2\pi$ and one is more interested in the size of the error $\phi_* - \phi$ than in the value of ϕ . In this way the cost function becomes an even function of a single variable, i.e. $C(\phi_*, \phi) \equiv C(\phi_* - \phi)$. It follows that also the optimal conditional probability will depend only on $\phi_* - \phi$, and the optimal POVM can be obtained by restricting the attention only to phase-covariant [30] POVMs, i.e. of the form

$$d\mu(\phi_*) = e^{-i\hat{a}^\dagger a \phi_*} \xi e^{i\hat{a}^\dagger a \phi_*} \frac{d\phi_*}{2\pi}, \quad (1.24)$$

where ξ is a positive operator satisfying the completeness constraints needed for the normalization of the POVM: $\int_0^{2\pi} d\mu(\phi) = 1$. Using Eqs. (1.23), (1.24) and the invariance of trace under cyclic permutations one can easily recognize that $p(\phi_*|\phi) \equiv p(\phi_* - \phi)$ if and only if $d\mu(\phi_*)$ is covariant³. Hence the optimization problem resorts to finding the best positive operator ξ for a given cost function $C(\phi)$ and a generic given state ρ_0 . Such optimization leads to the following POVM firstly obtained by Holevo:

$$d\mu(\phi) = \frac{d\phi}{2\pi} |e(\phi)\rangle\langle e(\phi)|, \quad (1.25)$$

where the (Dirac) normalizable vectors $|e(\phi)\rangle$ are given by

$$|e(\phi)\rangle = \sum_{n=0}^{\infty} e^{in\phi} |n\rangle. \quad (1.26)$$

²In this case we deal with a density of POVM for the phase is a continuous variable.

³In fact if $d\mu(\phi)$ is covariant it holds: $p(\phi_*|\phi)d\phi_* = \text{Tr}[d\mu(\phi_*)e^{-i\phi a^\dagger a}\rho_0 e^{i\phi a^\dagger a}] = \text{Tr}[e^{i\phi a^\dagger a}d\mu(\phi_*)e^{-i\phi a^\dagger a}\rho_0] = \text{Tr}[d\mu(\phi_* - \phi)\rho_0] = p(\phi_* - \phi)$

Therefore, the optimal POVM $d\mu(\phi)$ is the projector on the state $|e(\phi)\rangle$. It is worth recalling that once the best strategy is obtained, one further optimizes the pure state ρ_0 . The fundamental result expressed in (1.25) is not valid for any generic cost function $C(\phi)$, but for a particular class of 2π -periodic function satisfying:

$$\int_0^\infty C(\phi) \cos k\phi \, d\phi \leq 0, \quad \text{with } k = 1, 2, \dots \quad (1.27)$$

Cost function of this type correspond to the most popular optimization criteria as:

- i)* the likelihood criterion for $C(\phi) = -\delta(\phi)$;
- ii)* the 2π -periodic ‘‘variance’’ for $C(\phi) = 4 \sin^2(\phi/2)$.

Finally it is worth recalling that the same average cost is achieved by restricting ϕ to the set of discrete values $\{\phi_s = \frac{2\pi s}{q}, \quad s \in \mathbb{Z}_q\}$, ($q \equiv \dim(\mathcal{H})$), and by using as the optimal POVM, the orthogonal projector-valued operator [79]

$$|e(\phi_s)\rangle\langle e(\phi_s)|. \quad (1.28)$$

The result expressed in Eq. (1.25) is very important because it is an application to the phase parameter of the estimation theory developed initially by Holevo in his pioneering book [30]. In the last part of the present work we will use this result to study the performances of phase estimation in the presence of loss.

The single mode case is useful when single shot measurements are used, in this case one is interested in the estimation of the absolute value of the phase. Unfortunately the optimal quantum measurement (1.28) is not physically realizable. A detailed analysis of the physically achievable single shot phase measurements has been given in [75].

In the following we will move to interferometric schemes involving bipartite systems and we will describe a theoretical proposal of phase estimation with non classical states of light.

1.4 Phase estimation in interferometry

Interferometry is one of the most important measurement techniques in physics. Its numerous variations include Ramsey spectroscopy in atomic physics, optical interferometry in gravitational wave detectors, laser gyroscopes, optical imaging etc. All these applications aim to estimate the quantity of interest, normally a relative phase, with the highest possible precision.

A figure of merit that can be used to characterize the performances of an interferometer is its sensitivity. In general there are different sources of noise which can limit sensitivity and one of these is due to the detection stage (photon-counting statistical errors), depending on the measurement process and on its quantum efficiency. On the other hand the sensitivity is ultimately limited by the *standard quantum limit* (SQL) or *shot noise* (SN).

This ultimate limit is related to the intrinsic obstacle that rises when quantum light is used in measurements of the interferometric phase shift: an input state with finite photon number variance necessarily has a non-zero phase variance, whereas states with zero phase variance are characterized by a divergent photon number variance. The following uncertainty relation holds:

$$\Delta\phi\Delta N \geq \frac{1}{4} \quad (1.29)$$

As already said in section 1.3, from this inequality it can be seen that the errors that limit precision in the phase estimation can be reduced. It is possible to beat the SQL, which is commonly considered the ultimate limit in precision and show that the boundary to the accessible information can be pushed further down when non classical states are employed in the interferometer. In the following we will introduce the task of the precision phase measurement performed by an interferometer in which the input states are Fock states.

1.4.1 Fock state interferometry

The general framework is the one in which the total energy, namely the total number of particles is kept fixed.

We have already seen that a generic classical interferometer has a shot noise limited sensitivity that scales as $N^{-1/2}$. With suitable quantum correlations between the particles⁴, the sensitivity can be ideally improved by a factor of \sqrt{N} and the scaling law becomes N^{-1} . Here N denotes the average number of particles passing through the interferometer during the measurement time.

In their pioneering work *M. J. Holland* and *K. Burnett* [43] showed that in a Mach-Zehnder interferometer with a *dual photons Fock state*, namely $|N, N\rangle$ as the input state it would be possible to obtain a precision on the phase at the Heisenberg limit.

With the following maximally path entangled state called NOON state

$$|N :: 0\rangle = \frac{1}{\sqrt{2}}(|N, 0\rangle_{a', b'} + |0, N\rangle_{a', b'}) \quad (1.30)$$

which will be presented more exhaustively in chapter 4, it would be indeed ideally possible to reach the Heisenberg limit.⁵ If one considers the following observable $A_N = |N, 0\rangle\langle 0, N| + |0, N\rangle\langle N, 0|$ and we let the NOON state

⁴It must be underlined here that, when we deal with interferometry, we consider path entanglement because the correlation between photons is due to their coexistence in one field mode, namely in a Fock state. The correlation due to entanglement between single photons is present instead in a state of this type:

$$1/\sqrt{2}(|1, 0\rangle_{a,b}^{\otimes N} + |0, 1\rangle_{a,b}^{\otimes N})$$

where one have N pairs of bosonic field modes a and b , populated by a single photon. We will come back to this problem in chapter 4.

⁵Note that in (1.30) we have specified the field modes a' and b' (see fig.(1.3)). The NOON state is not an input state; it must be obtained inside the interferometer.

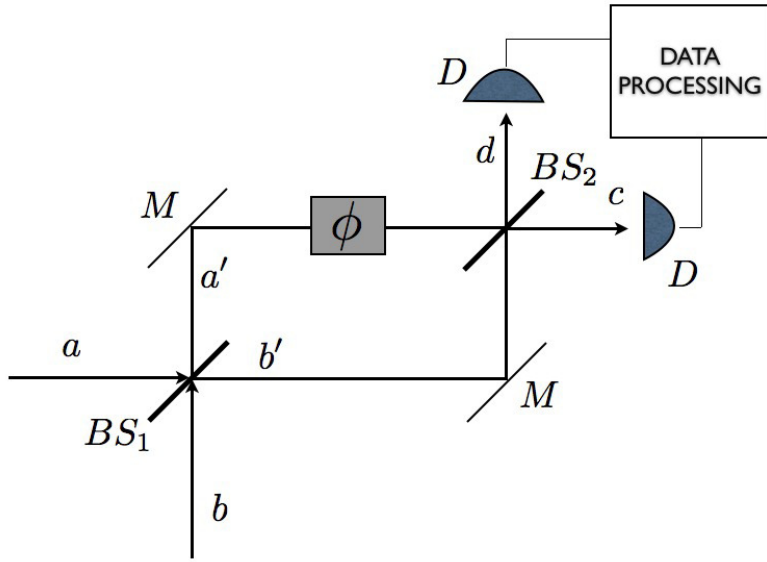


Figure 1.3: Typical Mach-Zehnder configuration: M denotes mirrors while $BS_{1,2}$ denotes balanced beam splitter. A dephasing medium is located in the upper arm. D are the detectors. The data are then processed depending on the measurement.

accumulate a phase ϕ it is easy to see:

$$\langle A_N \rangle_\phi = \cos N\phi$$

$$(\Delta A_N)_\phi^2 = 1 - \cos^2 N\phi$$

from which we obtain, thanks to formula (1.15),

$$\Delta\phi = \frac{\Delta A_N}{|\partial \langle A_N \rangle_\phi / \partial \phi|} = \frac{1}{N}$$

Unfortunately such a state is very sensitive to the loss of photons and we will see that, even if it would be possible to create a NOON state, it would require a noiseless environment. Moreover, with current interferometric set-up, it is not possible to deterministically create a state of this type, they can only be

1.4. Phase estimation in interferometry

approximated. Recently *R. Okamoto et al.* [44] have exploited the performance of a MZ interferometer with a 4 photon input state of the form $|2, 2\rangle_{a,b}$. The interferometer output state is of the form:

$$\sum_{k=0}^2 c(\phi)_k (|4-k, k\rangle_{c,d} + |k, 4-k\rangle_{c,d}), \quad (1.31)$$

with a, b and c, d (see Fig 1.3) input and output fields mode respectively. From Eq. (1.31) we can recognize the presence of the NOON state component. This experiment gives a better result than any classical interferometer but does not achieve the Heisenberg limit $\frac{1}{4}$ as a NOON state would do. We will see now how an interferometric measurement with input state of the form $|N, N\rangle$ can be described.

State projection method

A method to increase the precision beyond the SQL and near to the Heisenberg limit is the quantum state projection method employed for example in Ramsey interferometry.

F. W. Sun et al. [41] have suggested a way to perform such a measurement in which a NOON state was initially employed. In a more recent work [42], the same authors have also experimentally implemented such a method for the state emerging from a beam splitter when the input state is $|N, N\rangle$. Anyway the original idea presented in [42] can be further simplified. In that case it is stressed that in order to obtain information about the phase accumulated by the state $|\Psi_{2N}(\phi)\rangle$ inside the interferometer (see Fig. 1.4) a measurement onto such a state must be performed. In particular it is proposed a projective measurement represented by the observable-projector: $|\Psi_{2N}\rangle\langle\Psi_{2N}|$.

Actually it is simple to prove that it is not necessary to consider such a projection: following the argument of *Sun et al.* in [42] one initially writes the expression of $|\Psi_{2N}\rangle$:

$$\begin{aligned} |\Psi_{2N}\rangle &= U_{bs} |N, N\rangle_{a,b} \\ &= \sum_{k=0}^N (-)^{N-k} \left[\binom{2k}{k} \binom{2N-2k}{N-k} (1/2)^{2N} \right]^{1/2} |2k, 2N-2k\rangle_{a',b'} \\ &= \sum_{k=0}^N (-)^{N-k} \left[\binom{2k}{k} \binom{2N-2k}{N-k} (1/2)^{2N} \right]^{1/2} \\ &\quad \frac{a'^{2k} b'^{2N-2k}}{\sqrt{2k!(2N-2k)!}} |0, 0\rangle_{a',b'} \\ &= \frac{1}{N!} \sum_{k=0}^N (-)^{N-k} \binom{N}{k} (1/2)^N a'^{2k} b'^{2N-2k} |0, 0\rangle_{a',b'} \\ &= \frac{1}{N!} (a'^2 - b'^2)^N / 2^N |0, 0\rangle_{a',b'} \end{aligned}$$

$$= \frac{1}{N!} [(a' - b')/\sqrt{2}]^N [(a' + b')/\sqrt{2}]^N |0, 0\rangle_{a', b'}, \quad (1.32)$$

where $U_{bs} = e^{i\pi/4(a^\dagger b + b^\dagger a)}$ is the operator representing the action of the beam splitter, and we have made use of the fact that the commutator $[a'; b'] = 0$.

At this point we note that if we apply the beamsplitter transformation to last expression we obtain

$$U_{bs} \frac{1}{N!} [(a' - b')/\sqrt{2}]^N [(a' + b')/\sqrt{2}]^N |0, 0\rangle_{a', b'} = |N, N\rangle_{c, d}. \quad (1.33)$$

And this can be rephrased by saying that if we consider a MZ interferometer, it is possible to represent the action of the whole apparatus by a unitary operator $U_{\phi, MZ} = e^{-\phi(a^\dagger b - b^\dagger a)/2}$. If $\phi = 0$, $U_{\phi=0, MZ} = \mathbf{1}$, namely the identity operator.

So the projection method turns now to considering the MZ output state that accumulated a phase ϕ and projecting it onto the MZ output state that did not accumulate any phase, which means the input state for what just explained. Finally one has to perform the measurement of the projector

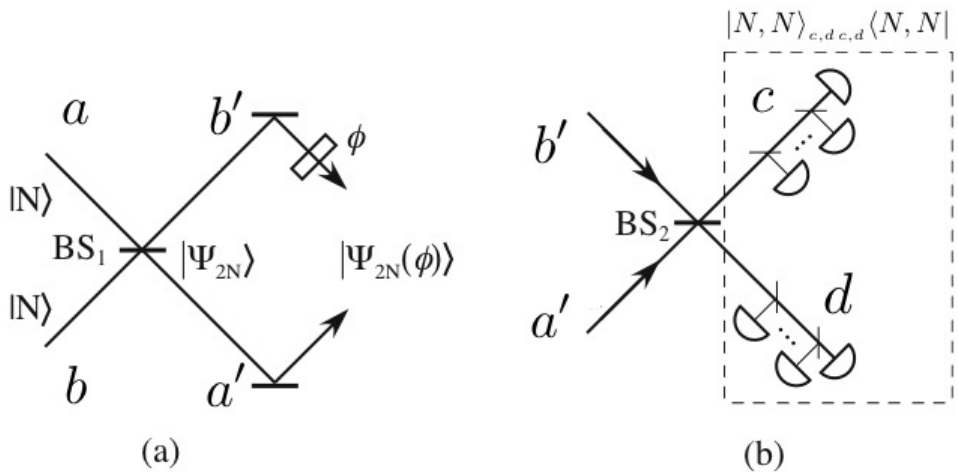


Figure 1.4: Projection measurement for phase measurement with twin Fock state in the framework of [42]. (a) generation of the state, (b) Projection measurement, see also [41] for an explanation of this method.

$$\mathbb{P} = |N, N\rangle_{c, d, c, d} \langle N, N| \quad (1.34)$$

over $|N, N\rangle_{c, d, \phi} := U_{\phi, MZ} |N, N\rangle_{a, b}$ which means a measure of the joint probability of detecting N photons at each output port of the second balanced beam splitter.

1.5. Comments

This is actually the argument of [42] but it has been presented in a slightly different way in order to see in a more intuitive way how the projection method could be achieved. Indeed the measurement of the projector $|\Psi_{2N}\rangle\langle\Psi_{2N}|$ as suggested in that work is actually a measure of \mathbb{P} .

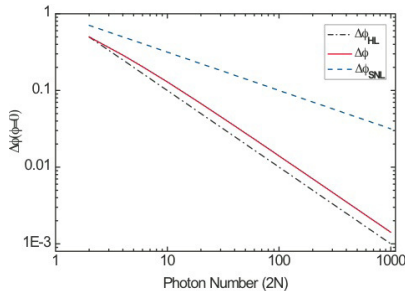


Figure 1.5: The figure has been taken from [42] and shows the theoretical phase uncertainty versus photon number N . The value of the phase to be estimated has been taken 0. Dashed line is SQL, dotted dashed is Heisenberg limit. The much closer solid line to Heisenberg limit is the precision obtained with the projection method described in the text.

The aim of the method is obviously to obtain information on the phase accumulated by the state inside the interferometer. This can be done by computing

$$\langle \mathbb{P} \rangle(\phi) = {}_{\phi} \langle N, N | \mathbb{P} | N, N \rangle_{\phi} = |\langle N, N | N, N \rangle_{\phi}|^2 \quad \text{and} \quad (1.35)$$

$$(\Delta \mathbb{P}(\phi))^2 = \langle \mathbb{P}^2 \rangle(\phi) - (\langle \mathbb{P} \rangle(\phi))^2 = \langle \mathbb{P} \rangle(\phi) [1 - \langle \mathbb{P} \rangle(\phi)] \quad (1.36)$$

from which it is possible to obtain:

$$\Delta \phi = \frac{\Delta \mathbb{P}(\phi)}{|\partial \langle \mathbb{P} \rangle(\phi) / \partial \phi|} \quad (1.37)$$

whose behaviour is presented in Fig. (1.5).

We have finally seen an interesting example which allows performing phase shift measurements near to the Heisenberg limit in an interferometric framework.

Several comments are now necessary.

1.5 Comments

In this introductory chapter an overview has been given on the research problems concerning phase estimation. This task has seen a great development in the last years but it must be said that a serious problem seems to be unavoidable at the moment for the difficulty in deterministically obtaining exotic states like NOON state and deterministic measurements.

How can a deterministic experiment in which the effect of noise is taken into account be realized? In [42] it is not only given a theoretical proposal but it is also presented an experimental realization and in [44] it is claimed that the SQL has been beaten with a MZ experiment and with a 4 photons input state of the form $|2, 2\rangle$.

In the first work it is explicitly said that the measurement is a *demonstration of principle* and so it is actually post selective, i.e., when noise is considered, one passes from measuring \mathbb{P} to measuring $\eta^2\mathbb{P}$ (see Eq. (1.34)), where $0 < \eta < 1$ represents the losses of photons. In practice the effect of noise is simply to decrease the success probability which only means that the number of trials must be increased. If one has N probes it needs now N/η . In this way the loss of photons is not actually considered, because between all the data coming from the fixed input probes to the detector, one considers only those related to a particular event, namely no photon loss. All information coming from many other events is rejected and in this way a piece of information depending on the input state is completely lost.

But why there should be other events? This is due to the noisy evolution suffered by the quantum states. For example, consider an interferometer pure input state ρ_ϕ that has accumulated a phase ϕ . If noise is present, it will evolve to a mixed state $\mathcal{L}(\rho_\phi)$ ⁶ that can be expressed in the following way:

$$\mathcal{L}(\rho_\phi) = c_\eta \rho_\phi + \chi_\eta(\phi), \quad (1.38)$$

where c_η is the probability that the input state remain unchanged and no photon is lost, while $\chi_\eta(\phi)$ is a term which can or not depend⁷ on the phase and correspond to further detection events in turn corresponding to the loss of one or more photons. From this term, some information about the phase can still be extracted, instead in [42] it is actually retrieved information coming from just the event that no photon is lost.

A problem of the same nature can be found in [44]: we have a MZ input state of the form $|2, 2\rangle$, so we obtain

$$|\psi_{out}\rangle = U_{\phi, MZ} |2, 2\rangle = \alpha(\phi)[|4, 0\rangle + |0, 4\rangle] + \beta(\phi)[|3, 1\rangle + |1, 3\rangle] + \gamma(\phi) |2, 2\rangle, \quad (1.39)$$

with

$$\alpha(\phi) = \sqrt{16}/6(1 - 2e^{2i\phi} + e^{4i\phi}) \quad (1.40)$$

$$\beta(\phi) = \sqrt{6}/8(1 - e^{4i\phi}) \quad (1.41)$$

$$\gamma(\phi) = 1/8(3 + 2e^{i2\phi} + 3e^{4i\phi}). \quad (1.42)$$

By observing that $\beta(\phi)$ has only the phase oscillation $e^{4i\phi}$ one computes the probability $P_{3,1}$ of detecting 3 photons on one detector and 1 photon on the

⁶We will see the effect of noise in detail in chapter 4

⁷This depends in turn on the input state, for the NOON state for example, we will see that $\chi_\eta(\phi)$ does not have a phase dependence and is completely useless.

other and vice-versa, namely $P_{1,3}$, at the output of the MZ. In fomula the probability becomes:

$$P_{3,1+1,3} = 3/8(1 - \cos 4\phi). \quad (1.43)$$

In their work, *Okamoto et al.* [44] develop a method to estimate the phase shift in which the experimenter concentrates only on this particular event neglecting the double fold coincidence that has a probability $P_{2,2} = 1/16(11 - 12 \cos 2\phi + 9 \cos 4\phi)$ or the event consisting in detecting 4 photons on one detector and viceversa that have a probability $P_{4,0+0,4} = 1/32(9 + 12 \cos 2\phi + 3 \cos 4\phi)$.

Such a measurement anyway can not be less noisy than a measurement in which it would be possible to recover information from all the events because many data containing information are not considered. Moreover, as explained in the paper, the loss of photons is not considered at all. So, if also the effect of noise at the detection stage were considered the only measurement of the event which gives the distribution $P_{3,1+1,3}$ would hardly give interesting results.

Unfortunately at the present time to have deterministic measurements seem to be pratically impossible.

We continue our work by introducing a peculiar class of quantum states widely employed in current technology which will be used in the following, namely the Gaussian states. The problem of phase estimation will be recovered in chapter 4, 5 and 6.

Chapter 2

A review on Gaussian states

This chapter will be devoted to the study of Gaussian states [30], a particular class of states widely employed in quantum optics and in quantum information processing with continuous variables. These states can be created in physical phenomena characterized by dynamical evolutions described through Hamiltonian operators at most bilinear in the field modes; such phenomena are studied in quantum non linear optics [89] and can be commonly reproduced in the laboratory. In the next chapter we will suggest a method, based on these states, to discriminate and estimate between two optical absorbers characterized by different damping constants, by means of a simple optical scheme based on the entangling property of a beam splitter for appropriate input states at fixed input energy.

2.1 Some preliminary notions

In this section some basic concepts and notations are given concerning Cartesian decomposition. For a deeper and more extensive analysis see [63].

Let us consider a system of n bosons described by the mode operators a_k , $k = 1, \dots, n$, with commutation relations $[a_k, a_l^\dagger] = \delta_{kl}$. The Hilbert space of the system $\mathcal{H} = \otimes_{k=1}^n \mathcal{F}_k$ is the tensor product of the infinite dimensional Fock spaces \mathcal{F}_k of the n modes, each spanned by the number basis $\{|m\rangle_k\}_{m \in \mathbb{N}}$, *i.e.* by the eigenstates of the number operator $a_k^\dagger a_k$. The free Hamiltonian of the system is given by $H = \sum_{k=1}^n (a_k^\dagger a_k + \frac{1}{2})$. Position- and momentum-like operators for each mode are defined through the Cartesian decomposition of the mode operators $a_k = \kappa_1 (q_k + ip_k)$ with $\kappa_1 \in \mathbb{R}$, *i.e.*

$$q_k = \frac{1}{2\kappa_1} (a_k + a_k^\dagger), \quad p_k = \frac{1}{2i\kappa_1} (a_k - a_k^\dagger). \quad (2.1)$$

The corresponding commutation relations are given by

$$[q_k, p_l] = \frac{i}{2\kappa_1^2} \delta_{kl}. \quad (2.2)$$

Canonical position and momentum operators are obtained for $\kappa_1 = 2^{-1/2}$, while the quantum optical convention corresponds to the choice $\kappa_1 = 1$. Introducing the vector of operators $\mathbf{R} = (q_1, p_1, \dots, q_n, p_n)^T$, Eq. (2.2) rewrites as

$$[R_k, R_l] = \frac{i}{2\kappa_1^2} \Omega_{kl}, \quad (2.3)$$

where Ω_{kl} are the elements of the symplectic matrix

$$\mathbf{\Omega} = \bigoplus_{k=1}^n \boldsymbol{\omega}, \quad \boldsymbol{\omega} = \begin{pmatrix} 0 & 1 \\ -1 & 0 \end{pmatrix}. \quad (2.4)$$

By a different grouping of the operators as $\mathbf{S} = (q_1, \dots, q_n, p_1, \dots, p_n)^T$, the commutation relations rewrite as

$$[S_k, S_l] = -\frac{i}{2\kappa_1^2} J_{kl}, \quad (2.5)$$

where J_{kl} are the elements of the $2n \times 2n$ symplectic antisymmetric matrix

$$\mathbf{J} = \begin{pmatrix} \mathbf{0} & -\mathbb{1}_n \\ \mathbb{1}_n & \mathbf{0} \end{pmatrix}, \quad (2.6)$$

$\mathbb{1}_n$ being the $n \times n$ identity matrix.

Analogously, for a quantum state of n bosons the *covariance matrix* is defined in the following way

$$\sigma_{kl} \equiv [\boldsymbol{\sigma}]_{kl} = \frac{1}{2} \langle \{R_k, R_l\} \rangle - \langle R_l \rangle \langle R_k \rangle, \quad (2.7a)$$

$$V_{kl} \equiv [\mathbf{V}]_{kl} = \frac{1}{2} \langle \{S_k, S_l\} \rangle - \langle S_l \rangle \langle S_k \rangle, \quad (2.7b)$$

where $\{A, B\} = AB + BA$ denotes the anticommutator and $\langle O \rangle \equiv \bar{O} = \text{Tr}[\rho O]$ is the expectation value of the operator O , ρ being the density matrix of the system.

The two vectors of operators \mathbf{R} and \mathbf{S} are related to each other through a simple $2n \times 2n$ permutation matrix $\mathbf{S} = \mathbf{P} \mathbf{R}$, whose elements are given by

$$P_{kl} = \begin{cases} \delta_{k,2l-1} & k \leq n \\ \delta_{n+k,2l} & l \leq n \end{cases}, \quad (2.8)$$

$\delta_{k,l}$ being the Krönecker delta. Correspondingly, the two forms of the covariance matrix, as well as the symplectic forms for the two orderings, are connected by

$$\mathbf{V} = \mathbf{P} \boldsymbol{\sigma} \mathbf{P}^T, \quad \mathbf{J} = -\mathbf{P} \mathbf{\Omega} \mathbf{P}^T.$$

The transformation from the Ω ordering to the \mathbf{J} ordering is called symplectic [86, 87, 88]. Now Gaussian states are introduced, some notions will be postponed in the Appendices at the end of the thesis.

We will see that such class of states embraces many quantum states widely employed in quantum optics such the coherent states $|\alpha\rangle$, the vacuum squeezed state $|\xi\rangle$ or the twin beam state $|\psi_{twb}\rangle = \sqrt{1 - |\zeta|^2} \sum_{n=0}^{\infty} \zeta^n |n\rangle |n\rangle$. The reason that allows to consider all these different states has to be found in the Gaussian form of the so called characteristic function as it will be now explained.

2.2 Gaussian states

This section is devoted to the characterization of the Gaussian states. We will analyze single and bipartite states giving some useful notion for the next chapter.

A quantum state ρ of the n bosonic modes is fully described by its characteristic function [62]

$$\chi[\rho](\boldsymbol{\lambda}) = \text{Tr}[\rho D(\boldsymbol{\lambda})] \quad (2.9)$$

where

$$D(\boldsymbol{\lambda}) = \bigotimes_{k=1}^n D_k(\lambda_k) \quad (2.10)$$

is the n -mode displacement operator, with $\boldsymbol{\lambda} = (\lambda_1, \dots, \lambda_n)^T$, $\lambda_k \in \mathbb{C}$, and where

$$D_k(\lambda_k) = \exp\{\lambda_k a_k^\dagger - \lambda_k^* a_k\}$$

is the single-mode displacement operator. We call a quantum state ρ Gaussian if its characteristic function has the Gaussian form

$$\chi[\rho](\boldsymbol{\Lambda}) = \exp\left\{-\frac{1}{2}\boldsymbol{\Lambda}^T \boldsymbol{\sigma} \boldsymbol{\Lambda} + \boldsymbol{\Lambda}^T \overline{\boldsymbol{X}}\right\} \quad (2.11)$$

where $\boldsymbol{\Lambda}$ is the real vector $\boldsymbol{\Lambda} = (\text{Re}\lambda_1, \text{Im}\lambda_1, \dots, \text{Re}\lambda_n, \text{Im}\lambda_n)^T$, $\overline{\boldsymbol{X}}$ is the vector of average values of the quadratures and $\boldsymbol{\sigma}$ is the covariance matrix. Of course, once the covariance matrix and the vector of the mean values are given, a Gaussian state is fully determined.

Note that we have introduced the cartesian coordinate as $\lambda_k = \kappa_3(\text{Re}\lambda_k + \text{Im}\lambda_k)$. A remark on parameters κ is given in appendix C. From now on we will assume $\kappa_h = \frac{1}{\sqrt{2}}$, $h = 1, 2, 3$.

Thanks to an important theorem, due to Williamson [90] it is possible to express every Gaussian state ρ as

$$\rho = U \nu U^\dagger, \quad (2.12)$$

where $\nu = \nu_1 \otimes \dots \otimes \nu_n$ is a product of single mode thermal states

$$\nu_k = (1 + N_k)^{-1} \sum_{n=0}^{\infty} (N_k / (1 + N_k))^n |n\rangle \langle n| \quad (2.13)$$

and U is a particular class of unitary transformations which in turn can be generated by linear and bilinear interactions. Examples of such unitary transformations are given by the unitary displacement and by the squeezing operators. We will see in one of the next section the explicit expression of the most general single mode Gaussian state, but first an important condition for the purity must be given.

2.2.1 Purity of Gaussian states

If we recall the definition of purity:

$$\mu = \text{Tr}[\rho^2] \quad (2.14)$$

for a Gaussian states it can be proved that:

$$\mu = \frac{1}{(2\kappa_2)^{2n} \sqrt{\text{Det}[\boldsymbol{\sigma}]}}. \quad (2.15)$$

So a Gaussian state is pure iff:

$$\text{Det}[\boldsymbol{\sigma}] = (2\kappa_2)^{-4n}. \quad (2.16)$$

In appendix B we will see how to compute the quantity (2.14) which actually involves integrations in the phase space because the characteristic function is taken into account. This computational technique will be widely employed in the next chapter.

Now the form of the single mode Gaussian states will be introduced.

2.2.2 Single mode Gaussian state

The decomposition (2.12) in this case becomes:

$$\rho_G = D(\alpha)S(\zeta)\nu S^\dagger(\zeta)D^\dagger(\alpha), \quad (2.17)$$

$D(\alpha)$ being the displacement operator (2.10), $S(\zeta) = \exp[\frac{1}{2}\zeta(a^\dagger)^2 - \frac{1}{2}\zeta^*a^2]$ is the squeezing operator, $\alpha, \zeta \in \mathbb{C}$, with $\zeta = re^{i\varphi}$, $r = |\zeta|$ and ν is a thermal state with N average number of photons (see Eq. (2.13)).

The explicit expression for the covariance matrix elements are:

$$\sigma_{11} = \frac{2N+1}{2} \left[\cosh(2r) + \sinh(2r) \cos(\varphi) \right], \quad (2.18a)$$

$$\sigma_{22} = \frac{2N+1}{2} \left[\cosh(2r) - \sinh(2r) \cos(\varphi) \right], \quad (2.18b)$$

$$\sigma_{12} = \sigma_{21} = -\frac{2N+1}{2} \sinh(2r) \sin(\varphi). \quad (2.18c)$$

From condition (2.16) it is possible to evaluate the expression for purity

$$\mu = (2N+1)^{-1},$$

from which we observe that the purity of a generic Gaussian state only depends on the average number of thermal photons, as one should expect since displacement and squeezing are unitary operations and they do not affect the value of the trace in Eq. (2.14).

Examples of the most important families of single mode Gaussian states are immediately derived considering Eq. (2.17): thermal states ν are obtained for $\alpha = r = \varphi = 0$, coherent states for $r = \varphi = N = 0$, while squeezed vacuum states are recovered for $\alpha = N = 0$. For $N = 0$ we have the vacuum and coherent states covariance matrix. The covariance matrix associated with the real squeezed vacuum state is recovered for $\varphi = 0$ and is given by $\sigma = \frac{1}{2}\text{Diag}(e^{-2r}, e^{2r})$.

2.2.3 Bipartite Gaussian states

Bipartite systems are the simplest scenario for investigation the fundamental issue of the entanglement in quantum information. Here, we are not interested in finding the most general covariance matrix¹: for our purpose it will be enough to consider 4×4 covariance matrices for a *separable* bipartite pure input state $\rho = \rho_A \otimes \rho_B$ of the following form:

$$\begin{pmatrix} A & 0 \\ 0 & B \end{pmatrix}, \quad (2.19)$$

where A and B are respectively the 2×2 covariance matrices of the single mode states ρ_A and ρ_B . Such initial form of Eq. (2.19) will be transformed by means of optical devices which will introduce entanglement and noise. We will see this in next chapter.

It is worth stressing that entanglement is not changed by local operations and that the vectors of the mean values $\overline{\mathbf{X}}$ appearing in the expressions Eq. (2.11) can be changed arbitrarily by phase-space translations, which are in turn local operations. So, Gaussian states are entirely characterized by their covariance matrix. This is a very relevant property of Gaussian states since it means that typical issues in continuous variables quantum information theory, which are generally difficult to handle in an infinite Hilbert space, can be analyzed with the help of finite matrix theory.

We conclude this brief section by recalling a particular subclass of Gaussian states constituted by the two mode squeezed thermal states:

$$\rho = S_2(\zeta) \rho_\nu S_2^\dagger(\zeta), \quad \rho_\nu = \nu_A \otimes \nu_B, \quad (2.20)$$

where ν_k , $k = A, B$, are thermal states with mean photon number N_1 and N_2 respectively.

After this short overview on Gaussian states, we can describe their behaviour under noisy channel making use of the results coming from the subject of the evolution of open quantum system in the Born-Markov approximation.

¹It should be now clear to the reader that it is more important to know the form of the covariance matrix than the density operator itself.

2.3 Noisy evolution of gaussian states

We are interested in the propagation of the modes of radiation (the *system*) in a noisy channel represented by a dissipative medium characterized by a damping parameter Γ .

Following the common way to describe damping of an electromagnetic field consisting in the coupling of each mode of the field to a reservoir of many modes, the evolution of the density matrix describing the radiation is obtained. This is the well known result regarding the derivation of the master equation [68, 67] in the Born-Markov approximation in the zero temperature limit². For a bipartite state in which one of the two modes suffers the noisy evolution³ we have:

$$\dot{\rho}(t) = \sum_{k=1}^2 (-i\omega[\hat{a}_k^\dagger \hat{a}_k, \rho]) + \frac{\Gamma}{2} (2\hat{a}_1 \rho \hat{a}_1^\dagger - \hat{a}_1^\dagger \hat{a}_1 \rho - \rho \hat{a}_1^\dagger \hat{a}_1) \quad (2.21)$$

After some manipulations [63] it is possible to obtain the covariance matrix and the mean values vector of the evolved state. For a single mode gaussian state, the mean values vector \mathbf{x} and the evolved covariance matrix $\boldsymbol{\sigma}$ at time t read as [63]:

$$\mathbf{x}(t) = \mathbb{G}_\eta^{1/2} \mathbf{x}(0), \quad (2.22)$$

$$\boldsymbol{\sigma}(t) = \mathbb{G}_\eta^{1/2} \boldsymbol{\sigma}(0) \mathbb{G}_\eta^{1/2} + (\mathbb{1}_2 - \mathbb{G}_\eta) \boldsymbol{\sigma}_\infty \quad (2.23)$$

where $\mathbb{G}_\eta = e^{-\eta} \mathbb{1}_2$, with $\eta \equiv \Gamma t$, $\boldsymbol{\sigma}_\infty = \frac{1}{2} \mathbb{1}_2$ is the asymptotic covariance matrix defined as the covariance matrix of the state after an interaction time $t \rightarrow \infty$ (corresponding to the covariance matrix of the vacuum) and $\mathbb{1}_m$ is the $m \times m$ identity matrix.

The above results can be extended to the evolution of an arbitrary n -mode Gaussian state in noisy channels [63], the mean values vector becomes:

$$\mathbf{X}(t) = \mathbb{G}^{1/2} \mathbf{X}(0) \quad \text{with} \quad \mathbb{G} = \bigoplus_{h=1}^n e^{-\Gamma h t} \mathbb{1}_2, \quad (2.24)$$

while the covariance matrix $\boldsymbol{\Sigma}(t)$ at time t is given by:

$$\boldsymbol{\Sigma}(t) = \mathbb{G}^{1/2} \boldsymbol{\Sigma}(0) \mathbb{G}^{1/2} + (\mathbb{1} - \mathbb{G}) \boldsymbol{\Sigma}_\infty. \quad (2.25)$$

Equation (2.25) describes the evolution of an initial Gaussian state $\boldsymbol{\Sigma}$ into the Gaussian environment $\boldsymbol{\Sigma}_\infty$ showing that the evolution preserves the Gaussian character of the state.

We have now the instruments necessary to clearly understand the study of the next chapter. We will consider the behaviour of some pure Gaussian states when exploited in extracting information on the damping constant of dissipative media. The above description of noisy evolution will be used to describe the dissipative medium which the radiation encounters.

²Since we are considering optical modes, the zero temperature assumption is reasonable.

³This will be the case under consideration in the next chapter.

Chapter 3

Interferometry with Gaussian states

Entanglement can be a resource because interesting results in the optical domain can be retrieved in binary communication and state discrimination [59, 60] to name but a few. The interferometric apparatus can be exploited also to retrieve information about damping constants and so it can be used to characterize dissipative media. Thanks to entangled light the estimation and the discrimination of two such constants can be more precise than in the cases in which non-entangled quantum state or classical state are employed.

It must be however said that for a deep understanding of the role of entanglement, the QET should be called into question, an in-depth study of which has been developed only in the last few years. For the damping constants a rudimental estimation method has been proposed by H. Venzel and M. Freyberger in [64]. There it is shown how an entangled state can give in principle better results than a scheme in which either classical light and or a state presenting only quantum superposition is employed.

This chapter is devoted to presenting an original method to attest the usefulness of entangled Gaussian states in a possible process of estimation or discrimination of two media characterized by different damping constants in which the input signal interacts several times with the damping media.

3.1 Set-up dynamics

In this section we describe the evolution of the Gaussian input states inside an optical set-up consisting of one Beam Splitter and a dissipative medium.

Let's consider the following two situations in which:

- a pure single mode gaussian state described by density operator $\rho_{\text{in}} = |\alpha, \zeta\rangle\langle\alpha, \zeta|$ enters a ring cavity where a medium characterized by a damping parameter Γ is placed, Fig. (3.1) top.

- a pure two mode gaussian state described by the operator $\omega_{\text{in}} = \rho_{\text{in}} \otimes \rho_0$ is a beam splitter input state, $\rho_0 = |0\rangle\langle 0|$ being the vacuum density operator. Along the path of the transmitted field we put the damping media and the ring cavity, Fig. (3.1) bottom.

Our aim is to compare the two setups for fixed energy impinging on the medium, as we will show in section 3.2, in order to see if the entangler¹ property of the beam splitter can improve the ability to discriminate between two different media characterized by two damping constant Γ_1 and Γ_2 .

After N cycles, that is, after the field has interacted with the medium N times, one obtains the output states ρ_{out} and ω_{out} coming out the cavity thanks to an optical switch, respectively for single mode and two mode gaussian state.

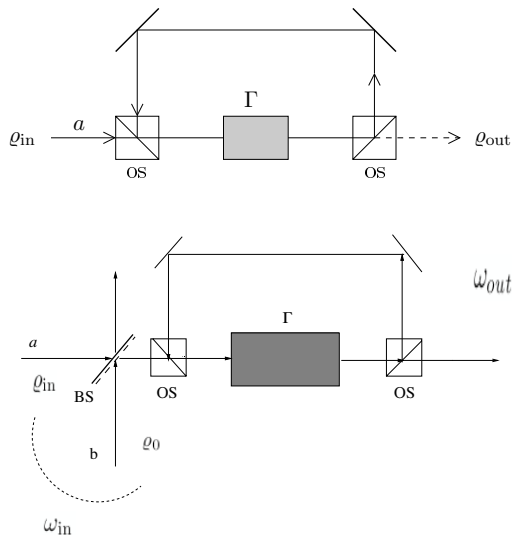


Figure 3.1: experimental setup for the discrimination of absorbers. Top: scheme for a single mode gaussian state entering directly the dissipative medium. Bottom: one mode of squeezed radiation impinges on a beam splitter of transmissivity τ and the transmitted field reaches the same medium employed in the simpler single mode case.

For the system concerning single mode gaussian state, we have an output state (see section 2.3), characterized by covariance matrix and mean values

¹Note that in order to obtain non classicality and so entanglement in the output state of a beam splitter, non classicality is needed in input as can be seen in [66]

3.1. Set-up dynamics

vector given by the following recursive formulas:

$$\begin{aligned}\boldsymbol{\sigma}_N(\eta) &\equiv \mathbb{S}_\eta[\boldsymbol{\sigma}_{N-1}(\eta)], \\ \mathbf{x}_N(\eta) &\equiv \mathbb{T}_\eta[\mathbf{x}_{N-1}(\eta)],\end{aligned}$$

where

$$\begin{aligned}\mathbb{S}_\eta[\boldsymbol{\sigma}] &\equiv \boldsymbol{\sigma} \rightarrow \boldsymbol{\sigma}(\eta) = \mathbb{G}_\eta^{1/2} \boldsymbol{\sigma} \mathbb{G}_\eta^{1/2} + (\mathbb{1}_2 - \mathbb{G}_\eta) \boldsymbol{\sigma}_\infty, \\ \mathbb{T}_\eta[\mathbf{x}] &\equiv \mathbf{x} \rightarrow \mathbf{x}(\eta) = \mathbb{G}_\eta^{1/2} \mathbf{x},\end{aligned}$$

and $\boldsymbol{\sigma}_0(\eta) = \boldsymbol{\sigma}_{\text{in}}$ and $\mathbf{x}_0(\eta) = \mathbf{x}_{\text{in}}$.

Let us now focus our attention to the two-mode product state: $\omega_{\text{in}} = \rho_{\text{in}} \otimes \rho_0$.

After the state has been passed through the BS and through the medium for the first time, the covariance matrix and the mean values vector become:

$$\begin{aligned}\boldsymbol{\Sigma}_{\text{in}} &\rightarrow \boldsymbol{\Sigma}_1(\eta) \equiv \mathbb{U}_\Gamma[\mathbf{S}_\tau^T \boldsymbol{\Sigma}_{\text{in}} \mathbf{S}_\tau], \\ \mathbf{X}_{\text{in}} &\rightarrow \mathbf{X}_1(\eta) \equiv \mathbb{V}_\Gamma[\mathbf{S}_\tau^T \mathbf{X}_{\text{in}}],\end{aligned}$$

where

$$\mathbf{S}_\tau = \begin{pmatrix} \sqrt{\tau} \mathbb{1}_2 & -\sqrt{1-\tau} \mathbb{1}_2 \\ \sqrt{1-\tau} \mathbb{1}_2 & \sqrt{\tau} \mathbb{1}_2 \end{pmatrix}, \quad (3.1)$$

is the symplectic matrix associated to the BS with transmissivity τ and

$$\begin{aligned}\mathbb{U}_\eta[\boldsymbol{\Sigma}] &\equiv \boldsymbol{\Sigma} \rightarrow \boldsymbol{\Sigma}(\eta) = \mathbb{G}_\eta^{1/2} \oplus \mathbb{1}_2 \boldsymbol{\Sigma} \mathbb{G}_\eta^{1/2} \oplus \mathbb{1}_2 + (\mathbb{1}_4 - \mathbb{G}_\eta \oplus \mathbb{1}_2) \boldsymbol{\Sigma}_\infty, \\ \mathbb{V}_\eta[\mathbf{X}] &\equiv \mathbf{X} \rightarrow \mathbf{X}(\eta) = \mathbb{G}_\eta^{1/2} \oplus \mathbb{1}_2 \mathbf{X},\end{aligned}$$

with $\eta = \Gamma t$ and $\boldsymbol{\Sigma}_\infty$ is the asymptotic covariance matrix.

After N cycles, the two-mode output state is characterized by a covariance matrix and a mean values vector given by the following formulas:

$$\begin{aligned}\boldsymbol{\Sigma}_N(\eta) &\equiv \mathbb{U}_\Gamma^N[\mathbf{S}_\tau^T \boldsymbol{\Sigma}_{\text{in}} \mathbf{S}_\tau], \\ \mathbf{X}_N(\eta) &\equiv \mathbb{V}_\Gamma^N[\mathbf{S}_\tau^T \mathbf{X}_{\text{in}}],\end{aligned}$$

We remind that in the case of such factorized Gaussian state: $\omega_{\text{in}} = \rho_{\text{in}} \otimes \rho_0$, the covariance matrix looks like:

$$\boldsymbol{\Sigma}_{\text{in}} = \boldsymbol{\sigma}_{\text{in}} \otimes \boldsymbol{\sigma}_0$$

and $\boldsymbol{\sigma}_0 = \frac{1}{2} \mathbb{1}_2$.

It is worth noticing that for this last case we could have employed a Mach-Zehnder interferometer, anyway to see whether entanglement could be a fruitful resource in the process of discriminating, the final beam splitter of a Mach-Zehnder interferometer is not necessary, as we will see in the next section.

3.2 Hilbert-Schmidt distance

The criterion we will adopt to see if an entangled state can be useful in the process of discrimination is the following: initially we consider the expression of the output state emerging from the set-up of Fig. (3.1) when a medium characterized by damping constant Γ_1 is inserted. Then, with the same input state, the procedure is repeated with another medium with a different constant damping Γ_2 . We find the form of these two Gaussian states. Specifically, we find the form of their covariance matrices, as explained in Chapter 2, and we compare them by quantifying their “similarity” through the *Hilbert-Schmidt distance* (HS) [69], which is defined as:

$$d(\rho_1, \rho_2) := \frac{1}{2} \text{Tr}(\rho_1 - \rho_2)^2 = \frac{\mu[\rho_1] + \mu[\rho_2] - 2\kappa[\rho_1, \rho_2]}{2}, \quad (3.2)$$

with $\mu[\rho_i] = \text{Tr}[\rho_i^2]$, $i = 1, 2$ and $\kappa[\rho_2, \rho_1] = \text{Tr}[\rho_1 \rho_2]$ denoting the purity of ρ and the overlap between ρ_1 and ρ_2 , respectively. Recalling expression (2.11) for the characteristic function of a gaussian state, Eqs. (2.15) and the following property

$$\int d^n \mathbf{X} \exp\left\{-\frac{1}{2} \mathbf{X}^T Q^{-1} \mathbf{X} + i \mathbf{\Lambda}^T X\right\} = \sqrt{(2\pi)^n \text{Det}[Q]} \exp\left\{-\frac{1}{2} \mathbf{\Lambda}^T Q \mathbf{\Lambda}\right\}, \quad (3.3)$$

valid for any symmetric positive-definite matrix $Q \in M(n, \mathcal{R})$, we get

$$\text{Tr}[\rho_i^2] = \frac{1}{2^n \sqrt{\text{Det}[\boldsymbol{\sigma}_i]}}.$$

Concerning the overlap, from Eq. (B.4)

$$\begin{aligned} \text{Tr}[\rho_1 \rho_2] &= \int \frac{d^{2n} \mathbf{\Lambda}}{(2\pi)^n} \chi[\rho_1](\mathbf{\Lambda}) \chi[\rho_2](-\mathbf{\Lambda}) = \\ &= \int \frac{d^{2n} \mathbf{\Lambda}}{(2\pi)^n} \exp\left\{-\frac{1}{2} \mathbf{\Lambda}^T \boldsymbol{\sigma}_1 \mathbf{\Lambda} + i \mathbf{\Lambda}^T \overline{X}_1\right\} \exp\left\{-\frac{1}{2} \mathbf{\Lambda}^T \boldsymbol{\sigma}_2 \mathbf{\Lambda} - i \mathbf{\Lambda}^T \overline{X}_2\right\} = \\ &= \int \frac{d^{2n} \mathbf{\Lambda}}{(2\pi)^n} \exp\left\{-\frac{1}{2} \mathbf{\Lambda}^T (\boldsymbol{\sigma}_1 + \boldsymbol{\sigma}_2) \mathbf{\Lambda} + i \mathbf{\Lambda}^T (\overline{X}_1 - \overline{X}_2)\right\} = \\ &= \frac{\exp\left\{-1/2 (\overline{X}_1 - \overline{X}_2)^T (\boldsymbol{\sigma}_1 + \boldsymbol{\sigma}_2)^{-1} (\overline{X}_1 - \overline{X}_2)\right\}}{\sqrt{\text{Det}[\boldsymbol{\sigma}_1 + \boldsymbol{\sigma}_2]}}. \end{aligned}$$

We can now write the expression of HS distance between two generic n-mode gaussian states:

$$\begin{aligned} d(\rho_1, \rho_2) &= \frac{1}{2} \left(\frac{1}{2^n \sqrt{\text{Det}[\boldsymbol{\sigma}_1]}} + \frac{1}{2^n \sqrt{\text{Det}[\boldsymbol{\sigma}_2]}} \right. \\ &\quad \left. - 2 \frac{\exp\left[-1/2 (\overline{X}_1 - \overline{X}_2)^T (\boldsymbol{\sigma}_1 + \boldsymbol{\sigma}_2)^{-1} (\overline{X}_1 - \overline{X}_2)\right]}{\sqrt{\text{Det}[\boldsymbol{\sigma}_1 + \boldsymbol{\sigma}_2]}} \right). \end{aligned} \quad (3.4)$$

3.2. Hilbert-Schmidt distance

The analytic expression of HS for the single mode state in the case we are considering reads as follows

$$d(\rho(\eta_1), \rho(\eta_2)) = \frac{1}{2} \left(\frac{1}{2\sqrt{\text{Det}[\boldsymbol{\sigma}_N(\eta_1)]}} + \frac{1}{2\sqrt{\text{det}[\boldsymbol{\sigma}_N(\eta_2)]}} - \frac{2 \exp[-1/2(\mathbf{x}_N(\eta_1) - \mathbf{x}_N(\eta_2))^T (\boldsymbol{\sigma}_N(\eta_1) + \boldsymbol{\sigma}_N(\eta_2))^{-1} (\mathbf{x}_N(\eta_1) - \mathbf{x}_N(\eta_2))] }{\sqrt{\text{det}[\boldsymbol{\sigma}_N(\eta_1) + \boldsymbol{\sigma}_N(\eta_2)]}} \right),$$

$\rho(\eta_k)$, $k = 1, 2$, being the state outgoing the ring cavity after N interactions with the dissipative medium with damping parameter η_k .

For the two mode case:

$$d(\omega(\eta_1), \omega(\eta_2)) = \frac{1}{2} \left(\frac{1}{4\sqrt{\text{Det}[\boldsymbol{\Sigma}_N(\eta_1)]}} + \frac{1}{4\sqrt{\text{Det}[\boldsymbol{\Sigma}_N(\eta_2)]}} - \frac{2 \exp[-1/2(\mathbf{X}_N(\eta_1) - \mathbf{X}_N(\eta_2))^T (\boldsymbol{\Sigma}_N(\eta_1) + \boldsymbol{\Sigma}_N(\eta_2))^{-1} (\mathbf{X}_N(\eta_1) - \mathbf{X}_N(\eta_2))] }{\sqrt{\text{Det}[\boldsymbol{\Sigma}_N(\eta_1) + \boldsymbol{\Sigma}_N(\eta_2)]}} \right),$$

$\omega(\eta_k)$, $k = 1, 2$, being the output state after N cycles.

If we consider the squeezed state $|\beta, \zeta\rangle$ as input states for the scheme in Fig. (3.1) top and $|\alpha, \xi\rangle$ for the one in Fig. (3.1) bottom, the total energy impinging on the medium is respectively:

$$E_0 = |\beta|^2 + \sinh^2 s \quad (3.5)$$

$$\mathcal{E}_0 = (|\alpha|^2 + \sinh^2 r) \tau \quad (3.6)$$

where we put $|\zeta| = s$ and $|\xi| = r$. In order to compare the two different schemes for fixed *total* energy absorbed by the lossy medium, we should have $E_0 = \mathcal{E}_0$. We address the following way to equate the energies: fixing $|\alpha|$ and r and putting $|\beta| = \sqrt{\tau}|\alpha|$ and $s = \sinh^{-1}[\sqrt{\tau} \sinh s]$. In Figs. (3.2) and (3.3) the behaviour of HS for a vacuum squeezed state as input state for both cases is plotted. As it can be seen from Fig. (3.2), the entanglement of the emerging state from the beam splitter increases the distance between two output states with respect to the distance between the input single mode gaussian states in the range of low trasmissivity τ .

Let's see in detail this behaviour of HS in the case of vacuum squeezed input state: for $\tau \rightarrow 0$ we have:

$$d(\rho(\eta_1), \rho(\eta_2)) = \frac{1}{2} \sinh^2 r (G_1^N - G_2^N)^2 \tau + o(\tau) \quad (3.7)$$

$$d(\omega(\eta_1), \omega(\eta_2)) = \sinh^2 r (\sqrt{G_1^N} - \sqrt{G_2^N})^2 \tau + o(\tau), \quad (3.8)$$

where $G_i = e^{-\eta_i}$. Calling $G_1 = G$, $G_2 = G + \delta G$ with $\delta G \simeq 0$ it is possible to rewrite the distances in this way:

$$d(\rho(\eta_1), \rho(\eta_2)) = \frac{1}{2} N^2 G^{2N} \left(\frac{\delta G}{G}\right)^2 \tau \sinh^2 r + o(\tau) \quad (3.9)$$

$$d(\omega(\eta_1), \omega(\eta_2)) = \frac{1}{4} N^2 G^N \left(\frac{\delta G}{G}\right)^2 \tau \sinh^2 r + o(\tau), \quad (3.10)$$

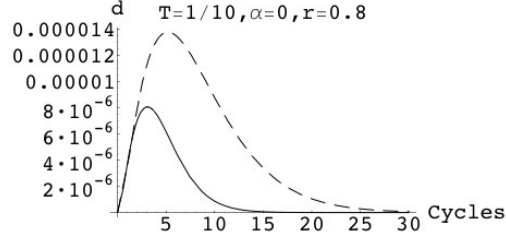


Figure 3.2: Plot of the HS-distances versus the number N of times the signal passes through the lossy media, for fixed total energy impinging on the medium (solid line refers to single mode gaussian state), in the case of vacuum squeezed state as input states. We set $\Gamma_2 = 0.71$ and $\Gamma_2 = 0.7$.

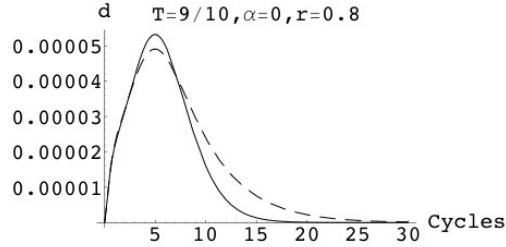


Figure 3.3: Plot of the HS-distances versus the number N of times the signal passes through the lossy media, for fixed total energy impinging on the medium (solid line refers to single mode gaussian state), in the case of vacuum squeezed as input states. We set $\Gamma_1 = 0.71$ and $\Gamma_2 = 0.7$. In this case both schemes are almost identical, if the transmissivity is one, the superposition of the curves is obtained. The result shows that, in the regime of high values of trasmissivity, there is no utility of entanglement.

from these expression it follows:

$$\frac{d(\omega(\eta_1), \omega(\eta_2))}{d(\rho(\eta_1), \rho(\eta_2))} \simeq \frac{1}{2G^N}. \quad (3.11)$$

This term is larger than 1 when N is not bigger than a threshold value: $N_{th} \simeq \frac{-\log 2}{\log G}$. We can also find out the analytic expressions for the N maximum in this approximation

$$N_{1 \text{ mode}} \simeq -\frac{1}{\log G} \quad (3.12)$$

$$N_{2 \text{ mode}} \simeq -\frac{2}{\log G} \quad (3.13)$$

3.2. Hilbert-Schmidt distance

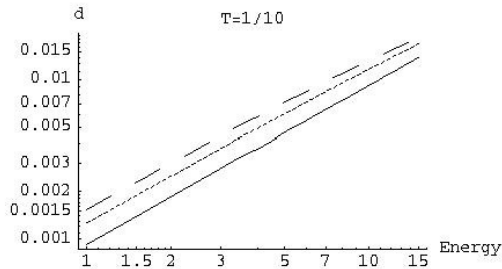


Figure 3.4: Bi-logarithmic plot of the two mode HS-distances optimized over the number of cycles versus the total energy impinging on the medium from Eq. (3.6). From bottom to top is $\gamma = 0.05, 0.5, 0.88$. So increasing squeezing is useful to achieve better discrimination between the two states.

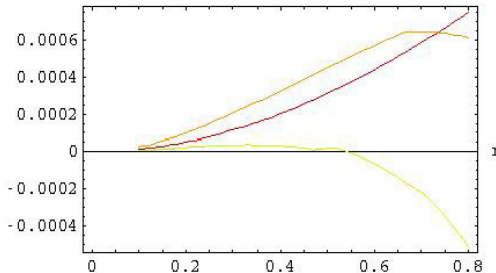


Figure 3.5: Vacuum squeezed input states for single mode and bipartite gaussian states employed in the set-up of figure (3.1): the number of cycles for which the HS reaches its maximum for both cases has been considered. Then the difference between these maximum values has been plotted as a function of the squeezed energy $\sinh^2 r$, see Eq. (3.6). Curve going through negative region is with $\tau = 0.9$. Red curve is for $\tau = 0.1$. This confirms the fact that for low transmissivity it is always convenient increasing squeezing energy for a vacuum squeezed state. The curve intersects the red one for $\tau = 0.5$.

and we observe that these last expressions are both smaller than N_{th} . This means that when we consider the optimized Hilbert Schmidt distance, i.e when we take the value for which the distances reach the maximum N , in the limit of low τ we can discriminate between two damping constants in cases in which very few photons reach the dissipative medium. We can interpret this result in the direction of a continuous variable version of the so called *Interaction Free Measurement* [70] for the fact that the interaction with the dissipative medium is kept low, see Fig. (3.2) for details. Moreover, our set-up, which is very similar to the one proposed in [64], could be also used in the process of estimation of the damping constant Γ .

In Fig. (3.4) it is shown how increasing squeezing energy can give bet-

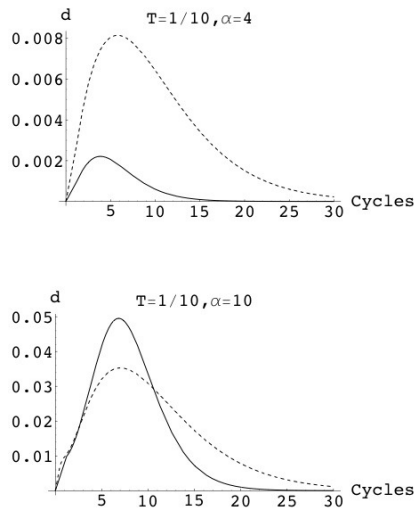


Figure 3.6: HS-distance as a function of cycles for the *cat state* $N_\alpha(|\frac{i\alpha}{2}\rangle + |-\frac{i\alpha}{2}\rangle)$ as input states for our experimental apparatus of Fig. (3.1). N_α is a suitable normalization constant. Dashed line is for bipartite state, continuous line is for *cat state* entering directly the dissipative medium. Note that increasing energy in this case destroys the effect of entanglement.

ter performances when the two mode gaussian state case is considered. The following parametrization has been assumed:

$$E_{tot} = (1 - \gamma)E_{tot} + \gamma E_{tot} \quad (3.14)$$

with $E_{tot} = |\alpha|^2 + \sinh^2 r$ and $\gamma = \frac{\sinh^2 r}{|\alpha|^2 + \sinh^2 r}$. Recalling Eq. (3.6) it is important to point out that $E_{tot} = \frac{\varepsilon_0}{\tau}$.

We finally recall that the use of Gaussian states makes the experimental realization more feasible than the cases in which other quantum states, as for example linear superposition of coherent state, the so called (not normalized) *cat state*,

$$\left| \frac{i\alpha}{2} \right\rangle + \left| \frac{-i\alpha}{2} \right\rangle,$$

are employed [64, 65]. In Fig. (3.6) the behaviour of this state for which the HS has been analitically evaluated is also shown.

3.3 Uhlman's fidelity

A further study to evaluate the similarity between the states has been performed by means of the Uhlman's fidelity [81]. In this case we have considered

3.3. Uhlman's fidelity

only one state entering the medium, the other one is assumed to remain pure, namely we have worked in the regime: $\Gamma_1 = \Gamma$ and $\Gamma_2 = 1$.

Uhlman's fidelity between two quantum states ρ_1, ρ_2 is defined as:

$$F(\rho_1, \rho_2) := \text{Tr}[\sqrt{\sqrt{\rho_1}\rho_2\sqrt{\rho_1}}]^2. \quad (3.15)$$

Such a quantity is very important in quantum information theory for which a fundamental problem is to define an upper limit (the channel capacity) to the amount of quantum information that can be transmitted with an arbitrarily highly fidelity.

Morover it can be employed to build the *Bures' distance*

$$d_B(\rho_1, \rho_2) := [2 - 2\sqrt{F(\rho_1, \rho_2)}]^{1/2}$$

which is a quantity used to evaluate the distance between two quantum states in the Hilbert space. For two pure states, the HS distance and the Bures' distance are identical.

As said, we can perform a study similar to the one performed in the previous sections and we can interpret the behaviour of the fidelity as an evaluation of similarity between two states in the Hilbert space.

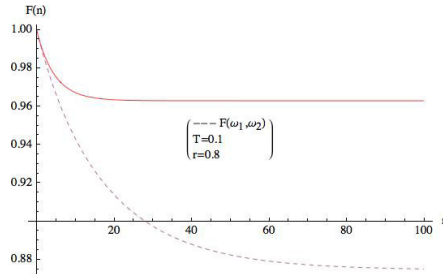


Figure 3.7: Fidelity as a function of cycles: dashed curve is two mode gaussian state. Continuous line is the single mode Gaussian state. $T = 0.1$

Now some properties follow:

1. $F(\rho_1, \rho_2) \leq 1$ and $F(\rho_1, \rho_2) = 1$ if and only if $\rho_1 = \rho_2$;
2. $F(\rho_1, \rho_2) = F(\rho_2, \rho_1)$;
3. If ρ_1 is a pure state, $\rho_1 = |\psi_1\rangle\langle\psi_1|$ then
 $F(\rho_1, \rho_2) = \langle\psi_1|\rho_2|\psi_1\rangle$;
4. $F(\rho_1, \rho_2)$ is invariant under unitary transformations on the state space;

Since the computation of the $\sqrt{\rho}$ factor in the continuous variable domain is quite often very demanding, few concrete examples of analytic calculations are

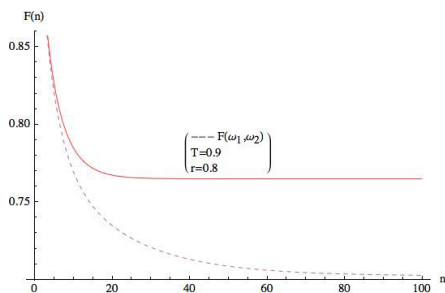


Figure 3.8: Fidelity as a function of cycles: dashed curve is two mode gaussian state. Continuous line is single mode Gaussian state. $T = 0.9$

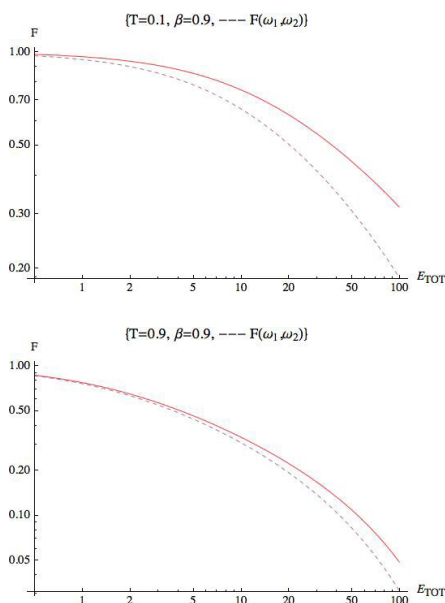


Figure 3.9: Optimized Fidelity over number of cycles as a function of total Energy: dashed curve is two mode gaussian state. Continuous line is single mode Gaussian state. Again in the case of high transmissivity the distance between the two bipartite states is bigger than the one for single mode. $\beta = \frac{\sinh^2 r}{|\alpha|^2 + \sinh^2 r}$, see parametrization of Eq. (3.14).

known. For multimode thermal squeezed states the fidelity has been calculated by *Gh.-S. Paraoanu et al.* [72].

We are interested in the case in which one of the two states remains pure.

3.4. Concluding remarks

Going back to Gaussian states, the Uhlman's fidelity reads:

$$F(\rho_1, \rho_2) = \langle \psi_1 | \rho_2 | \psi_1 \rangle = \frac{1}{\sqrt{\text{Det}[\boldsymbol{\sigma}_1 + \boldsymbol{\sigma}_2]}} \quad (3.16)$$

where $\boldsymbol{\sigma}_i, i = 1, 2$ are covariance matrices. By evaluating the fidelity, it seems that the behaviour we found by exploiting the HS extends also for the values of transmissivity τ ranging from 0 to 1, namely the fidelity curve for the scheme involving the two mode Gaussian state is always below the curve for the single mode state, see Figs. (3.7), (3.8) and (3.9). Unfortunately, specializing the study, which in the previous section was performed with the HS distance, to the fidelity is not a simple task, due to some technicality encountered when two mixed states are involved in the computation of the fidelity itself. Some remarks will be now given.

3.4 Concluding remarks

Exploiting our simple set up of fig. (3.1), we have studied the behaviour of the HS as a function of the number of times the radiation enters the medium. We have fixed the energy impinging on the medium and compared two different cases: single mode vacuum squeezed state and single mode vacuum squeezed state mixed with vacuum by means of a beam splitter. From the comparison, it results that in the particular regime of low transmissivity τ , entanglement makes the HS bigger than what can be obtained for the single vacuum squeezed state. This fact leads to another important result, *i.e.*: if τ is kept low, we may discriminate between two damping parameters even if the radiation does not interact so much with the medium, analogously to what happens in the fundamental task of the so called *Interaction free measurement* [71].

Moreover we note that, contrarily to the single mode case, with the entangled Gaussian state, one does not exploit the interaction of the radiation field with the medium, but the increased entanglement due to the presence of the beam splitter: if entanglement is present, it is possible to obtain more information about the damping constant by having few interaction between the field and the medium!

Once again we discover the intriguing and special behaviour of entangled quantum states.

At this point, we will turn to discrete variable domain and we will deal with the problem of estimation in bosonic systems.

Chapter 4

Quantum metrology with loss in Bosonic systems

Typical quantum \sqrt{N} enhancement predicted by quantum estimation theory is the main contribution given by quantum effects (such as squeezing and entanglement). When estimating an unknown parameter in a quantum system we typically prepare a probe and let it interact with the system and then we measure the probe. Once the dynamics of the system is known, it is possible to deduce the value of the parameter by comparing the input and the output state of the probe. It is well known that quantum states are rarely distinguishable with certainty. For this reason there is always an inherent statistical uncertainty in estimation.

If N identical independent probes are used and the results coming from each single probe are averaged, from the central limit theorem we have that the error on the average decreases as $1/\sqrt{N}$. Exploiting the same physical resources with the addition of quantum effects, a better precision can often be achieved with a customary \sqrt{N} enhancement, *i.e.* a scaling of $1/N$. Unfortunately, to fully exploit such resources, it is not a simple task when loss is introduced.

As it will be explained in section 4.3 of this chapter, with an N photons maximally path entangled state, called NOON state, it is possible to achieve and saturate the Heisenberg limit, *i.e.* the scale law of the minimum phase error:

$$\delta\phi_{min} = 1/N, \tag{4.1}$$

but if we look at how the pure NOON state evolves under a lossy map, we will see how crucial is the loss of only a single photon [29, 33], revealing the high sensitivity of this state to the noisy map.

It is tempting to attribute this behaviour to the fact that we are considering a maximally entangled state, but for our case, namely Fock state interferometry [43], we will see that this intuition is not true in general.

We are going to deal with bosonic systems, so our probes will be photons and the NOON state will be characterized by path entanglement. Moreover

there will be a further correlation between the probes due to their *coexistence* in a Fock state (as we will see), a correlation that is not considered in standard quantum metrology. In [27] the treatment is performed with qubits, and the most natural way to encode logical information in physical system is by means of *dual railing encoding* [81] in which the logical bit is encoded in a two mode Fock state, where one of two mode is populated by exactly one photon, while the other mode is left in the vacuum state.

In such a framework, we will see (section 4.5) that being maximally entangled could be a resource for a state if noise is considered, contrary to what was pointed out, for example, in [54] and to what is general assumed in the literature.

4.1 Physical information encoding

In this section we will deal with the problem of physical encoding, starting from the description of the *dual railing code*, we will see how logical information can be encoded in optical systems.

Logical information must be encoded in physical systems. In quantum information theory information is carried by qubits and an example of physical information encoding is the *dual railing encoding* [81].

We express the formal equivalence:

$$|0\rangle \equiv |1, 0\rangle_{a,b} \quad (4.2)$$

$$|1\rangle \equiv |0, 1\rangle_{a,b} . \quad (4.3)$$

With this particular encoding two field modes (labelled by a and b) are employed, and they can be populated only by one particle or left in the vacuum state. Such encoding is widely employed in quantum information theory since it permits to reproduce logical algorithms and operations performed on qubits in real systems. An example is the realization of C-NOT gate by means of Kerr-media (see [81] chapter 7). Moreover, in a recent work [37], a method to obtain maximally multipartite entangled states has been proposed exploiting such encoding with polarization modes by means of QND measurements.

Suppose now to have a N -qubit system. It is possible to make the following equivalence which is not an encoding anyway:

$$|0\rangle^{\otimes N} \equiv |N, 0\rangle_{a,b} \quad (4.4)$$

$$|1\rangle^{\otimes N} \equiv |0, N\rangle_{a,b} \quad (4.5)$$

$$\frac{1}{\sqrt{2}}(|0\rangle^{\otimes N} + |1\rangle^{\otimes N}) \equiv \frac{1}{\sqrt{2}}(|N, 0\rangle_{a,b} + |0, N\rangle_{a,b}), \quad (4.6)$$

and we have introduced the N -photon Fock states. As it will be explained in chapter 6, we have in this case a N qubit system which can be interpreted as an optical system involving N Fock state interferometry. [43, 44]. In this way

we will see how it is ideally possible to have a phase precision at the Heisenberg limit. Note how the entanglement between probes which characterizes qubit systems become now an entanglement between field modes. This poses a conceptual change due to the fact that probes are bunched in a single (spatial or polarization) bosonic field mode, and the entanglement does not involve them individually.

4.2 Description of lossy map

At this point is necessary to study the evolution of quantum states in presence of loss. First of all we will see how to describe noise: it can be shown [50] that a lossy channel of quantum efficiency η (which also takes into account the detection efficiency) can be described by considering a perfect channel and inserting a beam splitter of transmissivity η . The second input port b of the beam splitter is in the vacuum state $|0\rangle$ and one output port is traced out (see Fig.(4.1)). This allows us to obtain the non-unitary evolution of a lossy

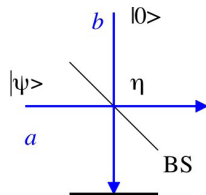


Figure 4.1: Description of a lossy channel mode through a beam splitter of transmissivity η equal to the channel quantum efficiency.

channel. It can be shown that, starting from the unitary evolution of the beam splitter

$$U = \exp \left[-\arctan \left(\sqrt{\frac{1-\eta}{\eta}} \right) (ab^\dagger - a^\dagger b) \right] \quad (4.7)$$

(where the mode definition for a and b is given in Fig. (4.1)), one obtains the following completely positive map for the density matrix evolution in the presence of loss

$$\rho = |\psi\rangle \langle \psi| \longrightarrow \rho = \text{Tr}_b [U \rho \otimes |0\rangle_b \langle 0| U^\dagger] = \sum_{n=0}^{\infty} V_n \rho V_n^\dagger, \quad (4.8)$$

with

$$V_n = \left(\frac{1-\eta}{\eta} \right)^{\frac{n}{2}} \frac{a^n}{\sqrt{n!}} \eta^{\frac{a^\dagger a}{2}}. \quad (4.9)$$

This description will be widely employed in the rest of the present work for, as we said, we are mostly interested in retrieving information from quantum state when photons are lost.

It is important to stress that with an N photon Fock state is not properly correct to state that we have N probes as it is not possible to extract deterministically N single photons from $|N\rangle$. When it is said that $n \leq N$ photons are lost, this must be considered as an *a posteriori* interpretation that is done considering the mixed state emerging from the noisy channel.

This section is very important because it states how to consider the noise in realistic scenarios and how to apply a lossy map to a quantum state. We will widely use such model in the remaining of the thesis.

4.3 Quantum estimation with NOON state

As we said in the introduction of this chapter, we will show how it is possible to ideally achieve the Heisenberg limit exploiting a particular quantum state. Such a state has been introduced in quantum estimation theory in order to see how it was possible to reach the Heisenberg limit. Unfortunately, as we will see, the property of being maximally entangled is not a guarantee of being a suitable state when noise is introduced.

Firstly we will be concerned with ideal case, namely no loss, and we will study the performances of this state in presence of noise.

4.3.1 NOON States and the Heisenberg Limit

Maximally entangled states of the form

$$|N :: 0\rangle_{a,b} = \frac{1}{\sqrt{2}} (|N, 0\rangle_{a,b} + |0, N\rangle_{a,b}), \quad (4.10)$$

are called NOON states [45, 51, 52], where

$$|m, n\rangle_{a,b} = |m\rangle_a |n\rangle_b, \quad (4.11)$$

and $|m\rangle_a$ is a Fock state with m quanta in mode a ,

$$|m\rangle_a = \frac{1}{\sqrt{m!}} (\hat{a}_a^\dagger)^m |0\rangle_a, \quad (4.12)$$

with \hat{a}_a^\dagger and $|0\rangle_a$ the usual creation operator and vacuum state for mode a . In interferometry, for example, modes a and b are different paths around the interferometer. The argument that NOON states allow phase measurement at the Heisenberg limit (4.1) is as follows. A phase shift of ϕ in mode b , which is obtained through the application of the unitary operator $U = e^{i\hat{b}^\dagger \phi}$, changes the state (4.10) to

$$|N :: 0; \phi\rangle_{a,b} = \frac{1}{\sqrt{2}} (|N, 0\rangle_{a,b} + \exp(iN\phi)|0, N\rangle_{a,b}). \quad (4.13)$$

4.3. Quantum estimation with NOON state

The phase ϕ can be determined by measuring the operator [48]

$$A_N = |0, N\rangle_{a,b} \langle N, 0| + |N, 0\rangle_{a,b} \langle 0, N|. \quad (4.14)$$

In the state (4.13), the expectation value of the operator (4.14) is

$$\begin{aligned} \langle A_N \rangle_\phi &= {}_{a,b} \langle N :: 0 ; \phi | A_N | N :: 0 ; \phi \rangle_{a,b} \\ &= \cos(N\phi), \end{aligned} \quad (4.15)$$

and its variance is

$$\begin{aligned} (\Delta A_N)^2 &= {}_{a,b} \langle N :: 0 ; \phi | A_N^2 | N :: 0 ; \phi \rangle_{a,b} - ({}_{a,b} \langle N :: 0 ; \phi | A_N | N :: 0 ; \phi \rangle_{a,b})^2 \\ &= \sin^2(N\phi). \end{aligned} \quad (4.16)$$

From error propagation

$$\delta\phi = \frac{\Delta A_N}{\left| \frac{\partial \langle A_N \rangle_\phi}{\partial \phi} \right|} = \frac{1}{N} \quad (4.17)$$

Phase measurement by this method is thus seen to be at the Heisenberg limit (4.1), with a precision that can be increased arbitrarily by increasing N .

4.3.2 NOON state Phase Measurement in the Presence of Loss

In any real system some photons will be inevitably lost prior to detection, a feature not represented in the model of phase measurement described above. Suppose we place beam splitters on both mode a , b of the NOON state characterized by different transmissivities, namely η_i , $i = 1, 2$: we evaluate the evolved state $\mathcal{L}(\rho_{NOON})$, ρ_{NOON} being density matrix of the NOON state. Once we let the NOON state accumulate a phase ϕ we have:

$$\begin{aligned} \mathcal{L}(\rho(\phi)_{NOON}) &= \frac{1}{2} \sum_{n,m=0}^{\infty} V_{1,n} V_{2,m} (|N, 0\rangle \langle N, 0| + |N, 0\rangle \langle 0, N| e^{-iN\phi} + \\ &\quad |0, N\rangle \langle N, 0| e^{iN\phi} + |0, N\rangle \langle 0, N|) V_{1,n}^\dagger V_{2,m}^\dagger, \end{aligned} \quad (4.18)$$

where $V_{i,n}$, $i = 1, 2$ are the operators

$$V_{i,n} = \left(\frac{1 - \eta_i}{\eta_i} \right)^{\frac{n}{2}} \frac{a^n}{\sqrt{n!}} \eta_i^{\frac{a^\dagger a}{2}}, \quad (4.19)$$

and the suffix i indicates the quantum efficiency η_i .

Observing that:

$$\sum_{n=0}^{\infty} V_n |N\rangle \langle N| V_n^\dagger = \sum_{n=0}^N \binom{N}{n} \eta^n (1 - \eta)^{N-n} |N - n\rangle \langle N - n| \quad (4.20)$$

$$\sum_{n=0}^{\infty} V_n |N\rangle \langle 0| V_n^\dagger = \eta^{N/2} |N\rangle \langle 0|, \quad (4.21)$$

we have the expression:

$$\begin{aligned} \mathcal{L}(\rho(\phi)_{NOON}) = & \frac{1}{2} \left[\sum_{n=1}^{N-1} \binom{N}{n} \eta_1^{N-n} (1-\eta_1)^n |N-n, 0\rangle \langle N-n, 0| + \right. \\ & \sum_{m=1}^{N-1} \binom{N}{m} \eta_2^{N-m} (1-\eta_2)^m |0, N-m\rangle \langle 0, N-m| + \\ & \left. (\eta_1 \eta_2)^{N/2} (|N, 0\rangle \langle 0, N| e^{-iN\phi} + |0, N\rangle \langle N, 0| e^{iN\phi}) \right]. \end{aligned} \quad (4.22)$$

Measuring the observable (4.14) we have:

$$\langle A_N \rangle_\phi = (\eta_1 \eta_2)^{N/2} \cos N\phi \quad (4.23)$$

$$\langle A_N^2 \rangle_\phi = \frac{1}{2} (\eta_1^N + \eta_2^N), \quad (4.24)$$

that lead to the following expression:

$$\delta\phi = \frac{\sqrt{\frac{1}{2}(\eta_1^N + \eta_2^N) - (\eta_1 \eta_2)^{N/2} \cos N\phi}}{|-N(\eta_1 \eta_2)^{N/2} \sin N\phi|}. \quad (4.25)$$

As would be the case in a practical quantum sensor [33], we assume loss in one arm, b , of the interferometer to be much greater than that of the delayed arm a , which we assume to be under controlled loss conditions. So we put $\eta_1 = 1, \eta_2 = \eta$ and obtain:

$$\delta\phi = \frac{[\frac{1}{2}(\eta^{-N} + 1) - \cos^2 N\phi]^{1/2}}{|-N \sin N\phi|}. \quad (4.26)$$

For fixed $\eta < 1$ and N , $\delta\phi$ is minimized for values of ϕ such that

$$N\phi = (n + 1/2)\pi, \quad n = 0, \pm 1, \pm 2, \dots \quad (4.27)$$

and

$$\delta\phi_{min} = \frac{\sqrt{(\eta^{-N} + 1)/2}}{N}. \quad (4.28)$$

It is worth reminding that in [35] the same result has been obtained using a master-equation model of continuous loss and entanglement.¹ For any nonzero amount of loss, i.e., for $\eta < 1$, we see from (4.28) that

$$\lim_{N \rightarrow \infty} \delta\phi'_{min} = \infty. \quad (4.29)$$

Putting $\eta_1 = \eta_2 = \eta$ we have:

$$\begin{aligned} \mathcal{L}(\rho(\phi)_{NOON}) = & \eta^N \rho(\phi)_{NOON} + \\ & \sum_{i=0}^{N-1} \binom{N}{i} \eta^i (1-\eta)^{N-i} \frac{1}{2} [|i, 0\rangle \langle i, 0| + |0, i\rangle \langle 0, i|]. \end{aligned} \quad (4.30)$$

¹The model of [35] corresponds to that of the present paper when the parameters $\bar{\gamma}t$, $\Gamma_1 t$ and $\Gamma_2 t$ of the former are set to values of 0, 0 and $-\log \eta$, respectively.

4.3. Quantum estimation with NOON state

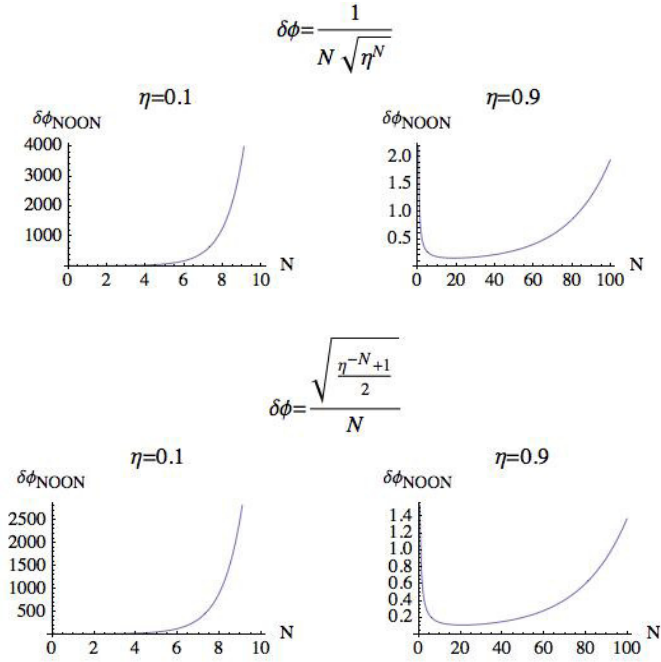


Figure 4.2: Top: Behaviour of $\delta\phi = \frac{1}{N\sqrt{\eta^N}}$. Bottom: $\delta\phi = \frac{\sqrt{\frac{1+\eta^{-N}}{2}}}{N}$.

Where we have explicitated the phase dependence in the density matrix, namely: $\rho(\phi)_{NOON} = |N :: 0; \phi\rangle_{a,b}\langle N :: 0; \phi|_{a,b}$, see Eq.(4.13). In this case it is possible to give an intuitive interpretation of Eq. (4.30): if none of the photons is lost, the state is unaffected with a probability η^N . If instead i photons are lost, the state is left in a mixture of density matrices of a mixed i photons state with probability: $\binom{N}{i} \eta^i (1-\eta)^{N-i}$. Always proceeding with the same measurement strategy, the following error precision is obtained:

$$\delta\phi_{min} = \frac{1}{N\sqrt{\eta^N}}. \quad (4.31)$$

From Fig.(4.2) it is possible to observe the high sensitivity to loss of NOON state.

The NOON state performances in realistic scenarios with attenuation have been pointed out in several works [33, 35, 36]: in practice, for most practical applications, the resolution of NOON state phase estimation not only does not achieve the Heisenberg Limit, but is actually worse than the Standard Quantum Limit.

In such a scenario, the need of a more robust state is required: such a suitable state will give, even in the ideal case, a lower precision in phase estimation, but it will retrieve phase information also from other terms of the

mixed state (4.8), contrary to NOON state case for which only a term is able to bear information after the lossy evolution, as it can be seen in Eq.(4.30).

4.4 Partially entangled states

We start to analyze our proposal of considering partially entangled state in the phase estimation problem. The idea we intend to investigate will be developed from time to time; now it will be presented the study of a state composed by groups of M NOON states.

Consider the following example, let an NM photon state be defined as:

$$\frac{1}{\sqrt{2}}(|N, 0\rangle + e^{iN\phi} |0, N\rangle)^{\otimes M} \quad (4.32)$$

We want to investigate the behaviour of states in which the photons are grouped, to see if it is possible to have more robustness. The contribution of every NOON state, if we consider lossy evolution [33] of state (4.32), is:

$$\delta\phi^N = \frac{\sqrt{\eta^{-N}}}{N} \quad (4.33)$$

We perform the measurement of the following observable:

$$A_{N,un} = \frac{1}{M} \oplus_{i=1}^M (|0, N\rangle \langle N, 0| + |N, 0\rangle \langle 0, N|)_i = \frac{1}{M} \oplus_{i=1}^M A_N^{(i)} \quad (4.34)$$

where $A_N^{(i)} = (|0, N\rangle \langle N, 0| + |N, 0\rangle \langle 0, N|)_i$, $i = 1, \dots, M$. We have:

$$(\Delta_\phi A_{N,un})^2 = \frac{1}{M} (\Delta_\phi A_N)^2. \quad (4.35)$$

This means that:

$$\Delta A_{N,un} = \frac{1}{\sqrt{M}} \Delta A_N \quad (4.36)$$

which translates into:

$$\delta\phi_{un}^N = \frac{\sqrt{\eta^{-N}}}{\sqrt{MN}}. \quad (4.37)$$

It is easy to interpret this expression in which the contributions of entanglement, $\frac{\sqrt{\eta^{-N}}}{N}$ term, from the contribution of the classical strategy, $\frac{1}{\sqrt{M}}$ term, are well separated. This precision can be improved by considering states showing entanglement between the M groups. Such states could be more robust to loss without anyway reaching the Heisenberg limit $\frac{1}{MN}$.

4.4.1 Entanglement between groups

We now search for states showing entanglement between groups of maximally entangled states to see if it is possible to exploit this further entanglement when lossy map is taken into account. First we present an exemplificative calculation and in next chapter we will deal with this task more deeply.

The behaviour of partially entangled states must now be considered in order to check whether these states can be useful in the presence of noise despite the precision is lower. The way we intend to investigate is suggested in [29], and consists in entangling groups of states, every group being composed by maximally entangled state. For sake of clarity, consider the following state:

$$|\psi\rangle_\phi = \frac{1}{\sqrt{2}} \left[\frac{|N-1, 0\rangle + e^{i(N-1)\phi}|0, N-1\rangle}{\sqrt{2}} \frac{|1, 0\rangle + e^{i\phi}|0, 1\rangle}{\sqrt{2}} \right] + \left[\frac{|1, 0\rangle + e^{i\phi}|0, 1\rangle}{\sqrt{2}} \frac{|N-1, 0\rangle + e^{i(N-1)\phi}|0, N-1\rangle}{\sqrt{2}} \right]. \quad (4.38)$$

This is a N photon state, where probes are grouped and a phase is accumulated between the groups. We measure this observable:

$$A_{N-1} = |N-1, 0, 1, 0\rangle\langle 0, N-1, 0, 1| + |0, N-1, 0, 1\rangle\langle N-1, 0, 1, 0| + |1, 0, N-1, 0\rangle\langle 0, 1, 0, N-1| + |0, 1, 0, N-1\rangle\langle 1, 0, N-1, 0| = \mathbf{A} + \mathbf{B} + \mathbf{C} + \mathbf{D}. \quad (4.39)$$

The initial state can be written as: $|\psi\rangle = \frac{1}{\sqrt{2}}(|I\rangle|II\rangle + |II\rangle|I\rangle)$.

Average value of A_{N-1} now is computed.

It is clear that:

$A_{N-1}|\psi\rangle = (\mathbf{A} + \mathbf{B})|II\rangle|I\rangle + (\mathbf{C} + \mathbf{D})|I\rangle|II\rangle$, then:

$$\begin{aligned} \mathbf{A}|II\rangle|I\rangle &= \frac{1}{2\sqrt{2}}|N-1, 0\rangle\langle 0, N-1| \left(\frac{(|N-1, 0\rangle + e^{i(N-1)\phi}|0, N-1\rangle)}{\sqrt{2}} \right) \\ &\otimes |1, 0\rangle\langle 0, 1| \left(\frac{(|1, 0\rangle + e^{i\phi}|0, 1\rangle)}{\sqrt{2}} \right) = \frac{1}{2\sqrt{2}}|N-1, 0\rangle e^{i(N-1)\phi}|1, 0\rangle e^{i\phi}. \end{aligned} \quad (4.40)$$

It follows:

$$\langle I|\langle II|\mathbf{A}|II\rangle|I\rangle = \frac{1}{8}e^{iN\phi}. \quad (4.41)$$

Concerning \mathbf{B} :

$$\begin{aligned} \mathbf{B}|II\rangle|I\rangle &= \frac{1}{2\sqrt{2}}|0, N-1\rangle\langle N-1, 0| \\ &\left(\frac{(|N-1, 0\rangle + e^{i(N-1)\phi}|0, N-1\rangle)}{\sqrt{2}} \right) \otimes \\ &|0, 1\rangle\langle 1, 0| \left(\frac{(|1, 0\rangle + e^{i\phi}|0, 1\rangle)}{\sqrt{2}} \right) = \frac{1}{2\sqrt{2}}|0, N-1\rangle|0, 1\rangle \end{aligned} \quad (4.42)$$

and we obtain:

$$\langle I | \langle II | \mathbf{B} | II \rangle | I \rangle = \frac{1}{8} e^{-iN\phi}. \quad (4.43)$$

Finally:

$$\langle \psi | A_{N-1} | \psi \rangle = \frac{1}{2} \cos N\phi. \quad (4.44)$$

Now we compute the variance, first of all:

$$A_{N-1}^2 = (\mathbf{A} + \mathbf{B} + \mathbf{C} + \mathbf{D})^2 = (\mathbf{A} + \mathbf{B})^2 + (\mathbf{C} + \mathbf{D})^2 + \quad (4.45)$$

$$(\mathbf{A} + \mathbf{B})(\mathbf{C} + \mathbf{D}) + (\mathbf{C} + \mathbf{D})(\mathbf{A} + \mathbf{B}) = \mathbf{AB} + \mathbf{BA} + \mathbf{CD} + \mathbf{DC} = \quad (4.46)$$

$$\underbrace{|N-1, 0, 1, 0\rangle\langle N-1, 0, 1, 0|}_{\mathbf{AB}} + \underbrace{|0, N-1, 0, 1\rangle\langle 0, N-1, 0, 1|}_{\mathbf{BA}} + \quad (4.47)$$

$$\underbrace{|1, 0, N-1, 0\rangle\langle 1, 0, N-1, 0|}_{\mathbf{CD}} + \underbrace{|0, 1, 0, N-1\rangle\langle 0, 1, 0, N-1|}_{\mathbf{DC}}. \quad (4.48)$$

In details:

$$\langle \psi | A_{N-1}^2 | \psi \rangle = \langle \psi | (\mathbf{AB} + \mathbf{BA} + \mathbf{CD} + \mathbf{DC}) | \psi \rangle, \quad (4.49)$$

from which follows:

$$\mathbf{AB} | II \rangle | I \rangle + \mathbf{BA} | II \rangle | I \rangle + \quad (4.50)$$

$$\mathbf{DC} | I \rangle | II \rangle + \mathbf{CD} | I \rangle | II \rangle =$$

$$\frac{1}{2\sqrt{2}} (|N-1, 0\rangle |1, 0\rangle + |1, 0\rangle |N-1, 0\rangle +$$

$$(|0, N-1\rangle |0, 1\rangle + |0, 1\rangle |0, N-1\rangle) e^{iN\phi} \quad (4.51)$$

so we have the second moment:

$$\langle \psi | A_{N-1}^2 | \psi \rangle = \frac{1}{2}$$

and in the end:

$$\Delta A_{N-1}^2 = \frac{1}{2} - \frac{1}{4} \cos^2 N\phi = \frac{1}{4} (1 + \sin^2 N\phi).$$

Through the usual expression for error propagation we obtain:

$$\delta\phi = \frac{\sqrt{1 + \sin^2[N\phi]}}{N \sin[N\phi]} > \frac{1}{N}.$$

4.4. Partially entangled states

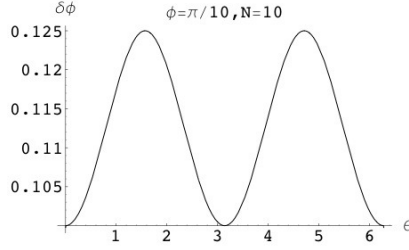


Figure 4.3: Behaviour of the phase error (4.56) as a function of θ : it can be seen that it lies between $\frac{1}{N-2}$ and $\frac{1}{N}$, in this case respectively $\frac{1}{8} = 0.125$ and $\frac{1}{10}$

From this example we see that state (4.38) is less precise than a N photon NOON state. Moreover, we may express (4.38) in this way:

$$|\psi\rangle_\phi = \frac{1}{\sqrt{2}}(|N\rangle_\phi + |\chi\rangle_\phi), \quad (4.52)$$

where

$$\begin{aligned} |N\rangle_\phi &= \frac{1}{2}[|1, 0, N-1, 0\rangle + |N-1, 0, 1, 0\rangle \\ &+ e^{iN\phi}(|0, 1, 0, N-1\rangle + |0, N-1, 0, 1\rangle)] \end{aligned}$$

and

$$\begin{aligned} |\chi\rangle_\phi &= e^{i\phi}(|0, 1, N-1, 0\rangle + |N-1, 0, 0, 1\rangle) \\ &+ e^{i(N-1)\phi}(|1, 0, 0, N-1\rangle + |0, N-1, 1, 0\rangle), \end{aligned}$$

note that $\langle N|\chi\rangle = 0$. Indeed, we could express this state in a more general way:

$$|\psi_\theta\rangle_\phi = \cos\theta |N\rangle_\phi + \sin\theta |\chi\rangle_\phi. \quad (4.53)$$

Starting from the projectors $|N\rangle\langle N|$ and $|\chi\rangle\langle\chi|$, the observable could be chosen in this way:

$$\begin{aligned} A_\theta &= 4|\psi_\theta\rangle\langle\psi_\theta| = 4(\cos^2\theta |N\rangle\langle N| + \sin^2\theta |\chi\rangle\langle\chi| \\ &+ \sin\theta \cos\theta(|N\rangle\langle\chi| + |\chi\rangle\langle N|)). \end{aligned} \quad (4.54)$$

We obtain the variance:

$$\begin{aligned} (\Delta A_\theta)^2 &:= {}_\phi\langle\psi_\theta| A_\theta^2 |\psi_\theta\rangle_\phi - {}_\phi\langle\psi_\theta| A_\theta |\psi_\theta\rangle_\phi^2 \\ &= 4 {}_\phi\langle\psi_\theta| A_\theta |\psi_\theta\rangle_\phi - {}_\phi\langle\psi_\theta| A_\theta |\psi_\theta\rangle_\phi^2 \\ &= (4 - {}_\phi\langle\psi_\theta| A_\theta |\psi_\theta\rangle_\phi) {}_\phi\langle\psi_\theta| A_\theta |\psi_\theta\rangle_\phi. \end{aligned} \quad (4.55)$$

So we have to compute:

$$\delta\phi = \frac{\sqrt{(4 - \phi \langle \psi_\theta | A_\theta | \psi_\theta \rangle_\phi) \langle \psi_\theta | A_\theta | \psi_\theta \rangle_\phi}}{\left| \frac{d_\phi \langle \psi_\theta | A_\theta | \psi_\theta \rangle_\phi}{d\phi} \right|}. \quad (4.56)$$

When $\theta = \pi$ we have a NOON like behaviour, namely we have $\delta\phi = \frac{1}{N}$, while for $\theta = \pi/2$, $\delta\phi = \frac{1}{N-2}$, see Fig. (4.3).

This example has been made in order to show how information on the phase can be extracted from the not-NOON component of Eq. (4.53).

Moreover our aim is to find some state tolerating the lost of more than one photon; starting from (4.38), we can generalize and consider:

$$|\psi\rangle = \frac{1}{\sqrt{2}}(|n :: 0\rangle |m :: 0\rangle + |m :: 0\rangle |n :: 0\rangle), \quad (4.57)$$

$n + m = N$. We call this state: *mn-loss*. As it can be seen in Appendix E, such a state can tolerate the loss of more than one photon. But as it will be explained in next chapter, it is not a simple task handling with the evolved density matrix of states like or similar to *mn-loss* state in order to describe a deterministic measurement.

We conclude this chapter by considering a state suitable for interferometry in which the desired characteristic of robustness to noise emerges in a very powerful way.

4.5 m&m states

We now present results concerning a particular quantum state and we try to give an example of a deterministic measurement as mentioned in section 1.5. Recently *Huver et al.* [38] have proposed a maximally path-entangled state together with a suitable interferometric measurement strategy revealing properties of robustness to loss. The state is the following:

$$|m :: m'\rangle_{a,b} = \frac{1}{\sqrt{2}} \left(|m, m'\rangle_{a,b} + |m', m\rangle_{a,b} \right). \quad (4.58)$$

By applying lossy map characterized by different quantum efficiencies to both modes, the emerging state is:

$$\begin{aligned} \rho_{a',b'} = & \sum_{k=0}^m \sum_{l=0}^{m'} |a_{k,l}|^2 |m-k, m'-l\rangle \langle m-k, m'-l| \\ & + |b_{k,l}|^2 |m'-l, m-k\rangle \langle m'-l, m-k| \\ & + \sum_{l,l'=0}^{m'} a_{l,l'}^* b_{l',l} |m'-l, m-l'\rangle \langle m-l, m'-l'| \\ & + a_{l',l} b_{l,l'}^* |m-l', m'-l\rangle \langle m'-l', m-l|, \end{aligned} \quad (4.59)$$

4.5. m&m states

where the coefficients are defined as

$$\begin{aligned}
 |a_{k,l}|^2 &\equiv \gamma_{k,l}^2 \eta_a^{m-k} (1-\eta_a)^k \eta_b^{m'-l} (1-\eta_b)^l \\
 |b_{k,l}|^2 &\equiv \gamma_{k,l}^2 \eta_a^{m'-l} (1-\eta_a)^l \eta_b^{m-k} (1-\eta_b)^k \\
 a_{l,l'}^* b_{l',l} &\equiv \gamma_{l,l'} \gamma_{l',l} \eta_a^{\frac{m+m'-2l}{2}} (1-\eta_a)^l \eta_b^{\frac{m+m'-2l'}{2}} (1-\eta_b)^{l'} e^{-i(m-m')\phi} \\
 a_{l',l} b_{l,l'}^* &\equiv \gamma_{l',l} \gamma_{l,l'} \eta_a^{\frac{m+m'-2l'}{2}} (1-\eta_a)^{l'} \eta_b^{\frac{m+m'-2l}{2}} (1-\eta_b)^l e^{i(m-m')\phi}, \quad (4.60)
 \end{aligned}$$

and

$$\gamma_{k,l} \equiv \sqrt{\frac{1}{2} \binom{m}{k} \binom{m'}{l}}. \quad (4.61)$$

As it can be seen in (4.60), mixed state (4.59) carries phase information thanks

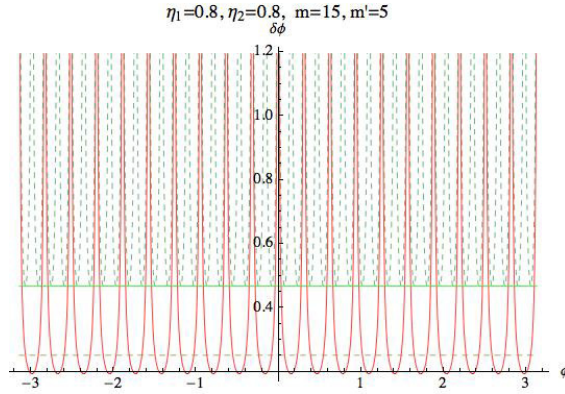


Figure 4.4: Dashed curve is NOON state, continuous curve is $m&m$ state ($m = 15, m' = 5$). See the beating of the rescaled SQL (dashed line), namey: $\delta\phi_{SQL} = \frac{1}{\sqrt{\eta N}}$

to the presence of interference terms which are multiplied by the quantity $e^{i(m-m')\phi}$.

The measured observable is:

$$\begin{aligned}
 A &= \sum_{r,s=0}^{m'} |m'-r, m-s\rangle \langle m-r, m'-s| \\
 &\quad + |m-r, m'-s\rangle \langle m'-r, m-s|, \quad (4.62)
 \end{aligned}$$

the average value and the average second moment are (see appendix F for explicit calculation):

$$\langle A \rangle = \text{Tr}[A\rho_{a',b'}] = \sum_{l,l'=0}^{m'} (a_{l,l'}^* b_{l',l} + a_{l',l} b_{l,l'}^*). \quad (4.63)$$

$$\langle A^2 \rangle = \text{Tr}[A^2 \rho_{a',b'}] = \sum_{k,l=0}^{m'} (|a_{k,l}|^2 + |b_{k,l}|^2), \text{ if } m' < \frac{m}{2} \quad (4.64)$$

and

$$\begin{aligned} \langle A^2 \rangle &\simeq \sum_{k,l=0}^{m'} (|a_{k,l}|^2 + |b_{k,l}|^2) + \\ &\sum_{k=m-m'}^m \sum_{l=0}^{2m'-m} (|a_{k,l}|^2 + |b_{k,l}|^2) \text{ if } m' \geq \frac{m}{2}. \end{aligned} \quad (4.65)$$

Through this expression we evaluate the expression for the phase error by means of Eq. (4.17). The following state is doubtless a very robust state. Even though the precision is lower than the one obtained in the absence of loss with a NOON state, it is possible to retrieve information since it is not so high-sensitive to the loss of photons.

In Fig. (4.4) we plot the phase precision that can be reached with the overexposed measurement strategy: we have considered both arms of the interferometer as two lossy channel with equal quantum efficiency. Note the beating of the rescaled SQL, $\delta\phi_{SQL} = \frac{1}{\sqrt{nN}}$, and the considerably better performances compared to NOON state. A little word must be spent about the observable (4.62). As explained in Appendix F it can be expressed in the following way:

$$A = \sum_{s,r=0}^{m'} \Pi_{r,s}^{(+)} - \Pi_{r,s}^{(-)}, \quad (4.66)$$

where $\Pi_{r,s}^{(\pm)}$ are the projectors onto the space generated by such vectors:

$$|\psi_{r,s}^{\pm}\rangle = \frac{1}{\sqrt{2}}(|m' - r, m - s\rangle \pm |m - r, m' - s\rangle). \quad (4.67)$$

This means that such measurement recovers all the terms of the evolved density matrix (F.10) that bear phase information. Every term corresponds to a different number of loss photons, but some loss are tolerated and so it is still possible to have phase information despite the noise. This is a clear example of a deterministic measurement in which the experimenter does not post-select data as explained in section 1.5, but he recovers information from the whole probes involved in the creation of the quantum state, for example the $m\&m$ state, with $m + m' = N$.

In this perspective the NOON state can be seen as a particular $m\&m$ state, with $m = N$ and $m' = 0$ with a high loss sensitivity due to the presence of only one term bearing phase information in the evolved density matrix (4.22).

Observable (4.14) becomes:

$$A_N = |0, N\rangle_{a,b} \langle N, 0| + |N, 0\rangle_{a,b} \langle 0, N| = \Pi_{NOON}^{(+)} - \Pi_{NOON}^{(-)}, \quad (4.68)$$

4.5. $m\&m$ states

with $\Pi_{NOON}^{(\pm)} := |N :: 0\rangle_{\pm} \pm |N :: 0\rangle$, where $|N :: 0\rangle_{\pm} := \frac{1}{\sqrt{2}}(|N, 0\rangle \pm |0, N\rangle)$. In this case in fact, the only important terms are those with zero losses [38].

Finally It is worth recalling that in their work [38], *Huver et al.* compare a N photon NOON state with a $m\&m$ state such that $m - m' = N$, i.e. $m + m' > N$. From our point of view this does not seem to be a good way to make comparison between two states due to their different mean photon number. In quantum metrology typically a framework is given in which the number of probes is fixed and we think that the right way to show the robustness of $m\&m$ states should be the one presented here, for it has been performed equating the photon number and not the information carried by the states.

At this point we are ready to introduce the idea of grouping photons in a more rigorous way.

Chapter 5

Grouping photons

As anticipated in the previous chapter, we intend to search for states that are less entangled but more robust, representing a tradeoff between precision and entanglement. Such a research is performed by analyzing states containing entanglement between groups of maximally entangled photon states.

In this way we will fall in with multipartite entangled states [83] diverging from a strictly interferometric point of view in which bipartite path entangled states are naturally assumed. The key idea can be retrieved in a work about quantum positioning [28, 29] in which it is suggested to use a partially entangled state in time coincidence measurements. In that case an estimation over time is given in order to give a better precision of position of some light sources.

In the followings two sections we will consider a precise NM photons state and we will see its contribution in phase estimation, firstly in the absence of noise. Then noise will be introduced and two particular observables will be measured. In section 5.1.2 we will compare our results with the $m\&m$ states introduced in previous chapter.

5.1 NOON-LIKE State

5.1.1 Ideal case

Now we study the behaviour of a particular multipartite (not maximally) entangled state. For the multimode case anyway is very difficult to consider an optimization over the measurement or over the input state as it has been done in single or double mode phase estimation (see chapter 6). A suggestion about which state can be used to obtain some preliminary result can come from a work previously mentioned about the possibility to exploit a particular entangled state in order to have a better precision in estimating the position of some light source, see *Maccone et al* [28, 29]. In practice one considers several maximally entangled states and entangles groups of these states in order to

have a further entanglement to exploit. Defining:

$$\begin{aligned} |\mathbf{N}\rangle &:= \frac{1}{\sqrt{2}}(|N, 0\rangle + |0, N\rangle), \\ |\mathbf{N}_+\rangle &:= \frac{1}{\sqrt{2}}(|N, 0\rangle + e^{iN\phi} |0, N\rangle), \\ |\mathbf{N}_-\rangle &:= \frac{1}{\sqrt{2}}(|N, 0\rangle + e^{-iN\phi} |0, N\rangle), \end{aligned}$$

the state in consideration is an NM [29] photon state:

$$|\psi'\rangle \propto \bigotimes_{i=1}^M |\mathbf{N}\rangle_i \otimes |0\rangle^{\otimes 2M} + \bigotimes_{i=1}^M |0\rangle^{\otimes 2M} |\mathbf{N}\rangle_i. \quad (5.1)$$

When we let it accumulate a phase we have:

$$|\psi'\rangle_\phi \propto \bigotimes_{i=1}^M |\mathbf{N}_+\rangle_i \otimes |0\rangle^{\otimes 2M} + \bigotimes_{i=1}^M |0\rangle^{\otimes 2M} |\mathbf{N}_-\rangle_i. \quad (5.2)$$

Note that we have inserted a negative phase term in the second term of (5.2) in order to have relative phase between the two term of the sum, namely the first $2M$ modes acquire a phase $+\phi$, the last $2M$ acquire a phase $-\phi$. Consider the following observable [40, 42, 41]:

$$A := 2 |\psi'\rangle \langle \psi'|. \quad (5.3)$$

$$A |\psi'\rangle_\phi = 2 |\psi'\rangle \langle \psi'| \psi'\rangle_\phi, \quad (5.4)$$

and evaluate $\langle \psi'| \psi'\rangle_\phi$ which is equal to:

$$\frac{1}{2} [\langle \mathbf{N} | \mathbf{N}_+\rangle^M + \langle \mathbf{N} | \mathbf{N}_-\rangle^M], \quad (5.5)$$

where $\langle \mathbf{N} | \mathbf{N}_+\rangle = (\frac{1+e^{iN\phi}}{2})^M$, $\langle \mathbf{N} | \mathbf{N}_-\rangle = (\frac{1+e^{-iN\phi}}{2})^M$. The average value is:

$$\phi \langle \psi'| A |\psi'\rangle_\phi = \frac{1}{2} \left[\left(\frac{1+e^{iN\phi}}{2} \right)^M + \left(\frac{1+e^{-iN\phi}}{2} \right)^M \right]^2, \quad (5.6)$$

and obviously:

$$A^2 = 2A. \quad (5.7)$$

The variance is:

$$\begin{aligned} (\Delta A)^2 &= \left[\left(\frac{1+e^{iN\phi}}{2} \right)^M + \left(\frac{1+e^{-iN\phi}}{2} \right)^M \right]^2 \\ &\quad \left\{ 1 - \frac{1}{4} \left[\left(\frac{1+e^{iN\phi}}{2} \right)^M + \left(\frac{1+e^{-iN\phi}}{2} \right)^M \right]^2 \right\}. \end{aligned} \quad (5.8)$$

The precision on the phase becomes:

$$\delta\phi = \frac{\sqrt{\left[\left(\frac{1+e^{iN\phi}}{2} \right)^M + \left(\frac{1+e^{-iN\phi}}{2} \right)^M \right]^2 \left(1 - \frac{1}{4} \left[\left(\frac{1+e^{iN\phi}}{2} \right)^M + \left(\frac{1+e^{-iN\phi}}{2} \right)^M \right]^2 \right)}}{\left| i \frac{MN}{2} \left[\left(\frac{1+e^{iN\phi}}{2} \right)^{M-1} e^{iN\phi} - \left(\frac{1+e^{-iN\phi}}{2} \right)^{M-1} e^{-iN\phi} \right] \right|}, \quad (5.9)$$

5.1. NOON-LIKE State

for $M = 1$, choosing $\frac{1}{\sqrt{2}}$ as normalization constant,

$$|\psi'\rangle_\phi = \frac{1}{\sqrt{2}} \left[\left(\frac{|N, 0\rangle + e^{iN\phi} |0, N\rangle}{\sqrt{2}} \right) |0\rangle |0\rangle + |0\rangle |0\rangle \left(\frac{|N, 0\rangle + e^{-iN\phi} |0, N\rangle}{\sqrt{2}} \right) \right] \quad (5.10)$$

and

$$\delta\phi = \frac{(1 + \cos N\phi) \sqrt{1 - \frac{1}{4}(1 + \cos N\phi)^2}}{|-N \sin N\phi(1 + \cos N\phi)|}. \quad (5.11)$$

This expression can be greater than $\frac{1}{N}$ and it is an effect of the different phase evolution suffered by the $2M$ modes ¹ After this overview in which phase estimation has been considered in the absence of noise, we start our lossy analysis.

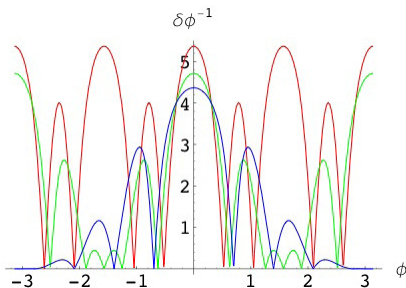


Figure 5.1: Behaviour of $\delta\phi_{min}^{-1}$ as a function of ϕ . $\eta = 1$ and $M = 1$, $N = 4$ (red), $M = 2$, $N = 2$ (green), $M = 4$, $N = 1$ (blue)

5.1.2 Lossy case

Having in mind the description of lossy map of section 4.2 we consider the effect of noise in these newer framework.

Suppose we apply the lossy map to the NOON-like state. If the quantum efficiencies are assumed equal for all the modes² the emerging mixed state is

¹Suppose for example that the NOON state accumulates phase in the following way: $1/\sqrt{2}(e^{-iN\phi} |N, 0\rangle + e^{iN\phi} |0, N\rangle)$. Measuring the usual observable $A_N = |N, 0\rangle \langle 0, N| + |0, N\rangle \langle N, 0|$ it can be seen that the phase uncertainty is $\delta\phi = \frac{1}{2N}$.

²See section 4.2

described by the following density matrix:

$$\begin{aligned}
 \rho'_M = & \frac{1}{2} [(\eta^N |\mathbf{N}_+\rangle \langle \mathbf{N}_+| + \rho_{MIX})^{\otimes M} \otimes \nu^{\otimes 2M} + \\
 & \nu^{\otimes 2M} \otimes (\eta^N |\mathbf{N}_-\rangle \langle \mathbf{N}_-| + \rho_{MIX})^{\otimes M} + \\
 & \eta^{NM} (|0\rangle^{\otimes 2M} \langle \mathbf{N}_+|^{\otimes M} \otimes |\mathbf{N}_-\rangle^{\otimes M} \langle 0|^{\otimes 2M} + \\
 & |\mathbf{N}_+\rangle^{\otimes M} \langle 0|^{\otimes 2M} \otimes |0\rangle^{\otimes 2M} \langle \mathbf{N}_-|^{\otimes M})] = \\
 & \eta^{NM} |\psi'\rangle_\phi \langle \psi'|_\phi + \rho_{MIX}^{\otimes M} \otimes \nu^{\otimes 2M} + \nu^{\otimes 2M} \otimes \rho_{MIX}^{\otimes M} + \rho_\chi, \quad (5.12)
 \end{aligned}$$

ρ_χ being the mixed terms emerging from the expansion of $(\eta^N |\mathbf{N}_\pm\rangle \langle \mathbf{N}_\pm| + \rho_{MIX})^{\otimes M}$ and

$\rho_{MIX} := \sum_{i=0}^{N-1} \binom{N}{i} \eta^i (1-\eta)^{N-i} \frac{1}{2} [|i, 0\rangle \langle i, 0| + |0, i\rangle \langle 0, i|]$. Derivation is given in appendix D. From this expression, a robustness to loss of photons stronger than that of NOON-states emerges, thanks to the presence of the term $(\eta^N |\mathbf{N}_\pm\rangle \langle \mathbf{N}_\pm| + \rho_{MIX})^{\otimes M}$, but it also highlights the difficulty in realizing a measure that would allow to extract phase information carried by every term of the emerging mixed density matrix in a deterministic way. In the following we will employ Heisenberg picture, contrary to what has been done in chapter 4, in which states were evolved (Schrodinger picture).

We present results considering in particular two observables A_{NM} and A_M :

Measure of A_{NM}

Let:

$$\begin{aligned}
 A_{NM} = & \bigotimes_i^M [|\mathbf{N}\rangle_{a'_i, b'_i} |0\rangle_i |0\rangle_i \langle 0|_i \langle 0|_{a'_i, b'_i} \langle \mathbf{N}|] \\
 & + \bigotimes_i [|0\rangle_i |0\rangle_i |\mathbf{N}\rangle_{a'_i, b'_i} \langle \mathbf{N}|_{a'_i, b'_i} \langle \mathbf{N}|_i \langle 0|_i \langle 0|] \quad (5.13)
 \end{aligned}$$

be a two mode (a', b') observable. The meaning of the prime ' will be clear in the following.

One can apply a lossy map to $n < M$ groups of photons and compare the result with a measure on an NM NOON-state with the lossy map applied to just one mode [33]. Regarding noise with the usual fictitious lossy beam splitter description [50] and considering an N photons NOON state, let:

$$A_N = |0, N\rangle \langle N, 0|_{a, b} + |N, 0\rangle \langle 0, N|_{a, b}, \quad (5.14)$$

a and b being the field mode unaffected by noise. Introducing two virtual beam splitters the field modes become

$$\begin{aligned}
 a' &= t_a a + r_a V_a \\
 b' &= t_b b + r_b V_b
 \end{aligned}$$

5.1. NOON-LIKE State

with t_i and r_i ($i = a, b$) being the respective transmission and reflection coefficients assumed to be real³, and V_i representing the vacuum field modes. The observable becomes [33]:

$$\begin{aligned} & |0, N\rangle \langle N, 0|_{a', b'} + |N, 0\rangle \langle 0, N|_{a', b'} = \\ & \frac{1}{N!} [(t^* a_b^\dagger + r^* V_b^\dagger)^N |0, 0\rangle \langle 0, 0|_{a, b} (ta_a + rV_a)^N \\ & + (t^* a_a^\dagger + r^* V_a^\dagger)^N |0, 0\rangle \langle 0, 0|_{a, b} (ta_b + rV_b)^N]^4. \end{aligned}$$

Note that we have taken the values of the trasmission and reflection coefficients equal for the two beam splitters. We have also assumed them to be real. Moreover remember that

$$|0\rangle_{a, b} = |0\rangle_{a', b'}, \quad (5.15)$$

For every NOON state appearing in Eq. (5.2), noise is introduced as just explained: we apply the lossy map to both modes for each NOON state $n < M$ times.

In details⁵ :

$$\begin{aligned} \langle A_{NM} \rangle = & \left[\frac{1}{2} (v_a \langle 0|_{v_b} \langle 0|_{a, b} \langle \mathbf{N}_+ | \mathbf{N} \rangle_{a', b'} \langle \mathbf{N} | \mathbf{N}_- \rangle_{a, b} |0\rangle_{v_a} |0\rangle_{v_b})^M \right. \\ & \left. + (v_a \langle 0|_{v_b} \langle 0|_{a, b} \langle \mathbf{N}_- | \mathbf{N} \rangle_{a', b'} \langle \mathbf{N} | \mathbf{N}_+ \rangle_{a, b} |0\rangle_{v_a} |0\rangle_{v_b})^M \right] \quad (5.16) \end{aligned}$$

So we must compute terms of this kind:

$$v_a \langle 0|_{v_b} \langle 0|_{a, b} \langle \mathbf{N}_\pm | \mathbf{N} \rangle_{a', b'}. \quad (5.17)$$

We observe that:

$$\begin{aligned} {}_{j'} \langle N | N \rangle_j |0\rangle_{V_j} &= v_{j'} \langle 0|_{j'} \langle 0| (a_j t + r V_j)^N |N\rangle_j |0\rangle_{V_j} \\ &= {}_{j'} \langle 0| (a_j t)^N |N\rangle_j \propto t^N = \eta^{N/2}, \quad (5.18) \end{aligned}$$

where $j^{(\prime)} = a^{(\prime)}, b^{(\prime)}$ and we have expanded the N -th power due to the fact V_j and a_j commute. Moreover we have used the fact that the quantum efficiency of the channel is the transmissivity of the fictious beam splitter (see section 4.2), namely: $\eta = |t|^2$ (remember that in our case $t \in \mathbf{R}$).

³In general such coefficients are complex number, but for pure loss, which is the case we are considering, they can be taken as real.

⁵We have done a simplification for we have subsumed the rigorous expression for the observable A_{NM} , because as it is here expressed, it seems that every mode is constrained to loss, infact all the field modes are marked with the prime ' symbol which stands for the application of lossy map to that mode. Actually not all modes suffer noisy evolution. But in prattice, the difference in the computation of the terms of type (5.17) and (5.19), when loss is applied, is the presence of the term η^N occouring the n number of modes that suffers evolution.

Moreover, recalling Eq. (5.15), we have (see Eq. (5.16)):

$$\begin{aligned} {}_{a',b'}\langle \mathbf{N} | \mathbf{N}_+ \rangle_{a,b} |0\rangle_{V_a} |0\rangle_{V_b} &= {}_{a'}\langle N | N \rangle_a + \\ {}_{b'}\langle N | N \rangle_b e^{iN\phi} &= \eta^{N/2} [1 + e^{iN\phi}] \end{aligned} \quad (5.19)$$

from which naturally follows that:

$${}_{a,b}\langle \mathbf{N}_\pm | \mathbf{N} \rangle_{a',b'} = {}_{a,b}\langle \mathbf{N} | \mathbf{N}_\mp \rangle_{a',b'}. \quad (5.20)$$

We can now easily obtain the expression for the average value:

$$\langle A_{NM} \rangle = \frac{1}{2} \eta^{nN} \left[\left(\frac{1 + e^{-iN\phi}}{2} \right)^{2M} + \left(\frac{1 + e^{iN\phi}}{2} \right)^{2M} \right]. \quad (5.21)$$

Now we compute $\langle A_{NM}^2 \rangle$. First of all, it is easy to check that:

$$A_{NM}^2 = \bigotimes_i^M [| \mathbf{N} \rangle_{a'_i, b'_i} |0\rangle_i |0\rangle_i {}_{a'_i, b'_i} \langle \mathbf{N} | {}_i \langle 0 | {}_i \langle 0 |] \quad (5.22)$$

$$+ \bigotimes_i^M [|0\rangle_i |0\rangle_i | \mathbf{N} \rangle_{a'_i, b'_i} \langle 0 | {}_i \langle 0 | {}_{a'_i, b'_i} \langle \mathbf{N} |]. \quad (5.23)$$

At this point we can write:

$$\begin{aligned} \langle A_{NM}^2 \rangle &= \frac{1}{2} [|_{a,b}\langle \mathbf{N}_+ | \mathbf{N} \rangle_{a',b'} |^{2M} + |_{a,b}\langle \mathbf{N}_- | \mathbf{N} \rangle_{a',b'} |^{2M}] \\ &= \eta^{nN} \left(\frac{1 + \cos N\phi}{2} \right)^M, \end{aligned} \quad (5.24)$$

and finally:

$$(\Delta A_{NM})^2 = \eta^{nN} \left[\left(\frac{1 + \cos N\phi}{2} \right)^M - \frac{1}{4} \eta^{nN} \left[\left(\frac{1 + e^{-iN\phi}}{2} \right)^{2M} + \left(\frac{1 + e^{iN\phi}}{2} \right)^{2M} \right]^2 \right],$$

which leads to a expression for $\delta\phi$ showing a non trivial ϕ dependence.

We would like to compare this measurement strategy with NOON state case and compare the different $\delta\phi_{min}$, that is, those computed in the phase value for which they reach its minimum.

Several numerical studies have been performed, in particular: $N = 4$ and $N = 20$ with different M and $n = M$.

First of all it is interesting observing the behaviour of the $\delta\phi_{min}$ for $N = 1$ and different M as a function of the quantum efficiency for the fixed value of ϕ_{min} , see Fig. (5.2). For value of η reaching 1 the precision increases as M becomes larger, while for lower value of η we can see how it is not always convenient to increase M (see also Fig. 5.3). Anyway, when more photons are involved, these states become more sensitive to loss, as can be again seen in Fig. (5.2), where $\delta\phi^{-1}$ starts to grow for high values of η , while for $M = 4$ sensitivity starts to increase very soon.

Coming back to fixed energy case we have this behaviour: for $NM = 4$ (Fig. 5.4) the curves are almost the same until a certain value of η and the

5.1. NOON-LIKE State

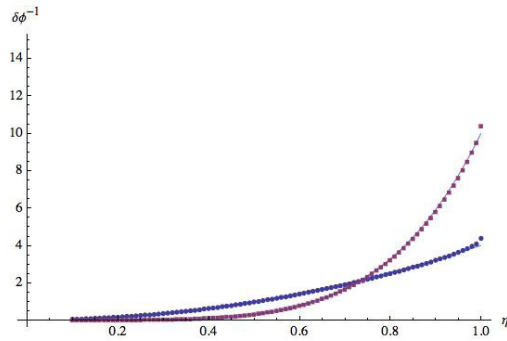


Figure 5.2: Plot of the $\delta\phi_{min}^{-1}$ as a function of the quantum efficiency η . Cases under consideration for the measure of A_{NM} : $M = 4, N = 1$ (points), $M = 10, N = 1$ (square). Superimposed continuous curves are NOON state with equal photon number.

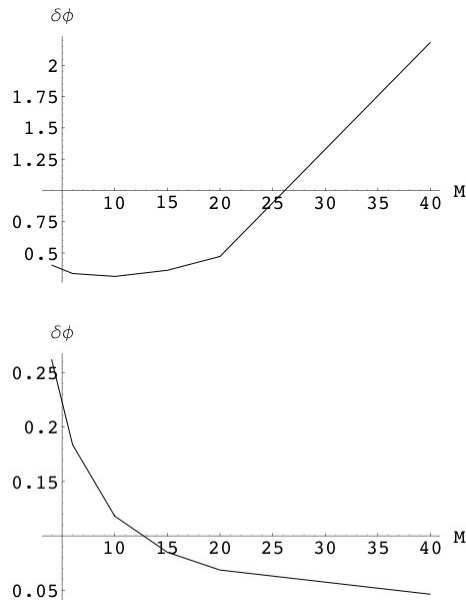


Figure 5.3: Top: Plot of the $\delta\phi_{min}$ as a function of M for $\eta = 0.8$, with $N = 1$. Increasing energy, namely in this case increasing M , is not always opportune. Bottom: Plot of the $\delta\phi_{min}$ as a function of M for $\eta = 0.97$, with $N = 1$. In this case increasing M improves precision.

highest value for $\delta\phi_{min}$ is reached when $M = 1$ and $N = 4$ as expected, for this state shows much more entanglement. These results anyway do not mean necessarily that NOON-like is not a good state, rather they tell us that we should consider a more efficient measurement strategy, infact the observable

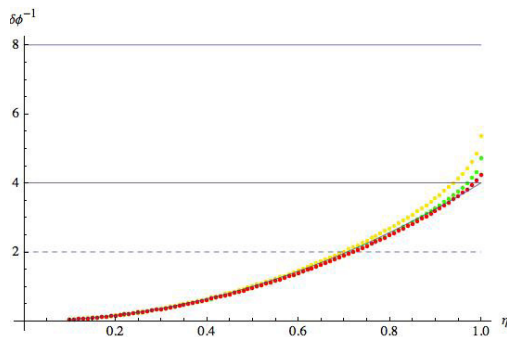


Figure 5.4: (Color on line). Plot of the $\delta\phi_{min}^{-1}$ as a function of the quantum efficiency η . Cases under consideration for the measure of A_{NM} : $M = 4, N = 1$ (red), $M = 2, N = 2$ (green), $M = 1, N = 4$ (yellow) and 4 photons NOON state (continuous curve). Dashed line is ideal shot noise $1/\sqrt{NM}$, continuous line is ideal Heisenberg Limit $1/MN$. See text for details.

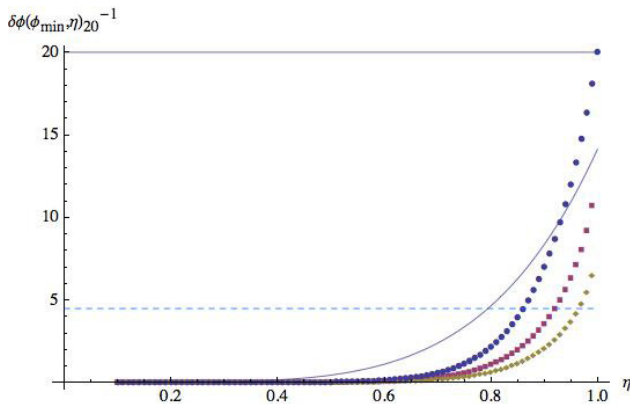


Figure 5.5: Measure of A_M : behaviour of $\delta\phi_{min}^{-1}$ as a function of η for different bunching of the fixed number of photons involved ($NM = 20$). $M = 1, N = 20$ (blue points), $M = 2, N = 10$ (violet square), $M = 5, N = 4$ (yellow turbots). Dotted curve is $\delta\phi_{M\ NOON} = \frac{1}{\sqrt{\eta^{NMN}}}$, corresponding to M unentangled N photons NOON state. Lines are Heisenberg limit (continuous) and shot noise limit (dashed) for a $NM=20$ photons NOON state.

(5.14) cannot extract information from other terms appearing in the expression (5.12) of the evolved density operator for the NOON-like state.

Actually these results are suitable only for the $M = 1$ case, for which the evolved density matrix is truly NOON-like:

$$\eta^N |\psi'\rangle_\phi \langle\psi'|_\phi + \rho_{MIX} \otimes |0\rangle\langle 0|^{\otimes 2} + |0\rangle\langle 0|^{\otimes 2} \otimes \rho_{MIX} \quad (5.25)$$

with $\rho_{MIX} = \sum_{i=0}^{N-1} \eta^i (1 - \eta)^{N-i} \frac{1}{2} [|i, 0\rangle\langle i, 0| + |0, i\rangle\langle 0, i|]$; this term does not

5.1. NOON-LIKE State

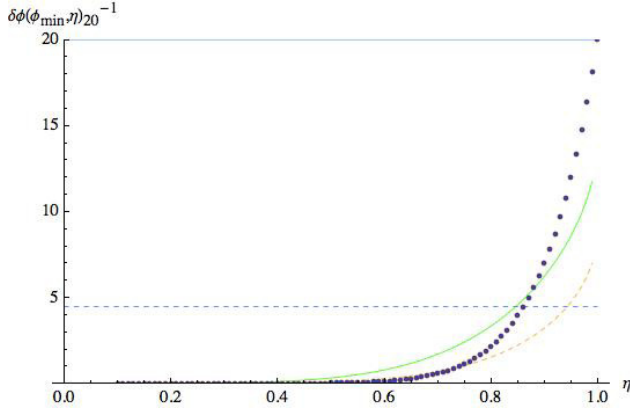


Figure 5.6: Same case as the previous figure. Now loss is applied to $n \geq \frac{M}{2}$ groups of photons. Blue points are NOON state, continuous green curve is for $N = 10, M = 2$. Dashed yellow curve is for $N = 5, M = 4$.

contribute to phase information. $|\psi'\rangle$ is the NOON-like state (5.2). This case is as the same as that of a single NOON state, for which you have:

$$\eta^N \rho(\phi)_{NOON} + \rho_{MIX} \quad (5.26)$$

and for which even the loss of one single photon is crucial (see section 4.3.2).

Measure of A_M

We now measure a more intuitive observable:

$$A_M = A_N^{\otimes M} \otimes |0\rangle \langle 0|^{\otimes 2M} + |0\rangle \langle 0|^{\otimes 2M} \otimes A_N^{\otimes M}, \quad (5.27)$$

where A_N is the usual observable (5.14) for the NOON state measurement. Again we apply loss to every mode and from the previous results we can easily obtain the expression

$$\delta\phi_{A_M} = \frac{\eta^{MN} (1 - \eta^{MN} \cos^{2M} N\phi)}{|-MN\eta^{MN} \cos(N\phi)^{M-1} \sin N\phi|}. \quad (5.28)$$

We can see $\delta\phi$ plotted in Fig.(5.5), for a fixed value of $MN = 20$; this strategy allows recognizing differences in precision when a different grouping is employed, but unfortunately increasing M does not help in having more robustness.

It has also been inserted $\delta\phi_{M\ NOON} = \frac{1}{\sqrt{\eta^{NMN}}}$ for a NM photon state of type (4.32) in which M NOON state are grouped without entangling them. In Fig. (5.6) we have the result for the case in which lossy map has been applied to $n = \frac{M}{2} < M$ group of photons. Note how the sensitivity to loss changes;

curves intersect not only the NOON state curve (black), but also the respective more sensitive curve corresponding to smaller M .

At this point it is important to use these results and compare them with the interesting maximally entangled state presented previously in chapter 4, the *m&m state*. We will see how it is fundamental to consider a suitable measurement which is able to preserve information in the presence of loss.

Comparison with m&m

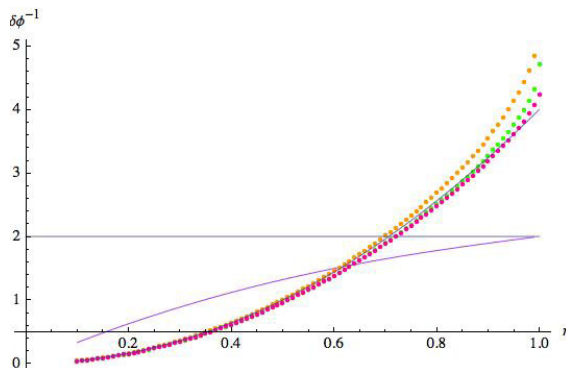


Figure 5.7: (Color on line) Continuous curve is $\delta\phi_{min}^{-1}$ for *m&m* state with $m = 3$, $m' = 1$. Points curves are NOON-like for the measure of A_{NM} and superimposed continuous curve to points curves is 4 photons NOON state. *m&m* is actually more robust.

In Fig. (5.7) and (5.8) the comparison with the *m&m state* previously introduced in chapter 4 is presented. As expected, this last state is more robust, thanks also to the particular chosen observable (see Eq. (4.62)) which is able to retrieve information from all the terms carrying information in the evolved density matrix (4.59), see section 4.5.

5.2 Comments

In the last two chapters we have investigated the behaviour of partially entangled states for bosonic systems in phase estimation problem. The idea of bunching photons, as explained in [29] has been translated for our systems in which photons have been squeezed in Fock states. In practice we tried to exploit the resource coming not only from single probes, namely photons, but also from the fact that they could be grouped in a single field mode.

In this way we have tried to translate what it was obtained with qubit in quantum metrology (see section 1.3) in the presence of bosonic field modes.

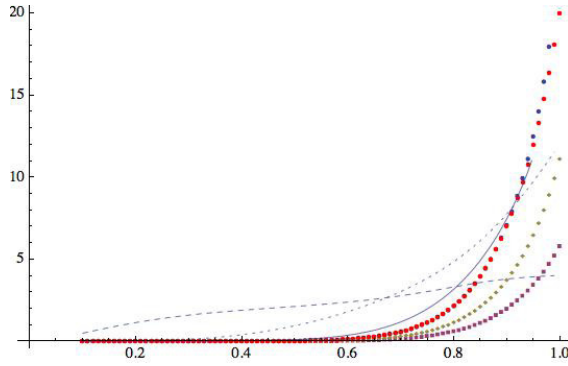


Figure 5.8: (Color on line) In this case we report the curves for 20 photons states. Points curves are NOON-like for the measurement of A_M . Dashed curve and dotted curve are respectively $m&m$ states with $m = 12, m' = 8$ and $m = 16, m' = 4$. Continuous curve is $m&m$ state with $m = 19, m' = 1$. It is worth to notice that $m&m$ states become more robust as photons are stolen from the mode populated by $m > m'$ photons, in practice as their structure aways from NOON-state.

The counterpart of the maximally entangled state (1.17)

$$|\Psi\rangle = \frac{1}{\sqrt{2}} \left(|\lambda_m\rangle_1 \cdots |\lambda_m\rangle_N + |\lambda_M\rangle_1 \cdots |\lambda_M\rangle_N \right) \quad (5.29)$$

becomes the NOON state

$$\frac{1}{\sqrt{2}} (|N, 0\rangle + |0, N\rangle). \quad (5.30)$$

We conclude by saying that the idea of bunching the photons as explained in this chapter must be considered carefully when applied to several physical systems. For example, in interferometry, it does not include the possibility to employ states as $m&m$ states, as these states describe a bipartite system while the idea of bunching necessarily force to consider multimode systems; as explained in the beginning of this chapter, the bunching rather takes into account multipartite entangled states preserving the NOON state form.

It would be anyway possible to make the following formal equivalence in order to build a physical encoding of logical information:

$$|0\rangle^{\otimes(m-m')} \equiv |m, m'\rangle \quad (5.31)$$

$$|1\rangle^{\otimes(m-m')} \equiv |m', m\rangle. \quad (5.32)$$

In next chapter we will deal with results belonging to general quantum estimation theory applied to standard interferometry problems.

Chapter 6

Robustness in absolute phase estimation

In his pioneering works [30] Holevo found out the optimal covariant estimation strategy thanks to which it is possible to give the optimal input phase state [49, 80], namely the state that gives an estimation as good as possible.

It has been suggested to make use of such results, for example, in adaptive single shot measurements [75] which seems to be an alternative and more powerful way for phase measurements for at least two reasons: it is not necessary to measure another observable, as for example happens in Homodyne tomography [78], and it is exploited the possibility to adjust the phase of a local oscillator by a feedback loop.

Unfortunately a purely quantum measurement of this type is impossible to be physically realized for it would require an unfeasible quantum canonical phase measurement [77].

In interferometry the task of finding the optimal quantum measurement [73, 76] and optimal quantum state [74] is also needed in order to enhance precision in phase shift estimation, in particular in the paradigm of the global QET.

Adaptive measurements are important also in this case for it is not possible to perform the optimal interferometric measurement and it has been demonstrated that such theoretical measurement can be in good agreement with results of ideal canonical measurements.

Anyway, to the best of our knowledge, such analysis are lead ignoring the effect of noise and loss of photons. Only very recently *Dorner et al.* [82] have performed an optimization by means of the Local QET showing an approximated form of the optimal state characterized by a strong robustness to loss in an interferometric framework. In this chapter we present an analysis of quantum phase measurement in the presence of noise for single mode photon optimal phase state and a suggestion for an interferometric apparatus is given.

6.1 Canonical phase measurement

This section is devoted to the introduction of the concept of a particular phase measurement which will be employed in a lossy scheme. We will also encounter the *optimal phase state* which permits to have an estimation at the Heisenberg limit.

In QET, one typically searches for the optimal POVM that minimizes the variance of an estimator¹. Actually the variance is not the only figure of merit that can be used, for the phase parameter it is also possible to define the so called Holevo variance [30], we will see anyway that for our purpose, it will be enough to consider the most common variance as a measure of uncertainty.

Considering the optical domain, the POVM Eq. (1.25) in the single mode case becomes $d\Pi(\phi) = \frac{d\phi}{2\pi} |\phi\rangle\langle\phi|$, where $|\phi\rangle$ is the normalizable vector $|\phi\rangle = \sum_{n=0}^{\infty} e^{in\phi} |n\rangle$, and $|n\rangle$ are Fock states. As it has been demonstrated by *D. T. Pegg* and *S. M. Barnett* in [79], it is possible to define the discrete version of the optimal covariant phase measurement in place of the one proposed by Holevo in which the phase variable runs continuously from 0 to 2π .

If one considers the following discrete set of phases: $\phi_m = \frac{2\pi}{N+1}m$, $m = 0, \dots, N$, the completeness relation can also be satisfied employing the orthonormal basis of the Hilbert space:

$$\{|\phi_m\rangle = \frac{1}{\sqrt{N+1}} \sum_{n=0}^N e^{in\phi_m} |n\rangle, \quad m = 0, \dots, N\}. \quad (6.1)$$

The measurement described by the POVM

$$|\phi_m\rangle\langle\phi_m| \quad (6.2)$$

is actually a projective one and is called *canonical phase measurement* [77]. From this result one can obtain the optimal input phase state which gives the minimum uncertainty achievable, namely the $N/2$ photons state:

$$|\varphi_{\text{opt}}\rangle = \sqrt{\frac{2}{N+1}} \sum_{n=0}^N \sin\left(\frac{n + \frac{1}{2}}{N+1}\pi\right) |n\rangle. \quad (6.3)$$

We will now study the behaviour of such a state when evolved by the loss map through a strategy employing this canonical measurement.

6.2 Robust strategy

Now that the measurement of the phase has been explained, we can show in detail the strategy that presents, as we will see, the feature of being robust to loss. The ideal case will be presented initially.

¹Given a sample $\phi_1, \phi_2, \dots, \phi_N$ of size N , an estimator $\hat{\phi}$ for the parameter ϕ is a function $\hat{\phi}(\phi_1, \phi_2, \dots, \phi_N)$.

6.2.1 Ideal measurement

We let $|\varphi_{ott}\rangle$ accumulate a phase obtaining:

$$|\varphi_{ott}\rangle_\phi = \sqrt{\frac{2}{N+1}} \sum_{n=0}^N \sin\left(\frac{n+\frac{1}{2}}{N+1}\pi\right) e^{in\phi} |n\rangle, \quad (6.4)$$

then we perform a canonical phase measurement onto the state (6.4) which gives the outcomes ϕ_m .

We evaluate

$$p(\phi_m|\phi) = |\langle\varphi_{ott}|\phi_m\rangle|^2, \quad (6.5)$$

namely the conditioned probability to obtain ϕ_m if the input state accumulated a phase ϕ . From Eq.(6.5) we obtain the first two moments of the statistic and

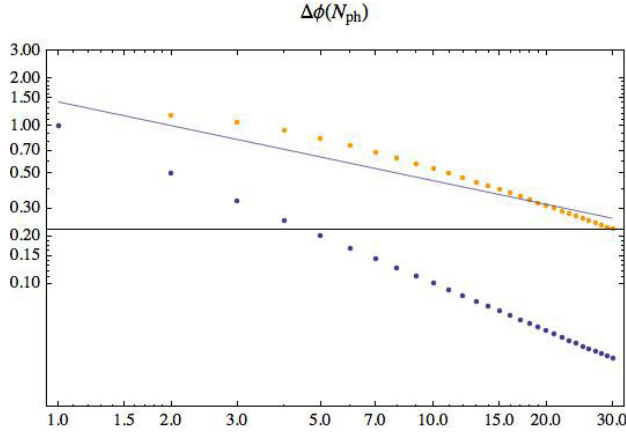


Figure 6.1: Bi-logarithmic scale. Dotted line represents SN, blue points the HL. Orange points crossing SN are $\overline{\Delta\phi}$ of Eq. (6.7). I remind that in this case we have to compare with $\frac{N}{2}$ photoh states for $\langle\phi_{ott}|a^\dagger a|\phi_{ott}\rangle = \frac{N}{2}$.

the variance of the phase, which in this case is treated as an operator:

$$\begin{aligned} \langle\phi\rangle_\phi &= \sum_{m=0}^N \phi_m p(\phi_m|\phi) \\ \langle\phi^2\rangle_\phi &= \sum_{m=0}^N \phi_m^2 p(\phi_m|\phi) \\ (\Delta\phi_\phi)^2 &= \langle\phi^2\rangle_\phi - \langle\phi\rangle_\phi^2. \end{aligned} \quad (6.6)$$

At this point an average over the phases is performed:

$$\overline{\Delta\phi} := \frac{1}{2\pi} \int_0^{2\pi} \sqrt{(\Delta\phi_\phi)^2}. \quad (6.7)$$

Its behaviour as a function of energy is plotted in Fig. (6.1). We can see that there is a crossing over the SN limit for a certain value ($\simeq 25$) of the average photon number N , namely, as expected, for large N , the precision scales as $1/N$. Now we perform a lossy analysis and we will focus on the values of the energy for which one has an estimation over the SN.

6.2.2 Noisy measurement

Taking into account also the effect of the loss of photons, defining $\rho(\phi)_{ott} := |\varphi_{ott}\rangle_{\phi} \langle \varphi_{ott}|$ we have the evolved state,

$$\begin{aligned} \mathcal{L}[\rho(\phi)_{ott}] &= \frac{2}{N+1} \sum_{n,m=0}^N \sum_{j=0}^{\min(n,m)} \sin\left(\frac{(n+\frac{1}{2})\pi}{N+1}\right) \sin\left(\frac{(m+\frac{1}{2})\pi}{N+1}\right) \\ &\quad \eta^{\frac{n+m}{2}-j} (1-\eta)^j \sqrt{\binom{m}{j} \binom{n}{j}} e^{i(n-m)\phi} |n-j\rangle \langle m-j|, \end{aligned} \quad (6.8)$$

obtained by applying the lossy map described in section 4.2.

We compute $p_{\eta}(\phi_m|\phi) = \langle \phi_m | \mathcal{L}[\rho(\phi)_{ott}] | \phi_m \rangle$ and employ the same argument of the previous section.

Now we have:

$$\begin{aligned} \langle \phi \rangle_{\phi,\eta} &= \sum_{m=0}^N \phi_m p_{\eta}(\phi_m|\phi) \\ \langle \phi^2 \rangle_{\phi,\eta} &= \sum_{m=0}^N \phi_m^2 p_{\eta}(\phi_m|\phi) \\ (\Delta \phi_{\phi,\eta})^2 &= \langle \phi^2 \rangle_{\phi,\eta} - \langle \phi \rangle_{\phi,\eta}^2. \end{aligned} \quad (6.9)$$

Averaging we define:

$$\overline{\Delta \phi_{\eta}} := \frac{1}{2\pi} \int_0^{2\pi} \sqrt{(\Delta \phi_{\phi,\eta})^2}. \quad (6.10)$$

In fig.(6.2) we have plotted the standard deviation $\overline{\Delta \phi_{\eta}}$ as a function of η and we can see the crossing of the SN curve.

We have compared our strategy with the one in which, as the input state that undergoes noisy map, the counterpart of the NOON state (blue points) in the single mode case is used, namely

$$\frac{1}{\sqrt{2}}(|0\rangle + e^{iN\phi}|N\rangle). \quad (6.11)$$

and the observable $A = |0\rangle \langle N| + |N\rangle \langle 0|$ is measured. The minimum detectable phase error $\delta\phi_{min}$ in this case is:

$$\delta\phi_{min} = \frac{1}{N\eta^{N/2}} \sqrt{1/2(1 + \eta^N + (1 - \eta)^N)}. \quad (6.12)$$

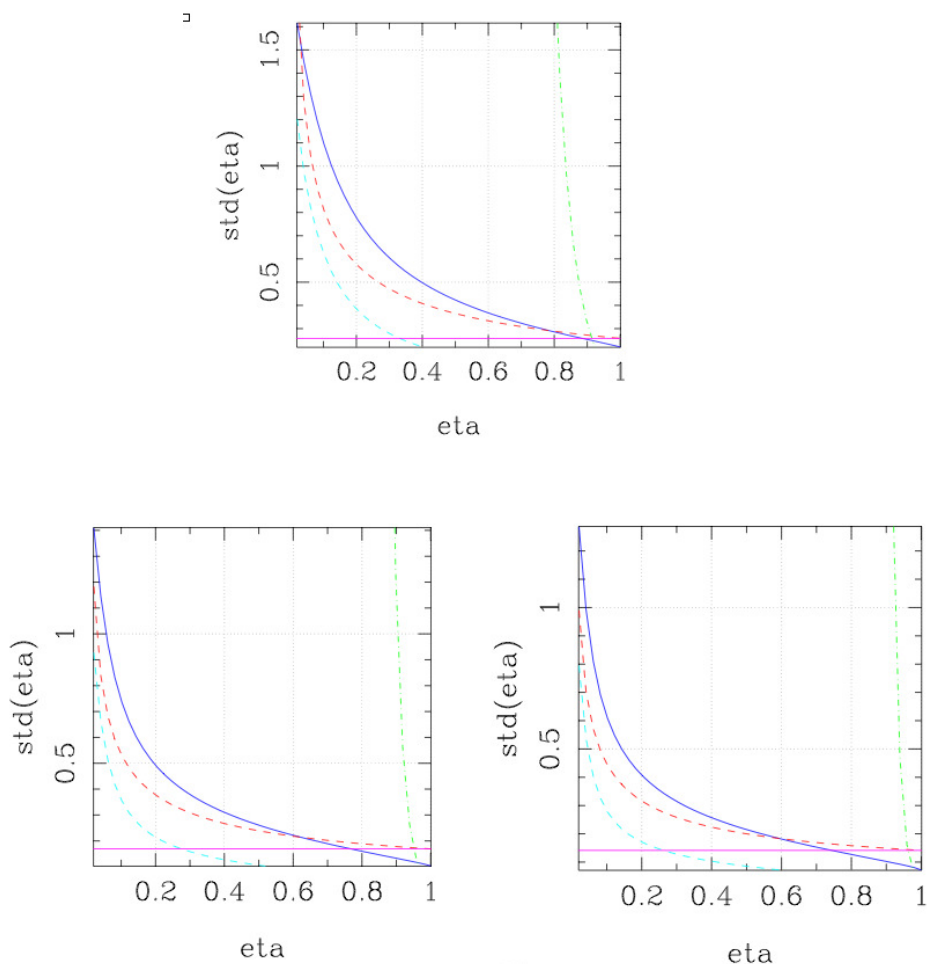


Figure 6.2: Averaged phase standard deviation $\overline{\Delta\phi}_\eta$ of Eq. (6.10) (Blue continuous curve) as a function of the quantum efficiency η with $N = 30$ (top) $N = 70$ (bottom left) and $N = 100$ (bottom right). Red dashed curve is SN, Green dashed and dotted curve is the function $\delta\phi = \frac{1}{N\eta^{N/2}}$ which for large values of N approximates the function (6.12). The cyan dashed line is the function (6.9) computed in the phase value for which it reaches the minimum. Note how, as far as N increases, the threshold η value for which $\overline{\Delta\phi}_\eta$ crosses the SN becomes lower and lower.

This result attests that the state $|\varphi_{out}\rangle_\phi$ behaves in robust way against loss of photons. That the strategy is overall a good one is also due to the fact that we have considered an average standard deviation, which means that there will be some phase values for which the crossing over the SN will be more considerable. This can be seen in figs. (6.2) and (6.3) where the behaviour of

the standard deviation (6.9) is also computed in its minimum.

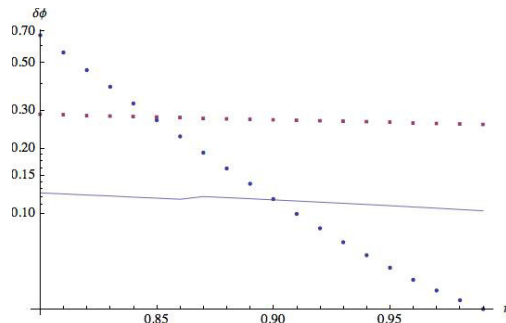


Figure 6.3: Logarithmic ordinate. $N = 30$. Plot of $\Delta\phi_{\phi,\eta}$ evaluated in its minimum for the phase as a function of η (continuous line). Points are $\delta\phi_{min}$ of Eq. (6.12) while squares are SN. η starts from 0.8.

An exhaustive lossy analysis is far from being completed and most of the work presented in the literature neglects the problem of noise. The same arguments hold if we move to interferometric framework. We will give a little contribution to this task presenting a preliminary example in which we will find again the required property of robustness in the next conclusive section.

6.3 Towards interferometric framework

This chapter has shown a preliminary result that gives a better understanding of the problem of estimation in the presence of noise in the optical domain. The most interesting consideration to hold should be that the POVM (6.2), when employed with the mixed state (6.8), can give a strategy robust to loss.

A rigorous treatment would expect to consider an input mixed state and to search for the optimal POVM as QET would require (see section 1.3.1).

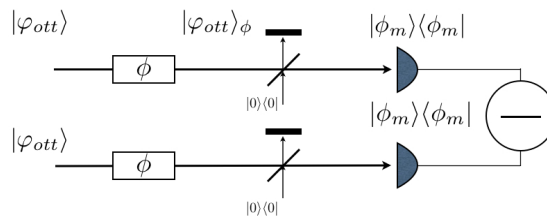


Figure 6.4: (Color on line) Interferometric set-up for the estimation of the phase shift in presence of noise

We have given a contribution to the first step, namely to beat the SN, a robust analysis at the HL is the necessary perspective.

Turning to the interferometric framework, it is possible to see such a beating of the SN in a very simple way: in the two arms of an inteferometer, see Fig.(6.4), are injected two optimal phase states $|\varphi_{opt}\rangle$ (6.3), both arms suffer a phase evolution and a canonical phase measurement is performed in each mode. Then the difference of the experimental data coming from both light fields is taken.

We compare our results of the standard deviation also showing its behaviour in the phase value for which it reaches its minimum. In fig.(6.5) we have also

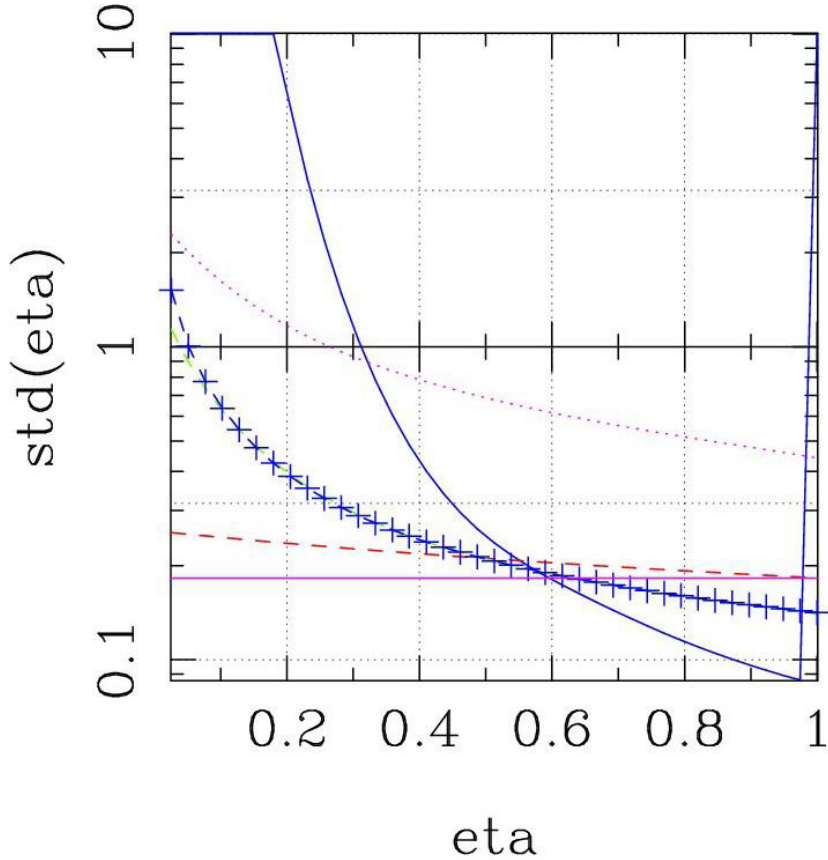


Figure 6.5: (Color on line) Semilogarithmic scale. Continuous blue line is $m\&m$ state with $m = 21$, $m' = 9$. Dashed line with + is the case of two optimal phase state as input state of an interferometer in which has been considered the minimum phase detectable error. Point line is the same case but for the average over ϕ . Dashed red curve is shot noise. Continuous pink line is ideal shot noise, namely in absence of loss.

inserted the behaviour of the $m\&m$ states and we can observe how robust this

state is.

This interferometric strategy shows its quantum features for the crossing of the shot noise limit, anyway, it does not seem to be as robust as we would expect. A deeper analysis similar to the very recent one performed by *U. Dorner et al.* in [39] will have to be done.

Conclusions

In the present work I have investigated the behaviour of multipartite entangled states in quantum optics when employed in the estimation of the damping constant in the continuous variable domain and in the estimation of the phase parameter in the discrete variable domain.

Concerning the problem of the damping constant estimation, I have studied how entangled Gaussian states can give in principle a better estimation than the one where unentangled states are employed. In this case the problem of noise has been neglected. Together with this problem of characterization of dissipative media, I have dealt with the general task of quantum metrology which has been specialized to the bosonic field. I have introduced the problem of estimation, in the presence of noise, of the phase shift in multipartite interferometry and of the absolute value of the phase in a single mode. I analyzed several types of non classical states. Some are reproducible in laboratory (as the Gaussian states), others were introduced to test our proposal of photon bunching (consider the *NOON-like* introduced in chapter 4) or taken from known results in quantum estimation theory (QET). These states have given surprising results, even in the case of lossy systems. The robustness to the loss of photons has been qualitatively demonstrated for some states, and quantitatively demonstrated for a particular known state.

A brief summary of the thesis follows. After an introduction to the main concepts of QET specialized for the phase parameter, I have shown how the shot noise limit can be beaten with Fock state interferometry, refining the result presented in [42]. **Chapter I** concludes with a dissertation on the problem of the deterministic measurements which cannot currently be performed. I explained how to interpret experimental results in the discrete variable domain presented in literature and how such measurements are actually *demonstrations of principle*. **Chapter II** has been devoted to give the most important properties of Gaussian states, I have presented our first original result in **Chapter III**. It consists in the behaviour of an entangled Gaussian state compared to that of a single mode Gaussian state in the characterization of dissipative media.

When one is interested in obtaining some information about the property of

absorption of some media, one typically measures the intensity of the damped field of light emerging from the medium. I have shown that it would be possible to obtain more precise information putting little energy in the medium and exploiting the entanglement that rises when a simple beam splitter is inserted in the optical set-up. This is a very interesting result showing a new use for entanglement. Our result is currently of theoretical interest only, because a measurement strategy has not been considered; this will be an obvious development of the work presented in this chapter. Moreover, on this task, a systematic analysis must be done and a powerful and fruitful application of QET, as has been done in phase estimation problem, has to be performed.

In **Chapter IV** I have introduced heuristically the problem of quantum metrology with loss when photons are employed as probes. Certainly a more formal analysis of this task is necessary. I presented NOON states and I have explained the reason why they are so sensitive to loss. From this, I introduced the idea of groupings photons as a possible strategy to obtain robust states and I presented the potentiality of the *MN loss* state calculating the evolved density matrix under loss map. After this result, I gave the behaviour of the more suitable NOON-like state for phase estimation, and this has been done in **Chapter V**. Such multipartite partially entangled state actually presents the feature of robustness, but it has not been possible to show this in a quantitative way. Again, by studying the evolution of the density matrix of this newer state under the noise, I have recognized in the form of the analytically evaluated output mixed state, the presence of several where the information on the phase survives despite of the noise. In the final section of this chapter I have analyzed the *m&m* states. These states needed a special mention because they are an example of a MES robust to loss of photons which are not considered as individual probes since they are bunched in a single bosonic mode. This means that a MES, in quantum optics, is not necessarily highly sensitive to loss as it might be expected.

Finally in **Chapter VI** the most important result of the present work is presented. I have proved that it is possible to obtain a measurement of the absolute value of the phase in a single mode case in a way that is robust to the loss of photons. This measurement employs the optimal POVM, due to Holevo, which minimizes a suitable cost function and the optimal phase state, which allows to reach the Heisenberg limit in the ideal case, namely no loss. In this way it becomes evident that QET will give the main contribution to find the necessary optimal robust measurement since the sensitivity to loss of our proposed strategy is not dramatic and seems promising! Only very recently an investigation on this task in the interferometric domain has began. Such result, from this point of view, must be considered as preliminary result, since it suggests a strategy to reconstruct the absolute value of the phase, not the phase shift in an interferometer.

Further efforts in applying QET in the presence of noise to multi mode interferometry will be the next step to be done. In this way it will be possible to

Conclusions

give a deterministic description of measurement and it will be possible extract as much information as possible from the employed state in the estimation strategy.

Symplectic transformations

It seems to us necessary to give some notion about symplectic transformation for their binding with Gaussian states. Let us first consider a classical system of n particles described by coordinates (q_1, \dots, q_n) and conjugated momenta (p_1, \dots, p_n) . If H is the Hamiltonian of the system, the equation of motion are given by

$$\dot{q}_k = \frac{\partial H}{\partial p_k}, \quad \dot{p}_k = -\frac{\partial H}{\partial q_k}, \quad (k = 1, \dots, n) \quad (\text{A.1})$$

where \dot{x} denotes time derivative. The Hamilton equations can be summarized as

$$\dot{\mathbf{R}}_k = \Omega_{kl} \frac{\partial H}{\partial R_l}, \quad \dot{\mathbf{S}}_k = -\mathbf{J}_{kl} \frac{\partial H}{\partial S_l}, \quad (\text{A.2})$$

where \mathbf{R} and \mathbf{S} are vectors of coordinates ordered as the vectors of canonical operators in section (2.1), whereas Ω and \mathbf{J} are the symplectic matrices defined in Eq. (2.4) and Eq. (2.6), respectively. The transformations of coordinates $\mathbf{R}' = \mathbf{F}\mathbf{R}$, $\mathbf{S}' = \mathbf{Q}\mathbf{S}$ are described by matrices

$$F_{kl} = \frac{\partial R'_k}{\partial R_l}, \quad Q_{kl} = \frac{\partial S'_k}{\partial S_l}, \quad (\text{A.3})$$

and lead to

$$\dot{R}'_k = F_{ks} \Omega_{st} F_{lt} \frac{\partial H}{\partial R_l}, \quad \dot{S}'_k = -Q_{ks} \mathbf{J}_{st} Q_{lt} \frac{\partial H}{\partial R_l}. \quad (\text{A.4})$$

Equations of motion thus remain invariant iff

$$\mathbf{F} \Omega \mathbf{F}^T = \Omega, \quad \mathbf{Q} \mathbf{J} \mathbf{Q}^T = \mathbf{J}, \quad (\text{A.5})$$

which characterize symplectic transformations and, in turn, describe the canonical transformations of coordinates. Notice that the identity matrix and the symplectic forms themselves satisfies Eq. (A.5).

Let us now focus our attention on a quantum system of n bosons, described by the mode operators \mathbf{R} or \mathbf{S} . A mode transformation $\mathbf{R}' = \mathbf{F}\mathbf{R}$ or $\mathbf{S}' = \mathbf{Q}\mathbf{S}$ leaves the kinematics invariant if it preserves canonical commutation relations (2.3) or (2.5). In turn, this means that the $2n \times 2n$ matrices \mathbf{F} and \mathbf{Q} should satisfy the symplectic condition (A.5). Since $\mathbf{\Omega}^T = \mathbf{\Omega}^{-1} = -\mathbf{\Omega}$ from (A.5) one has that $\text{Det}[\mathbf{F}]^2 = 1^1$ and therefore \mathbf{F}^{-1} exists. Moreover, it is straightforward to show that if \mathbf{F} , \mathbf{F}_1 and \mathbf{F}_2 are symplectic then also \mathbf{F}^{-1} , \mathbf{F}^T and $\mathbf{F}_1\mathbf{F}_2$ are symplectic, with $\mathbf{F}^{-1} = \mathbf{\Omega}\mathbf{F}^T\mathbf{\Omega}^{-1}$. Analogue formulas are valid for the \mathbf{J} -ordering. Therefore, the set of $2n \times 2n$ real matrices satisfying (A.5) form a group, the so-called *symplectic group* $\text{Sp}(2n, \mathbb{R})$ with dimension $n(2n + 1)$. Together with phase-space translation, it forms the *affine* (inhomogeneous) symplectic group $\text{ISp}(2n, \mathbb{R})$. If we write a $2n \times 2n$ symplectic matrix in the block form

$$\mathbf{F} = \begin{pmatrix} \mathbf{A} & \mathbf{B} \\ \mathbf{C} & \mathbf{D} \end{pmatrix}, \quad (\text{A.6})$$

with \mathbf{A} , \mathbf{B} , \mathbf{C} , and \mathbf{D} $n \times n$ matrices, then the symplectic conditions rewrites as the following (equivalent) conditions

$$\begin{cases} \mathbf{A}\mathbf{D}^T - \mathbf{B}\mathbf{C}^T = \mathbb{1} \\ \mathbf{A}\mathbf{B}^T = \mathbf{B}\mathbf{A}^T \\ \mathbf{C}\mathbf{D}^T = \mathbf{D}\mathbf{C}^T \end{cases}, \quad \begin{cases} \mathbf{A}^T\mathbf{D} - \mathbf{C}^T\mathbf{B} = \mathbb{1} \\ \mathbf{A}^T\mathbf{C} = \mathbf{C}^T\mathbf{A} \\ \mathbf{B}\mathbf{D}^T = \mathbf{D}^T\mathbf{B} \end{cases}. \quad (\text{A.7})$$

The matrices $\mathbf{A}\mathbf{B}^T$, $\mathbf{C}\mathbf{D}^T$, $\mathbf{A}^T\mathbf{C}$, and $\mathbf{B}^T\mathbf{D}$ are symmetric and the inverse of the matrix \mathbf{F} writes as follows

$$\mathbf{F}^{-1} = \begin{pmatrix} \mathbf{D}^T & -\mathbf{B}^T \\ -\mathbf{C}^T & \mathbf{A}^T \end{pmatrix}. \quad (\text{A.8})$$

For a generic real matrix the polar decomposition is given by $\mathbf{F} = \mathbf{T}\mathbf{O}$ where \mathbf{T} is symmetric and \mathbf{O} orthogonal. If $\mathbf{F} \in \text{Sp}(2n, \mathbb{R})$ then also $\mathbf{T}, \mathbf{O} \in \text{Sp}(2n, \mathbb{R})$. A matrix \mathbf{O} which is symplectic and orthogonal writes as

$$\mathbf{O} = \begin{pmatrix} \mathbf{X} & \mathbf{Y} \\ -\mathbf{Y} & \mathbf{X} \end{pmatrix}, \quad \begin{cases} \mathbf{X}\mathbf{X}^T + \mathbf{Y}\mathbf{Y}^T = \mathbb{1} \\ \mathbf{X}\mathbf{Y}^T - \mathbf{Y}\mathbf{X}^T = \mathbf{0} \end{cases}, \quad (\text{A.9})$$

which implies that $\mathbf{U} = \mathbf{X} + i\mathbf{Y}$ is a unitary $n \times n$ complex matrix. The converse is also true, *i.e.* any unitary $n \times n$ complex matrix generates a symplectic matrix in $\text{Sp}(2n, \mathbb{R})$ when written in real notation as in Eq. (A.9).

A useful decomposition of a generic symplectic transformation $\mathbf{F} \in \text{Sp}(2n, \mathbb{R})$ is the so-called *Euler decomposition*

$$\mathbf{F} = \mathbf{O} \begin{pmatrix} \mathbf{D} & \mathbf{0} \\ \mathbf{0} & \mathbf{D}^{-1} \end{pmatrix} \mathbf{O}', \quad (\text{A.10})$$

where \mathbf{O} and \mathbf{O}' are orthogonal and symplectic matrices, while \mathbf{D} is a positive diagonal matrix. About the real symplectic group in quantum mechanics see Refs. [87, 86], for details on the single mode case see Ref. [88].

¹Actually $\text{Det}[\mathbf{F}] = +1$ and never -1 . This result may be obtained by showing that if e is an eigenvalue of a symplectic matrix, than also e^{-1} is an eigenvalue [86].

Appendix **B**

Characteristic function

The characteristic function of a generic operator O has been introduced in Eq. (2.9). For a quantum state ϱ we have $\chi[\varrho](\boldsymbol{\lambda}) = \text{Tr}[\varrho D(\boldsymbol{\lambda})]$. In the following, for the sake of simplicity, we will sometime omit the explicit dependence on ϱ . The characteristic function $\chi(\boldsymbol{\lambda})$ is also known as the moment-generating function of the signal ϱ , since its derivatives in the origin of the complex plane generates symmetrically ordered moments of mode operators. In formula

$$(-)^q \frac{\partial^{p+q}}{\partial \lambda_k^p \partial \lambda_l^{*q}} \chi(\boldsymbol{\lambda}) \Big|_{\boldsymbol{\lambda}=0} = \text{Tr} \left[\varrho \left[(a_k^\dagger)^p a_l^q \right]_S \right]. \quad (\text{B.1})$$

For the first non trivial moments we have $[a^\dagger a]_S = \frac{1}{2}(a^\dagger a + a a^\dagger)$, $[a a^\dagger^2]_S = \frac{1}{3}(a^\dagger^2 a + a a^\dagger^2 + a^\dagger a a^\dagger)$, $[a^\dagger a^2]_S = \frac{1}{3}(a^2 a^\dagger + a^\dagger a^2 + a^\dagger a)$ [91]. In order to evaluate the symmetrically ordered form of generic moments, one should expand the exponential in the displacement operator

$$\begin{aligned} D(\boldsymbol{\lambda}) &= \sum_{k=0}^{\infty} \frac{1}{k!} (\lambda a^\dagger - \lambda^* a)^k = \sum_{k=0}^{\infty} \frac{1}{k!} \sum_{l=0}^k \binom{k}{l} \lambda^k \lambda_l^* [a^{\dagger k} a^l]_S \\ &= \sum_{k=0}^{\infty} \sum_{l=0}^{\infty} \frac{\lambda^k \lambda_l^*}{k! l!} [a^{\dagger k} a^l]_S. \end{aligned} \quad (\text{B.2})$$

We recall that the set of displacement operators $D(\boldsymbol{\lambda})$ with $\boldsymbol{\lambda} \in \mathcal{C}^n$ is complete, namely any generic operator O on the Hilbert space \mathcal{H} can be written as:

$$O = \int_{\mathcal{C}^n} \frac{d^{2n} \boldsymbol{\lambda}}{\pi^n} \text{Tr}[O D(\boldsymbol{\lambda})] D(\boldsymbol{\lambda})^\dagger, \quad (\text{B.3})$$

where $\chi[O](\boldsymbol{\lambda}) = \text{Tr}[O D(\boldsymbol{\lambda})]$. From this consideration it follows that for any pair of generic operators acting on the Hilbert space of n modes we have¹

$$\text{Tr}[O_1 O_2] = \frac{1}{\pi^n} \int_{\mathcal{C}^n} d^{2n} \boldsymbol{\lambda} \chi[O_1](\boldsymbol{\lambda}) \chi[O_2](-\boldsymbol{\lambda}), \quad (\text{B.4})$$

¹The computation is showed at the end of this section

which allows to evaluate a quantum trace as a phase-space integral in terms of the characteristic function. Other important properties of the characteristic function follow from the definition, for example we have $\chi[O](0) = \text{Tr}[O]$ and

$$\int_{\mathbb{C}^n} \frac{d^{2n}\boldsymbol{\lambda}}{\pi^n} |\chi[O](\boldsymbol{\lambda})|^2 = \text{Tr}[O^2]. \quad (\text{B.5})$$

We have seen that the introduction of the characteristic function allows to evaluate operators' traces as integrals in the phase space. This is useful in order to evaluate correlation functions and the statistics of a measurement since we are mostly dealing with Gaussian states and also many detectors are described by Gaussian operators.

Now we explicitly derive equality (B.4) for the trace of two generic operators in terms of their characteristic functions. The starting point is the Glauber expansions of an operator in terms of the characteristic, *i.e.* formula (B.3). For the characteristic function we have

$$\begin{aligned} \text{Tr}[O_1 O_2] &= \int_{\mathbb{C}^n} \frac{d^{2n}\boldsymbol{\lambda}_1}{\pi^n} \chi[O_1](\boldsymbol{\lambda}_1) \int_{\mathbb{C}^n} \frac{d^{2n}\boldsymbol{\lambda}_2}{\pi^n} \chi[O_2](\boldsymbol{\lambda}_2) \text{Tr}[D(\boldsymbol{\lambda}_1) D(\boldsymbol{\lambda}_2)], \\ &= \int_{\mathbb{C}^{2n}} \frac{d^{2n}\boldsymbol{\lambda}_1}{\pi^n} \frac{d^{2n}\boldsymbol{\lambda}_2}{\pi^n} \chi[O_1](\boldsymbol{\lambda}_1) \chi[O_2](\boldsymbol{\lambda}_2) \\ &\quad \times \text{Tr}[D(\boldsymbol{\lambda}_1 + \boldsymbol{\lambda}_2)] \exp\left\{\boldsymbol{\lambda}_1^\dagger \boldsymbol{\lambda}_2 - \boldsymbol{\lambda}_2^\dagger \boldsymbol{\lambda}_1\right\}, \\ &= \int_{\mathbb{C}^n} \frac{d^{2n}\boldsymbol{\lambda}}{\pi^n} \chi[O_1](\boldsymbol{\lambda}) \chi[O_2](-\boldsymbol{\lambda}), \end{aligned} \quad (\text{B.6})$$

where we have used the trace rule for the displacement $\text{Tr}[D(\boldsymbol{\gamma})] = \pi^n \delta^{(2n)}(\boldsymbol{\gamma})$.

To recover expression Eq. (2.15) is it sufficient to recall property (3.3).

Appendix C

A remark about parameters κ

In order to encompass the different notations used in the literature to pass from complex to Cartesian notation, we have introduced the three parameters κ_h , $h = 1, 2, 3$, in the decomposition of the mode operator, the phase-space coordinates and the reciprocal phase-space coordinates respectively. We report here again their meaning

$$a_k = \kappa_1(q_k + ip_k), \quad \alpha_k = \kappa_2(x_k + iy_k), \quad \lambda_k = \kappa_3(a_k + ib_k). \quad (\text{C.1})$$

The three parameters are not independent on each other and should satisfy the relations $2\kappa_1\kappa_3 = 2\kappa_2\kappa_3 = 1$, *i.e.* $\kappa_1 = \kappa_2 = (2\kappa_3)^{-1}$. The so-called canonical representation corresponds to the choice $\kappa_1 = \kappa_2 = \kappa_3 = 2^{-1/2}$, while the quantum optical convention corresponds to $\kappa_1 = \kappa_2 = 1$, $\kappa_3 = 1/2$. We have already seen that $2\kappa_2\kappa_3 = 1$; in order to prove that $2\kappa_1\kappa_3 = 1$, it is enough to consider the vacuum state of a single mode and evaluate the second moment of the “position” operator $\langle q^2 \rangle = \text{Tr}[\varrho q^2]$, which coincides with the variance $\langle \Delta q^2 \rangle$, since the first moment $\langle q \rangle = 0$ vanishes. Starting from the commutation relation $[q, p] = (2\kappa_1^2)^{-1}$ it is straightforward to show that the vacuum is a minimum uncertainty state with

$$\langle \Delta q^2 \rangle = (4\kappa_1^2)^{-1}. \quad (\text{C.2})$$

On the other hand, the so called Wigner¹ and the characteristic functions of a single-mode vacuum state are given by

$$W_0(x, y) = \frac{2}{\pi} \exp \left\{ -2\kappa_2^2(x^2 + y^2) \right\}, \quad \chi_0(a, b) = \exp \left\{ -\frac{1}{2}\kappa_3^2(a^2 + b^2) \right\}. \quad (\text{C.3})$$

¹The Wigner function is another fundamental quantity in quantum optics, for the present purposes it is enough recalling that it is defined as the Fourier transform of the characteristic function.

Therefore, using the properties of W as quasiprobability, and of χ as moment generating function, respectively, we have

$$\langle \Delta q^2 \rangle = \int_{\mathbb{R}^2} dx dy \kappa_2^2 x^2 W_0(x, y) = (4\kappa_2^2)^{-1}, \quad (\text{C.4a})$$

$$\langle \Delta q^2 \rangle = - \left. \frac{\partial^2}{\partial_a^2} \chi_0(a, b) \right|_{a=b=0} = \kappa_3^2, \quad (\text{C.4b})$$

from which the thesis follows, upon using Eqs. (C.2), (C.4a) and (C.4b) and assuming positivity of the parameters. Now, thanks to these results and denoting by $\boldsymbol{\sigma}_0 = \mathbf{V}_0 = (4\kappa_1^2)^{-1} \mathbb{1}_{2n} = (4\kappa_2^2)^{-1} \mathbb{1}_{2n} = \kappa_3^2 \mathbb{1}_{2n}$ the covariance matrix of the n -mode vacuum, we have that the characteristic and the Wigner functions can be rewritten as

$$\chi_0(\boldsymbol{\Lambda}) = \exp \left\{ -\frac{1}{2} \boldsymbol{\Lambda}^T \boldsymbol{\sigma}_0 \boldsymbol{\Lambda} \right\}, \quad \chi_0(\mathbf{K}) = \exp \left\{ -\frac{1}{2} \mathbf{K}^T \mathbf{V}_0 \mathbf{K} \right\}, \quad (\text{C.5})$$

and

$$W_0(\mathbf{X}) = \frac{\exp \left\{ -\frac{1}{2} \mathbf{X}^T \boldsymbol{\sigma}_0^{-1} \mathbf{X} \right\}}{(2\pi)^n \kappa_2^{2n} \sqrt{\text{Det}[\boldsymbol{\sigma}_0]}} = \left(\frac{2}{\pi} \right)^n \exp \left\{ -\frac{1}{2} \mathbf{X}^T \boldsymbol{\sigma}_0^{-1} \mathbf{X} \right\}, \quad (\text{C.6a})$$

$$W_0(\mathbf{Y}) = \frac{\exp \left\{ -\frac{1}{2} \mathbf{Y}^T \mathbf{V}_0^{-1} \mathbf{Y} \right\}}{(2\pi)^n \kappa_2^{2n} \sqrt{\text{Det}[\mathbf{V}_0]}} = \left(\frac{2}{\pi} \right)^n \exp \left\{ -\frac{1}{2} \mathbf{Y}^T \mathbf{V}_0^{-1} \mathbf{Y} \right\}, \quad (\text{C.6b})$$

respectively, independently on the choice of parameters κ_h . So we see that the vacuum is a Gaussian state.

Appendix D

Calculation of damped NOON-like

Consider the state (5.2):

$$|\psi'\rangle_\phi = \frac{1}{\sqrt{2}} \left(\bigotimes_{i=1}^M |\mathbf{N}_+\rangle_i \otimes |0\rangle^{\otimes 2M} + \bigotimes_{i=1}^M |0\rangle^{\otimes 2M} |\mathbf{N}_-\rangle_i \right), \quad (\text{D.1})$$

For $M = 1$ becomes:

$$|\psi'\rangle_\phi = \frac{1}{\sqrt{2}} (|\mathbf{N}_+\rangle \otimes |0\rangle^{\otimes 2} + |0\rangle^{\otimes 2} |\mathbf{N}_-\rangle) \quad (\text{D.2})$$

Let the projector $\rho := |\psi'\rangle_\phi \langle \psi'|_\phi$: we want to know the evolution of this state under a lossy channel, so let us apply the lossy beam splitters model to all 4 modes and consider the case in which the quantum efficiency is the same for every mode.

The evolved quantum state must be calculated in this way, for every mode we have: $\rho' = \mathbf{Tr}[U\rho \otimes |0\rangle \langle 0| U^\dagger] = \sum_{n=0}^{\infty} V_n \rho V_n^\dagger$, where $V_n := \left(\frac{1-\eta}{\eta}\right)^{n/2} \frac{a^n}{\sqrt{n!}} \eta^{\frac{a^\dagger a}{2}}$, and a is annihilation operator describing the mode of radiation impinging on the fictious beam splitters. So we have to consider 4 beam splitter.

First of all I write explicitly ρ : $\rho = \frac{1}{2} [|\mathbf{N}_+\rangle \langle \mathbf{N}_+| \otimes |0\rangle \langle 0|^{\otimes 2} + |0\rangle \langle 0|^{\otimes 2} \otimes |\mathbf{N}_-\rangle \langle \mathbf{N}_-| + |\mathbf{N}_+\rangle \langle 0|^{\otimes 2} \otimes |0\rangle^{\otimes 2} \langle \mathbf{N}_-| + |0\rangle^{\otimes 2} \langle \mathbf{N}_+| \otimes |\mathbf{N}_-\rangle \langle 0|^{\otimes 2}]$. The evolved density matrix ρ' is¹:

$$\begin{aligned} \frac{1}{2} \sum_{n_1=0}^{\infty} \sum_{n_2=0}^{\infty} \sum_{n_3=0}^{\infty} \sum_{n_4=0}^{\infty} V_{n_1} V_{n_2} V_{n_3} V_{n_4} & (|\mathbf{N}_+\rangle \langle \mathbf{N}_+| \otimes |0\rangle \langle 0|^{\otimes 2} + \\ & |0\rangle \langle 0|^{\otimes 2} \otimes |\mathbf{N}_-\rangle \langle \mathbf{N}_-| + |\mathbf{N}_+\rangle \langle 0|^{\otimes 2} \otimes |0\rangle^{\otimes 2} \langle \mathbf{N}_-| \\ & + |0\rangle^{\otimes 2} \langle \mathbf{N}_+| \otimes |\mathbf{N}_-\rangle \langle 0|^{\otimes 2}) V_{n_1}^\dagger V_{n_2}^\dagger V_{n_3}^\dagger V_{n_4}^\dagger. \end{aligned} \quad (\text{D.3})$$

¹ $\frac{1}{2}$ term will be omitted

I differentiate between diagonal elements and off diagonal elements: For the first ones, considering that lossy channel does not perturb the vacuum density matrix $\nu = |0\rangle\langle 0|$, we have just to compute the evolution under lossy map of the noon state, so we have:

$$(\eta^N |\mathbf{N}_+\rangle \langle \mathbf{N}_+| + \rho_{MIX}) \otimes \nu^{\otimes 2} \quad (\text{D.4})$$

and

$$\nu^{\otimes 2} \otimes (\eta^N |\mathbf{N}_-\rangle \langle \mathbf{N}_-| + \rho_{MIX}) \quad (\text{D.5})$$

with $\rho_{MIX} = \sum_{i=0}^{N-1} \eta^i (1-\eta)^{N-i} \frac{1}{2} [|i, 0\rangle \langle i, 0| + |0, i\rangle \langle 0, i|]$.

Concerning the off diagonal element I have to compute terms like the following: $\sum_{n=0}^{\infty} V_n |N\rangle \langle 0| V_n^\dagger$ where $|N\rangle$ now must be meant as a N photon fock state. These terms give a non zero expression only for the term with $n = 0$ and what is obtained is: $\eta^{N/2} |N\rangle \langle 0|$. At this point we compute:

$$\sum_{n_1=0}^{\infty} \sum_{n_2=0}^{\infty} \sum_{n_3=0}^{\infty} \sum_{n_4=0}^{\infty} V_{n_1} V_{n_2} V_{n_3} V_{n_4} |0\rangle^{\otimes 2} \langle \mathbf{N}_+| \otimes \underbrace{|\mathbf{N}_-\rangle \langle 0|}_{(*)}^{\otimes 2} V_{n_1}^\dagger V_{n_2}^\dagger V_{n_3}^\dagger V_{n_4}^\dagger. \quad (\text{D.6})$$

(*) = $\frac{1}{\sqrt{2}} (|N, 0\rangle + e^{-iN\phi} |0, N\rangle) \langle 0|^{\otimes 2} = \frac{1}{\sqrt{2}} |N, 0\rangle \langle 0, 0| + |0, N\rangle \langle 0, 0| e^{-iN\phi}$, we see that, if we apply the lossy map we have: $\eta^{N/2} (|N, 0\rangle \langle 0, 0| + |0, N\rangle \langle 0, 0| e^{-iN\phi}) = \eta^{N/2} |\mathbf{N}_-\rangle \langle 0|^{\otimes 2}$, and more generally for Eq. (D.6) the result is: $\eta^N (|0\rangle^{\otimes 2} \langle \mathbf{N}_+| \otimes |\mathbf{N}_-\rangle \langle 0|^{\otimes 2})$. Finally, the expression of the evolved noon-like density matrix is:

$$\begin{aligned} \rho' &= \frac{1}{2} [(\eta^N |\mathbf{N}_+\rangle \langle \mathbf{N}_+| + \rho_{MIX}) \otimes \nu^{\otimes 2} \\ &\quad + \nu^{\otimes 2} \otimes (\eta^N |\mathbf{N}_-\rangle \langle \mathbf{N}_-| + \rho_{MIX}) + \\ &\quad \eta^N (|0\rangle^{\otimes 2} \langle \mathbf{N}_+| \otimes |\mathbf{N}_-\rangle \langle 0|^{\otimes 2} + \\ &\quad |\mathbf{N}_+\rangle \langle 0|^{\otimes 2} \otimes |0\rangle^{\otimes 2} \langle \mathbf{N}_-|)] = \\ &\eta^N |\psi'\rangle_\phi \langle \psi'|_\phi + \rho_{MIX} \otimes \nu^{\otimes 2} + \nu^{\otimes 2} \otimes \rho_{MIX}. \end{aligned} \quad (\text{D.7})$$

When $M = 2$:

$$\begin{aligned} &\eta^{2N} |\psi'\rangle_\phi \langle \psi'|_\phi + \eta^N [\nu^{\otimes 4} \otimes (|\mathbf{N}_-\rangle \langle \mathbf{N}_-| \otimes \rho_{MIX} + \rho_{MIX} \otimes |\mathbf{N}_-\rangle \langle \mathbf{N}_-|) + \\ &(|\mathbf{N}_+\rangle \langle \mathbf{N}_+| \otimes \rho_{MIX} + \rho_{MIX} \otimes |\mathbf{N}_+\rangle \langle \mathbf{N}_+|) \otimes \nu^{\otimes 4}] + \rho_{MIX}^{\otimes 2} \otimes \nu^{\otimes 4} + \nu^{\otimes 4} \otimes \rho_{MIX}^{\otimes 2}, \end{aligned}$$

where $|\psi'\rangle_\phi \langle \psi'|_\phi$ is the $M = 2$ pure noon-like state. It seems now that the state is more robust due to the presence of the second term in the sum multiplied by η^N .

More generally, for $M > 2$ what is obtained is:

$$\begin{aligned} \rho'_M &= \frac{1}{2} [(\eta^N |\mathbf{N}_+\rangle \langle \mathbf{N}_+| + \rho_{MIX})^{\otimes M} \otimes \nu^{\otimes 2M} + \nu^{\otimes 2M} \otimes (\eta^N |\mathbf{N}_-\rangle \langle \mathbf{N}_-| + \rho_{MIX})^{\otimes M} + \\ &\eta^{NM} (|0\rangle^{\otimes 2M} \langle \mathbf{N}_+|^{\otimes M} \otimes |\mathbf{N}_-|^{\otimes M} \langle 0|^{\otimes 2M} + |\mathbf{N}_+|^{\otimes M} \langle 0|^{\otimes 2M} \otimes |0\rangle^{\otimes 2M} \langle \mathbf{N}_-|^{\otimes M})] = \\ &\eta^{NM} |\psi'\rangle_\phi \langle \psi'|_\phi + \rho_{MIX}^{\otimes M} \otimes \nu^{\otimes 2M} + \nu^{\otimes 2M} \otimes \rho_{MIX}^{\otimes M} + \rho_\chi. \end{aligned} \quad (\text{D.8})$$

ρ_χ being the mixed terms emerging from the expression $(\eta^N |\mathbf{N}_\pm\rangle \langle \mathbf{N}_\pm| + \rho_{MIX})^{\otimes M}$ and responsible of the robustness of the state.

Appendix **E**

Calculation of damped MN-loss

Suppose the following state: $|\psi\rangle = \frac{1}{\sqrt{2}}(|n :: 0\rangle |m :: 0\rangle + |m :: 0\rangle |n :: 0\rangle)$, where $|q :: 0\rangle$ is a q photons noon state, $q = m, n, n + m = N$. I call such a term *MN-loss* state. Let every noon state accumulate a phase in one of its field modes, so we have: $|\psi\rangle_\phi = \frac{1}{\sqrt{2}}(|n :: 0\rangle_\phi |m :: 0\rangle_\phi + |m :: 0\rangle_\phi |n :: 0\rangle_\phi)$, with $|q :: 0\rangle = \frac{1}{\sqrt{2}}(|q, 0\rangle + e^{iq\phi} |0, q\rangle)$ and $q = m, n$.

Now follows the explicit calculation of the evolution of this state under lossy map: first of all I write the density operator, namely:

$\rho_\phi = |m :: 0\rangle_\phi |n :: 0\rangle_\phi \langle m :: 0|_\phi \langle n :: 0|_\phi + |m :: 0\rangle_\phi |n :: 0\rangle_\phi \langle n :: 0|_\phi \langle m :: 0|_\phi + |n :: 0\rangle_\phi |m :: 0\rangle_\phi \langle m :: 0|_\phi \langle n :: 0|_\phi + |n :: 0\rangle_\phi |m :: 0\rangle_\phi \langle n :: 0|_\phi \langle m :: 0|_\phi$. Then I consider four lossy channels characterized by the same efficiency η , and after having traced out the four vacuum modes as usual, I have: $\mathcal{L}[\rho_\phi] = \sum_{n_1, n_2, n_3, n_4} V_1 V_2 V_3 V_4 \rho_\phi V_1^\dagger V_2^\dagger V_3^\dagger V_4^\dagger$. I rewrite ρ_ϕ in a more feasible way:

$$\rho_{|m::0\rangle_\phi} \otimes \rho_{|n::0\rangle_\phi} + \rho_{|n::0\rangle_\phi} \otimes \rho_{|m::0\rangle_\phi} + \text{OFF DIAG. TERMS.} \quad (\text{E.1})$$

The behaviour under loss of the first two terms is easy to recover, $\rho_{|q::0\rangle_\phi}$ is the density matrix of the pure q -photons noon state, $q = n, m$. I consider instead the OFF DIAGONAL TERMS, namely:

$$|m :: 0\rangle_\phi |n :: 0\rangle_\phi \langle n :: 0|_\phi \langle m :: 0|_\phi \quad (\text{E.2})$$

$$|n :: 0\rangle_\phi |m :: 0\rangle_\phi \langle m :: 0|_\phi \langle n :: 0|_\phi. \quad (\text{E.3})$$

Expresion (E.4) can be also written in the following way:

$|m :: 0\rangle_\phi \langle n :: 0|_\phi \otimes |n :: 0\rangle_\phi \langle m :: 0|_\phi$. After little manipulation we have, considering that

$$\mathcal{L}[|m\rangle \langle n|] = \sum_j V_j |m\rangle \langle n| V_j^\dagger =$$

$$\eta^{\frac{n+m}{2}} \sum_{j=0}^{\min[m,n]} \left(\frac{1-\eta}{\eta}\right)^j \sqrt{\binom{m}{j} \binom{n}{j}} |m-j\rangle \langle n-j|.$$

$$\begin{aligned} \mathcal{L}[|m::0\rangle_\phi \langle n::0|_\phi \otimes |n::0\rangle_\phi \langle m::0|_\phi] = \\ \eta^{\frac{n+m}{2}} (\rho_{m,n,0} + \rho_{0,m,n} e^{i(m-n)\phi} + |0,m\rangle \langle n,0| e^{im\phi} + |m,0\rangle \langle 0,n| e^{-im\phi}) \\ \otimes \eta^{\frac{n+m}{2}} (\rho_{n,m,0} + \rho_{0,n,m} e^{-i(m-n)\phi} + |0,n\rangle \langle m,0| e^{in\phi} + |n,0\rangle \langle 0,m| e^{-in\phi}) \end{aligned}$$

$$\text{with } \rho_{m,n,0} := \sum_{j=0}^{\min[m,n]} \left(\frac{1-\eta}{\eta}\right)^j \sqrt{\binom{m}{j} \binom{n}{j}} |m-j\rangle \langle n-j| \otimes \nu$$

$$\rho_{0,m,n} := \nu \otimes \sum_{j=0}^{\min[m,n]} \left(\frac{1-\eta}{\eta}\right)^j \sqrt{\binom{m}{j} \binom{n}{j}} |m-j\rangle \langle n-j|$$

$$\rho_{n,m,0} := \sum_{j=0}^{\min[m,n]} \left(\frac{1-\eta}{\eta}\right)^j \sqrt{\binom{m}{j} \binom{n}{j}} |n-j\rangle \langle m-j| \otimes \nu$$

$$\rho_{0,m,n} := \nu \otimes \sum_{j=0}^{\min[m,n]} \left(\frac{1-\eta}{\eta}\right)^j \sqrt{\binom{m}{j} \binom{n}{j}} |n-j\rangle \langle m-j|, \text{ where } \nu \text{ is}$$

the vacuum density matrix. This terms will obviously carry information about the phase, but the presence of the term $\eta^{n+m} = \eta^N$ indicates the fact that such an information will be preserved only if no photons is lost. Manipulating further the evolved state I have finally:

$$\begin{aligned} \mathcal{L}[\rho] = \eta^N \rho_\phi + \eta^m (\rho_{|m::0\rangle_\phi} \otimes \rho_{mix}^{(n)} + \rho_{mix}^{(n)} \otimes |m::0\rangle_\phi) + \\ \eta^n (\rho_{|n::0\rangle_\phi} \otimes \rho_{mix}^{(m)} + \rho_{mix}^{(m)} \otimes |n::0\rangle_\phi) + \\ \rho_{mix}^{(m)} \otimes \rho_{mix}^{(n)} + \rho_{mix}^{(n)} \otimes \rho_{mix}^{(m)} + \eta^N \rho(\phi)_\chi. \end{aligned} \quad (\text{E.4})$$

$\rho_{mix}^{(q)} = \sum_{i=0}^{q-1} \binom{q}{i} \eta^i (1-\eta)^{q-i} \frac{1}{2} [|i,0\rangle \langle i,0| + |0,i\rangle \langle 0,i|]$, where the suffix indicate the fact that the state is a q photon state. The term $\rho(\phi)_\chi$ instead is related to the OFF DIAGONAL TERMS previously given. The MN-loss state presents a robustness to loss for the presence of the second and third term in (E.4), thanks to which we can say that the lost of n or m photons is tolerated and phase information can still be extracted.

Appendix **F**

Analytical evaluation of $(\Delta A)^2$ for the m&m state

The A operator of Eq. (4.62) can be written as:

$$A = \sum_{s,r=0}^{m'} \Pi_{r,s}^{(+)} - \Pi_{r,s}^{(-)}, \quad (\text{F.1})$$

where $\Pi_{r,s}^{(\pm)}$ is the projector onto the space generated the vectors:

$$|\psi_{r,s}^{\pm}\rangle = \frac{1}{\sqrt{2}}(|m' - r, m - s\rangle \pm |m - r, m' - s\rangle). \quad (\text{F.2})$$

The evaluation of A^2 now follows:

$$A^2 = \sum_{s,r=0}^{m'} \sum_{s',r'=0}^{m'} \Pi_{r,s}^{(+)} \Pi_{r',s'}^{(+)} + \Pi_{r,s}^{(-)} \Pi_{r',s'}^{(-)}. \quad (\text{F.3})$$

Infact $\Pi_{r,s}^{(\pm)} \Pi_{r',s'}^{(\mp)} = 0 \forall r, s, r', s'$, due to the fact that both projectors will always project onto ortogonal subspaces.

In order to compute: $\Pi_{r,s}^{(+)} \Pi_{r',s'}^{(+)}$, we evaluate $\langle \psi_{r,s}^+ | \psi_{r',s'}^+ \rangle$.

$$\langle \psi_{r,s}^+ | \psi_{r',s'}^+ \rangle = \frac{1}{2} (\delta_{m'-r, m'-r'} \delta_{m-s, m-s'} + \delta_{m-r, m'-r'} \delta_{m'-s, m-s'} + \quad (\text{F.4})$$

$$\delta_{m'-r, m-r'} \delta_{m-s, m'-s'} + \delta_{m-r, m-r'} \delta_{m'-s, m'-s'}). \quad (\text{F.5})$$

Summing over r' and s' :

$$1 + \frac{1}{2} \sum_{r',s'}^{m'} (\delta_{m-r, m'-r'} \delta_{m'-s, m-s'} + \delta_{m'-r, m-r'} \delta_{m-s, m'-s'}). \quad (\text{F.6})$$

We obtain the following condition on r', s' :

$$\begin{aligned} r' &= m' - m + r \\ s' &= m - m' + s \end{aligned} \quad (\text{F.7})$$

$$\begin{aligned} r' &= m - m' + r \\ s' &= m' - m + s \end{aligned} \quad (\text{F.8})$$

which cannot be satisfied if $m > 2m'$.

For the present purposes we can take into account the case $m < 2m'$ and the evaluation is simplified. We have:

$$\sum_{s,r=0}^{m'} \sum_{s',r'=0}^{m'} \Pi_{r,s}^{(+)} \Pi_{r',s'}^{(+)} = \sum_{s,r=0}^{m'} \sum_{s',r'=0}^{m'} |\psi_{r,s}^+\rangle \langle \psi_{r,s}^+ | \psi_{r',s'}^+\rangle \langle \psi_{r',s'}^+ | = \sum_{s,r=0}^{m'} |\psi_{r,s}^+\rangle \langle \psi_{r,s}^+|. \quad (\text{F.9})$$

Now we must calculate: $\text{Tr} \{ \mathcal{L}(\rho) A^2 \}$.

I recall the expression of the evolved m&m density matrix under lossy evolution:

$$\begin{aligned} \mathcal{L}(\rho) = \hat{\rho}_{a',b'} &= \sum_{k=0}^m \sum_{l=0}^{m'} \underbrace{|a_{k,l}|^2 |m-k, m'-l\rangle \langle m-k, m'-l|}_{X} \\ &\quad + \underbrace{|b_{k,l}|^2 |m'-l, m-k\rangle \langle m'-l, m-k|}_{Y} \\ &\quad + \sum_{l,l'=0}^{m'} a_{l,l'}^* b_{l',l} |m'-l, m-l'\rangle \langle m-l, m'-l'| \\ &\quad + a_{l',l} b_{l,l'}^* |m-l', m'-l\rangle \langle m'-l', m-l| \end{aligned} \quad (\text{F.10})$$

with:

$$\begin{aligned} |a_{k,l}|^2 &\equiv \gamma_{k,l}^2 \eta_a^{m-k} (1-\eta_a)^k \eta_b^{m'-l} (1-\eta_b)^l \\ |b_{k,l}|^2 &\equiv \gamma_{k,l}^2 \eta_a^{m'-l} (1-\eta_a)^l \eta_b^{m-k} (1-\eta_b)^k \\ a_{l,l'}^* b_{l',l} &\equiv \gamma_{l,l'} \gamma_{l',l} \eta_a^{\frac{m+m'-2l}{2}} (1-\eta_a)^l \eta_b^{\frac{m+m'-2l'}{2}} (1-\eta_b)^{l'} e^{-i(m-m')\phi} \\ a_{l',l} b_{l,l'}^* &\equiv \gamma_{l',l} \gamma_{l,l'} \eta_a^{\frac{m+m'-2l'}{2}} (1-\eta_a)^{l'} \eta_b^{\frac{m+m'-2l}{2}} (1-\eta_b)^l e^{i(m-m')\phi}, \end{aligned} \quad (\text{F.11})$$

and

$$\gamma_{k,l} \equiv \sqrt{\frac{1}{2} \binom{m}{k} \binom{m'}{l}}. \quad (\text{F.12})$$

It can be immediately said that no contribution is given by *off diagonal* terms of the evolved density matrix, namely third and fourth terms Eq. (F.10).

So, first we compute:

$$\text{Tr} \{A^2 X\} \text{ and } \text{Tr} \{A^2 Y\}. \quad (\text{F.13})$$

Reexpressing A^2 we have:

$$A^2 = \sum_{r,s=0}^{m'} \underbrace{|m' - r, m - s\rangle \langle m' - r, m - s|}_{(i)} + \underbrace{|m - r, m' - s\rangle \langle m - r, m' - s|}_{(ii)} \quad \text{if } m - m' > m' \quad (\text{F.14})$$

From Eq.F.14 we have:

$$\begin{aligned} \text{Tr} \{(i)X\} &= \text{Tr} \{|m' - r, m - s\rangle \langle m - k, m' - l|\} \delta_{m' - r, m - k} \delta_{m - s, m' - l} \\ \text{Tr} \{(ii)X\} &= \text{Tr} \{|m - r, m' - s\rangle \langle m - k, m' - l|\} \delta_{m - r, m - k} \delta_{m' - s, m' - l} \\ \text{Tr} \{(i)Y\} &= \text{Tr} \{|m' - r, m - s\rangle \langle m' - l, m - k|\} \delta_{m' - r, m' - l} \delta_{m - s, m - k} \\ \text{Tr} \{(ii)Y\} &= \text{Tr} \{|m - r, m' - s\rangle \langle m' - l, m - k|\} \delta_{m - r, m' - l} \delta_{m' - s, m - k} \end{aligned} \quad (\text{F.15})$$

From the first and last term, no contribution is given, infact for that expression, what must be obeyed is:

$r = m' - m + k$ and $s = m - m' + l$ for the first and,

$r = m - m' + l$ and $s = m' - m + k$ for the fourth, but this is not the case.

For second and third expressions instead is: $r = k, s = l$ for the second,

$r = l, s = k$ for the third. Provided that k now must run from 0 to m' , we have:

$$\langle A^2 \rangle = \sum_{k,l=0}^{m'} (|a_{k,l}|^2 + |b_{k,l}|^2). \quad (\text{F.16})$$

With these results we can compute the variance $(\Delta A)^2$ and finally the precision over the phase $\delta\phi$.

Bibliography

- [1] C. W. Helstrom, Phys. Lett. A **25**, 1012 (1967).
- [2] H. P. Yuen, M. Lax, IEEE Trans. Inf. Th. **19**, 740 (1973).
- [3] C. W. Helstrom, R. S. Kennedy, IEEE Trans. Inf. Th. **20**, 16 (1974).
- [4] S. Braunstein and C. Caves, Phys. Rev. Lett. **72**, 3439 (1994).
- [5] S. Braunstein, C. Caves, and G. Milburn, Ann. Phys. **247**, 135 (1996).
- [6] O. E. Barndorff-Nielsen, R. D. Gill, J. Phys. A **33**, 4481 (2000).
- [7] A. S. Holevo, Rep. Math. Phys. **16**, 385 (1979).
- [8] S. L. Braunstein, C. M. Caves and G. J. Milburn, Ann. Phys. **247**, 135 (1996);
S. L. Braunstein, C. M. Caves, Phys. Rev. Lett. **72**, 3439 (1994).
- [9] M. D'Ariano et al., Phys. Lett. A **248**, 103 (1998).
- [10] C. W. Helstrom, Found. Phys. **4**, 453 (1974).
- [11] G. J. Milburn et al., Phys. Rev. A **50**, 801 (1994).
- [12] G. Chiribella et al., Phys. Rev. A **73**, 062103 (2006).
- [13] G. M. D'Ariano, M. G. A. Paris, P. Perinotti, J. Opt. B **3**, 337 (2001).
- [14] A. Monras, Phys. Rev. A **73**, 033821 (2006).
- [15] M. Sarovar, G. J. Milburn, J. Phys. A **39**, 8487 (2006).
- [16] M. Hotta et al., Phys. Rev. A **72**, 052334 (2005); J. Phys. A **39** (2006).
- [17] A. Fujiwara, Phys. Rev. A **63**, 042304 (2001); A. Fujiwara, H. Imai, J. Phys. A **36**, 8093 (2003).
- [18] J. Zhenfeng et al., preprint LANL quant-ph/0610060
- [19] A. Monras, M. G. A. Paris Phys. Rev. Lett. **98**, 160401 (2007).

-
- [20] V. D'Auria et al., *J. Phys. B* **39**, 1187 (2006).
- [21] P. Grangier et al., *Phys. Rev. Lett.* **59**, 2153 (1987).
- [22] E. S. Polzik et al., *Phys. Rev. Lett.* **68**, 3020 (1992).
- [23] B. R. Frieden, *Opt. Comm.* **271**, 7 (2007).
- [24] S. Boixo, A. Monras, *Phys. Rev. Lett.* **100**, 100503 (2008).
- [25] P. Zanardi, M. G A Paris, arXiv:0708.1089
- [26] B.L. Higgins et al., *Nature*, **450**, 393, (2007)
- [27] V. Giovannetti, S.Lloyd and L. Maccone, *Phys. Rev. Lett.* **96**,10401 (2006).
- [28] V. Giovannetti, S. Lloyd, and L. Maccone, *Nature* **412**, 417 (2001).
- [29] V. Giovannetti, S. Lloyd, and L. Maccone, *Phys. Rev. A* **65**, 022309 (2002).
- [30] A. S. Holevo, *Probabilistic and Statistical Aspect of Quantum Theory*, (North-Holland, Amsterdam, 1982).
- [31] C. W. Helstrom, *Quantum Detection and Estimation Theory*, (Academic Press, New York, 1976)
- [32] Giulio Chiribella, PhD thesis, XIX ciclo, A. A. 2003-2006.
- [33] M. A. Rubin, and S. Kaushik, *Phys. Rev. A* **75**, 053805 (2007) .
- [34] R. H. Kingstone, *Optical Sources, Detectors, and System*, Academic, San Diego, 1995.
- [35] X,-Y., Chen, L.-z. Jiang and Han, L., quant-ph/0605184
- [36] G. Gilbert, M. Hamrick, Y.S. Weinstein, quant-ph/0612156v1
- [37] Yu-Bo Sheng, Fu-Guo Deng, Hong-Yu Zhou arXiv:0806.0115v2
- [38] S. D. Huver, C. F. Wildfeuer, and J. P. Dowling, arXiv:0805.0296v1 [quant-ph].
- [39] U. Dorner et al. arXiv:0807.3659v1 [quant-ph].
- [40] Z. Y. Ou, *Phys. Rev. A* **55**, 2598 (1997)
- [41] F. W. Sun, Z.Y. Ou, and G. C. Guo, *Phys. Rev. A* **73**, 023808 (2006).
- [42] F. W. Sun, B. H. Liu, Y. X. Gong, Y. F. Huang, Z.Y. Ou, G. C. Guo, arXiv:0710.2922v1 [quant-ph].
- [43] M. J. Holland and K. Burnett, *Phys. Rev. Lett.* **71**, 1355 (1993)
- [44] Ryo Okamoto, H. F. Hofmann, T. Nagata, J. L. O' Brien, Keiji Sasaki, and Shigeki Takeuchi, arXiv:0804.0087v1 [quant-ph] (2008)

BIBLIOGRAPHY

- [45] J. J. Bollinger, Wayne M. Itano and D. J. Wineland, Phys. Rev. A **54**, R4649 (1996)
- [46] J. Eisert, M.B. Plenio, Int. J. Quant. Inf. **1**, 479 (2003).
- [47] S. L. Braunstein, P. van Loock, quant-ph/0410100, Rev. Mod. Phys., in press.
- [48] Lee, H., Kok, P. and Dowling, J.P., J. Mod. Opt., **49**, 2325-2338 (2002)
- [49] V., Buek, R., Derka, and S., Massar, Phys. Rev. Lett, **82** 2207 (1999)
- [50] H. Carmichael, *An Open Quantum System Approach to Quantum Optics* (Springer-Verlag, Heidelberg, 1993).
- [51] P. Kok, H. Lee, and J. P. Dowling Phys. Rev. A **65**, 052104 (2002)
- [52] M. W. Mitchell, J. S. Lundeen & A. M. Steinberg, Nature **429**, 161-164, 2004
- [53] A. N. Boto, P. Kok, D. S. Abrams, S. L. Braunstein, C. P. Williams, and J. P. Dowling, Phys. Rev. Lett. **85**, 2733 (2000).
- [54] S. F. Huelga, C. Macchiavello, T. Pellizzari, A. K. Ekert, M. B. Plenio, and J. I. Cirac, Phys. Rev. Lett. **79**, 3865 (1997).
- [55] J.M. Geremia *et al.*, Phys. Rev. Lett. **91**, 250801(2003).
- [56] C. M. Caves, Phys. Rev. Lett. **45**, 75 (1980); Phys. Rev. Lett. **54**, 2465 (1985)
- [57] R. S. Bondurant and J. H. Shapiro, Phys. Rev. D **30**, 2548 (1984).
- [58] A. Monras, and Matteo G. A. Paris, Phys. Rev. Lett. **98**, 160401 (2007)
- [59] S. Olivares and M. G. A. Paris, J. Opt. B, **6** 69 (2004)
- [60] G. M. D'Ariano, M. G. A. Paris, and P. Perinotti, Phys. Rev. A **65** 062106
- [61] V. D'Áuria *et al.*, J. Phys. **B39**, 1187 (2006), P. Grangier *et al.*, Phys. Rev. Lett. **59**, 2153(1987), E.S. Polzik *et al.*, Phys. Rev. Lett. **68**, 3020(1992)
- [62] K. E. Cahill and R. J. Glauber, Phys. Rev. **177**, 1882 (1969).
- [63] A. Ferraro, S. Olivares, and M. G. A. Paris, *Gaussian States in Quantum Information* (Bibliopolis, Napoli, 2005).
- [64] H. Venzl and Matthias Freyberger, Phys. Rev. A **75**, 042322 (2007).
- [65] W. Schleich, M. Pernigo, and F. L.Kien, Phys. Rev. A **44**, 2172 (1991).
- [66] Wang Xiang-bin, Phys. Rev. A **66**, 024303 (2002).
- [67] W. H. Louisell, *Quantum Statistical Properties of Radiation* (Wiley, New York,1990).

-
- [68] H. J. Carmichael, *Statistical Methods in Quantum Optics 1: Master Equations and Fokker-Planck Equations* (Springer, Berlin, 1999).
- [69] M. G. Genoni, M. G. A. Paris and Konrad Banaszek, Phys. Rev. A **76**, 042327 (2007).
- [70] A. C. Elitzur, L. Vaidman, Found. Phys. **23**, 987 (1993).
- [71] P. Kwiat, H. Weinfurter, T. Herzog, and A. Zeilinger Phys. Rev. Lett. **74**, 4763 (1995)
- [72] Gh.-S. Paraoanu, H. Scutaru, arXiv:quant-ph/9907068v1
- [73] B. C. Sanders G. J. Milburn, Phys. Rev. Lett. **76**, 2944 (1995).
- [74] D. W. Berry and H. M. Wiseman, Phys. Rev. Lett. **85**, 5098 (2000).
- [75] H. M. Wiseman and R. B. Killip, Phys. Rev. A **56**, 944 (1997).
- [76] B. C. Sander, G. J. Milburn, and Z. Zhang, J. Mod. Opt. **44**, 1309 (1997).
- [77] U. Leonhardt, J. A. Vaccaro, B. Böhmer, and H. Paul, Phys. Rev. A **51**, 84 (1995).
- [78] M. G. Raymer, M. Beck, and D. F. McAlister, Phys. Rev. Lett. **72**, 1137 (1994).
- [79] D., T., Pegg, and S., M., Barnett EuroPhys. Lett. **6**, 483 (1988).
- [80] Zhengfeng Ji, Guoming Wang, Runyao Duan, Yuan Feng, Mingsheng Ying, arXiv:quant-ph/0610060v4 (2006)
- [81] M. A. Nielsen and I. L. Chuang, *Quantum Computation and Quantum Communication*, Cambridge University Press, 2000.
- [82] U. Dorner, R. Demkowicz-Dobrzanski, B. J. Smith, J. S. Lundeen, W. Wasilewski, K. Banaszek, and I. A. Walmsley, quant-ph/0807.3659
- [83] R. Horodecki, P. Horodecki, M. Horodecki, K. Horodecki, quant-ph/07022205.
- [84] R. Simon, E. C. G. Sudarshan, and N. Mukunda, Phys. Rev. A **36**, 3868 (1987); R. Simon, N. Mukunda, and B. Dutta, Phys. Rev. A **49**, 1567 (1994).
- [85] P. Lo Presti, *Nuove misurazioni quantistiche*, Tesi di Laurea Università di Pavia, a.a. 1998/1999; G. M. D'Ariano, P. Lo Presti, and M. F. Sacchi, Phys. Lett. A **272**, 32 (2000).
- [86] R. Littlejohn, Phys. Rep. **138**, 193 (1986).
- [87] R. Simon, E. C. G. Sudarshan, and N. Mukunda, Phys. Rev. A **37**, 3028 (1988); Arvind, B. Dutta, N. Mukunda, and R. Simon, Pramana-Journ. Phys. **45**, 471 (1995) (e-print quant-ph/9509002).
- [88] A Wunschë, J. Opt. B **4**, 1 (2002).

BIBLIOGRAPHY

- [89] L. Mandel, E. Wolf, *Optical Coherence and Quantum Optics*, (Cambridge Univ. Press, 1995)
- [90] J. Williamson, *Am. J. of Math.* **58**, 141 (1936).
- [91] H. J. Carmichael, *Statistical methods in quantum optics 1*, (Springer, Berlin, 1999).